



## Applied Chemistry Project

**Project title**      Synthesis of depsides and their biological activity

**Student names**   Miss Thamolwan Arnanthigo    ID    6033817623

                         Miss Napassakorn                                    ID    6033821023

                         Chuaycharoen

**Program**            Bachelor of Science in Applied Chemistry

**Academic year**   2020

# **Synthesis of depsides and their biological activity**

**by**

**Miss Thamolwan Arnanthigo**

**Miss Napassakorn Chuaycharoen**

**In Partial Fulfillment for the Degree of Bachelor of Science**

**Program in Applied Chemistry (International Program)**

**Department of Chemistry, Faculty of Science**

**Chulalongkorn University**

**Academic Year 2020**

Project        Synthesis of depsides and their biological activity

By        Miss Thamolwan Arnanthigo and Napassakorn Chuaycharoen

Accepted by Department of Chemistry, Faculty of Science, Chulalongkorn University in Partial Fulfillment of the Requirements for the Degree of Bachelor of Science Program in Applied Chemistry (International Program)

Examination committees

- |  |           |
|--|-----------|
| 1. Associate Professor Dr. Apichat Imyim           | Chairman  |
| 2. Assistant Professor Dr. Tanatorn Khotavivattana | Committee |
| 3. Assistant Professor Dr. Warinthorn Chavasiri    | Advisor   |

Endorsed and approved by the Head of Department of Chemistry

*Warinthorn Chavasiri*

.....  
(Assistant Professor Dr. Warinthorn Chavasiri)

Advisor

*Vp. Hoven*

.....  
(Associate Professor Voravee Hoven, PhD.)

Head of department of chemistry

Date *28 December 2020*

Project Title            Synthesis of depsides and their biological activity  
Student Name            **Miss Thamolwan Arnanthigo**  
Student ID                6033817623  
Student Name            **Miss Napassakorn Chuaycharoen**  
Student ID                6033821023  
Advisor Name            Assistant Professor Dr. Warinthorn Chavasiri  
Department of Chemistry, Faculty of Science, Chulalongkorn University, Academic Year 2020

### **Abstract**

Synthesized depsides were modified based on the core structure of jaboticabin, to enhance its biological activities. Desired depsides were synthesized through an esterification with methyl 2-(2-hydroxyphenyl) acetate (**NT0**) and a carboxylic acid compound. DCC and DMAP were required to activate the carboxylic group and solvent used was DCM. 2-(2-Methoxy-2-oxoethyl)phenyl 3-nitrobenzoate (**NT1**) and 2-(2-methoxy-2-oxoethyl)phenyl (*E*)-3-(2,6-dichlorophenyl)acrylate (**NT18**) showed powerful anti  $\alpha$ -glucosidase activity with an  $IC_{50}$  value of 68.7  $\mu$ M and 84.8  $\mu$ M. The  $IC_{50}$  values obtained from assay were lower than that of Acarbose, the standard reference ( $IC_{50}$  = 93.6  $\mu$ M). On the other hand, none of the compounds showed good potential towards antioxidant activities.

Keywords: Depsides, Jaboticabin, ester, esterification, anti  $\alpha$ -glucosidase, antioxidant, extraction

## **Acknowledgement**

We would like to express our deepest appreciation to our project advisor, Assistant Professor Warinthon Chavasiri for valuable guidance, assistance and providing us with an opportunity to explore new experiences throughout the research project. We would also like to extend our deepest gratitude to all members of Warinthorn's lab, especially Mr. Dinh Phuoc Nguyen for valuable advice and providing us with encouragement throughout the research project. In addition, we are extremely grateful for the opportunity arranged by the Department of Chemistry, Faculty of Science at Chulalongkorn University.

## Table of Content

### Page

Abstract	III
Acknowledgement	IV
Table of Content	V
List of figures	VII
List of schemes	IX
List of tables	X
List of abbreviations	XI
<b>Chapter 1 Introduction</b>	<b>1</b>
1.1 Introduction to the research problem and significance	1
1.2 Research objectives	1
1.3 Literature search	2
1.3.1 Phenolic compounds	2
1.3.2 Jaboticabin	2
1.3.3 Depsides	3
1.3.4 Biological activities of depsides	4
1.3.4.1 Antioxidant	4
1.3.4.2 Antibacterial	4
1.3.4.3 Anti $\alpha$ -glucosidase	4
1.3.4.4 Antiviral	5
<b>Chapter 2 Experimental</b>	<b>6</b>
2.1 List of equipment and instrument	6
2.2 List of chemicals and materials	6
2.3 Experimental procedure	7
2.3.1 Synthesis of methyl 2-(2-hydroxyphenyl) acetate (NT0)	7
2.3.2 General esterification reaction procedure for the synthesis of NT1-NT22	7
2.3.3 General purification for NT3-NT6, NT8-NT13, NT15, NT19-NT21 and NT23	8
2.3.4 Purification by silica gel column chromatography	8
2.3.5 Synthesis and purification of 2-(2-methoxy-2-oxoethyl)phenyl ( <i>E</i> )-3-(2,6-dichlorophenyl)acrylate (NT23)	18
2.3.6 Synthesis and purification of 2-(2-(2-(2,6-dichlorophenyl)acetoxy)phenyl)acetic acid (NT24)	19

2.3.7 Synthesis and purification of 2-(2-(2,6-dichlorophenyl)acetoxy)benzoic acid (NT25)	20
2.3.8 Biological activity tests of synthesized compounds	21
2.3.8.1 Anti $\alpha$ -glucosidase activity	21
2.3.8.2 Antioxidant activity	22
<b>Chapter 3 Results and discussion</b>	<b>23</b>
3.1 Structural modification	23
3.2 Tentative $^1\text{H}$ - and $^{13}\text{C}$ -NMR spectroscopic data of synthesized depsides	24
3.3 Biological test of synthesized depsides	77
3.3.1 Anti $\alpha$ -Glucosidase activity	77
3.3.2 Antioxidant activity	82
<b>Chapter 4 Conclusions</b>	<b>84</b>
References	85
Biography	86

**List of figures**

Figure 1.1	Top 10 global causes of deaths, 2016	1
Figure 1.2	Structure of jaboticabin	3
Figure 1.3	Jaboticaba	3
Figure 1.4	Structure of depside	3
Figure 1.5	Green lichen	3
Figure 3.1	Synthesized depside based structure	23
Figure 3.2	The $^1\text{H}$ NMR spectrum of <b>NT0</b>	24
Figure 3.3	The $^{13}\text{C}$ NMR spectrum of <b>NT0</b>	24
Figure 3.4	The $^1\text{H}$ NMR spectrum of <b>NT1</b>	26
Figure 3.5	The $^{13}\text{C}$ NMR spectrum of <b>NT1</b>	26
Figure 3.6	The $^1\text{H}$ NMR spectrum of <b>NT2</b>	28
Figure 3.7	The $^{13}\text{C}$ NMR spectrum of <b>NT2</b>	28
Figure 3.8	The $^1\text{H}$ NMR spectrum of <b>NT3</b>	30
Figure 3.9	The $^{13}\text{C}$ NMR spectrum of <b>NT3</b>	30
Figure 3.10	The $^1\text{H}$ NMR spectrum of <b>NT4</b>	32
Figure 3.11	The $^{13}\text{C}$ NMR spectrum of <b>NT4</b>	32
Figure 3.12	The $^1\text{H}$ NMR spectrum of <b>NT5</b>	34
Figure 3.13	The $^{13}\text{C}$ NMR spectrum of <b>NT5</b>	34
Figure 3.14	The $^1\text{H}$ NMR spectrum of <b>NT6</b>	36
Figure 3.15	The $^{13}\text{C}$ NMR spectrum of <b>NT6</b>	36
Figure 3.16	The $^1\text{H}$ NMR spectrum of <b>NT7</b>	38
Figure 3.17	The $^{13}\text{C}$ NMR spectrum of <b>NT7</b>	38
Figure 3.18	The $^1\text{H}$ NMR spectrum of <b>NT8</b>	40
Figure 3.19	The $^{13}\text{C}$ NMR spectrum of <b>NT8</b>	40
Figure 3.20	The $^1\text{H}$ NMR spectrum of <b>NT9</b>	42
Figure 3.21	The $^{13}\text{C}$ NMR spectrum of <b>NT9</b>	42
Figure 3.22	The $^1\text{H}$ NMR spectrum of <b>NT10</b>	44
Figure 3.23	The $^{13}\text{C}$ NMR spectrum of <b>NT10</b>	44
Figure 3.24	The $^1\text{H}$ NMR spectrum of <b>NT11</b>	46
Figure 3.25	The $^{13}\text{C}$ NMR spectrum of <b>NT11</b>	46
Figure 3.26	The $^1\text{H}$ NMR spectrum of <b>NT12</b>	48
Figure 3.27	The $^{13}\text{C}$ NMR spectrum of <b>NT12</b>	48
Figure 3.28	The $^1\text{H}$ NMR spectrum of <b>NT13</b>	50



Figure 3.29	The $^{13}\text{C}$ NMR spectrum of <b>NT13</b>	50
Figure 3.30	The $^1\text{H}$ NMR spectrum of <b>NT14</b>	52
Figure 3.31	The $^{13}\text{C}$ NMR spectrum of <b>NT14</b>	52
Figure 3.32	The $^1\text{H}$ NMR spectrum of <b>NT15</b>	54
Figure 3.33	The $^{13}\text{C}$ NMR spectrum of <b>NT15</b>	54
Figure 3.34	The $^1\text{H}$ NMR spectrum of <b>NT16</b>	56
Figure 3.35	The $^{13}\text{C}$ NMR spectrum of <b>NT16</b>	56
Figure 3.36	The $^1\text{H}$ NMR spectrum of <b>NT17</b>	58
Figure 3.37	The $^{13}\text{C}$ NMR spectrum of <b>NT17</b>	58
Figure 3.38	The $^1\text{H}$ NMR spectrum of <b>NT18</b>	60
Figure 3.39	The $^{13}\text{C}$ NMR spectrum of <b>NT18</b>	60
Figure 3.40	The $^1\text{H}$ NMR spectrum of <b>NT19</b>	62
Figure 3.41	The $^{13}\text{C}$ NMR spectrum of <b>NT19</b>	62
Figure 3.42	The $^1\text{H}$ NMR spectrum of <b>NT20</b>	64
Figure 3.43	The $^{13}\text{C}$ NMR spectrum of <b>NT20</b>	64
Figure 3.44	The $^1\text{H}$ NMR spectrum of <b>NT21</b>	66
Figure 3.45	The $^{13}\text{C}$ NMR spectrum of <b>NT21</b>	66
Figure 3.46	The $^1\text{H}$ NMR spectrum of <b>NT22</b>	68
Figure 3.47	The $^{13}\text{C}$ NMR spectrum of <b>NT22</b>	68
Figure 3.48	The $^1\text{H}$ NMR spectrum of <b>NT23</b>	71
Figure 3.49	The $^{13}\text{C}$ NMR spectrum of <b>NT23</b>	71
Figure 3.50	The $^1\text{H}$ NMR spectrum of <b>NT24</b>	73
Figure 3.51	The $^{13}\text{C}$ NMR spectrum of <b>NT24</b>	73
Figure 3.52	The $^1\text{H}$ NMR spectrum of <b>NT25</b>	75
Figure 3.53	The $^{13}\text{C}$ NMR spectrum of <b>NT25</b>	75
Figure 3.54	The 96-well plate after the addition of enzyme, substrate and incubation	77
Figure 3.56	Before the addition of DPPH	82
Figure 3.57	After incubation and addition of DPPH into the samples (top 3 rows) and Ascorbic acid (bottom 3 rows)	82

**List of schemes**

Scheme 2.1	Synthesis pathway of 2-(2-methoxy-2-oxoethyl)phenyl 3-(3-nitrophenyl)propanoate (NT23)	18
Scheme 2.2	Synthesis pathway of 2-(2-(2-(2,6-dichlorophenyl)acetoxy)phenyl)acetic acid (NT24)	19
Scheme 2.3	Synthesis pathway of 2-(2-(2-(2,6-dichlorophenyl)acetoxy)benzoic acid (NT25)	20

**List of tables**

Table 3.1	The <sup>1</sup> H and <sup>13</sup> C NMR spectral assignment of <b>NT0</b> in CDCl <sub>3</sub> and reference compound in DMSO-d <sub>6</sub>	25
Table 3.2	The <sup>1</sup> H and <sup>13</sup> C NMR spectral assignment of <b>NT1</b> and reference compound in DMSO-d <sub>6</sub>	27
Table 3.3	The <sup>1</sup> H and <sup>13</sup> C NMR spectral assignment of <b>NT2</b>	29
Table 3.4	The <sup>1</sup> H and <sup>13</sup> C NMR spectral assignment of <b>NT3</b> in CDCl <sub>3</sub>	31
Table 3.5	The <sup>1</sup> H and <sup>13</sup> C NMR spectral assignment of <b>NT4</b> and reference compound in DMSO-d <sub>6</sub>	33
Table 3.6	The <sup>1</sup> H and <sup>13</sup> C NMR spectral assignment of <b>NT5</b>	35
Table 3.7	The <sup>1</sup> H and <sup>13</sup> C NMR spectral assignment of <b>NT6</b>	37
Table 3.8	The <sup>1</sup> H and <sup>13</sup> C NMR spectral assignment of <b>NT7</b> reference compound in DMSO-d <sub>6</sub>	39
Table 3.9	The <sup>1</sup> H and <sup>13</sup> C NMR spectral assignment of <b>NT8</b>	41
Table 3.10	The <sup>1</sup> H and <sup>13</sup> C NMR spectral assignment of <b>NT9</b>	43
Table 3.11	The <sup>1</sup> H and <sup>13</sup> C NMR spectral assignment of <b>NT10</b>	45
Table 3.12	The <sup>1</sup> H and <sup>13</sup> C NMR spectral assignment of <b>NT11</b>	47
Table 3.13	The <sup>1</sup> H and <sup>13</sup> C NMR spectral assignment of <b>NT12</b>	49
Table 3.14	The <sup>1</sup> H and <sup>13</sup> C NMR spectral assignment of <b>NT13</b>	51
Table 3.15	The <sup>1</sup> H and <sup>13</sup> C NMR spectral assignment of <b>NT14</b>	53
Table 3.16	The <sup>1</sup> H and <sup>13</sup> C NMR spectral assignment of <b>NT15</b>	55
Table 3.17	The <sup>1</sup> H and <sup>13</sup> C NMR spectral assignment of <b>NT16</b>	57
Table 3.18	The <sup>1</sup> H and <sup>13</sup> C NMR spectral assignment of <b>NT17</b>	59
Table 3.19	The <sup>1</sup> H and <sup>13</sup> C NMR spectral assignment of <b>NT18</b>	61
Table 3.20	The <sup>1</sup> H and <sup>13</sup> C NMR spectral assignment of <b>NT19</b>	63
Table 3.21	The <sup>1</sup> H and <sup>13</sup> C NMR spectral assignment of <b>NT20</b>	65
Table 3.22	The <sup>1</sup> H and <sup>13</sup> C NMR spectral assignment of <b>NT21</b>	67
Table 3.23	The <sup>1</sup> H and <sup>13</sup> C NMR spectral assignment of <b>NT22</b>	69
Table 3.24	The <sup>1</sup> H and <sup>13</sup> C NMR spectral assignment of <b>NT23</b>	72
Table 3.25	The <sup>1</sup> H and <sup>13</sup> C NMR spectral assignment of <b>NT24</b>	74
Table 3.26	The <sup>1</sup> H and <sup>13</sup> C NMR spectral assignment of <b>NT25</b>	76
Table 3.27	The anti α-glucosidase activity of NT1-25 as % inhibition at 200 μM and IC <sub>50</sub> value	78
Table 3.28	The % inhibition at 1mM of <b>NT5</b> , <b>NT7</b> , <b>NT11-NT16</b> , <b>NT21</b> and <b>NT24</b>	83

**LIST OF ABBREVIATIONS**

Equiv	Equivalence
HCl	Hydrochloric acid
NaHCO <sub>3</sub>	Sodium bicarbonate
DCM	Dichloromethane
DMAP	4-Dimethylaminopyridine
NaOH	Sodium hydroxide
DMSO	Dimethyl sulfoxide
Na <sub>2</sub> CO <sub>3</sub>	Sodium carbonate
MeOH	Methanol
DPPH	2,2-diphenyl-1-picrylhydrazyl
CuCl	Copper(I) chloride
NaBH <sub>4</sub>	Sodium borohydride
i-PrOH	Isopropyl alcohol
tert-BuOK	Potassium tert-butoxide
tert-BuOH	tert-Butyl alcohol
KHCO <sub>3</sub>	Potassium bicarbonate
DMF	Dimethylformamide
EtOAc	Ethyl acetate
Pd/C	Palladium on carbon

## Chapter 1

### Introduction

#### 1.1 Introduction to the research problem and significance

From the past to the present, the leading causes of death globally are mainly noncommunicable diseases, such as, heart disease, trachea, bronchus, lung cancers, diabetes mellitus, and more. According to WHO organization, the number one reason of death in 2016, was Ischaemic heart disease, with trachea, bronchus, lung cancers, and diabetes mellitus being in the top 10 causes of death, as shown in Figure 1.1. Scientists and researchers in the pharmaceutical industry are aiming to discover and modify new drugs and chemicals, serving the purpose of efficiently treating the diseases with least to no harm to human health.

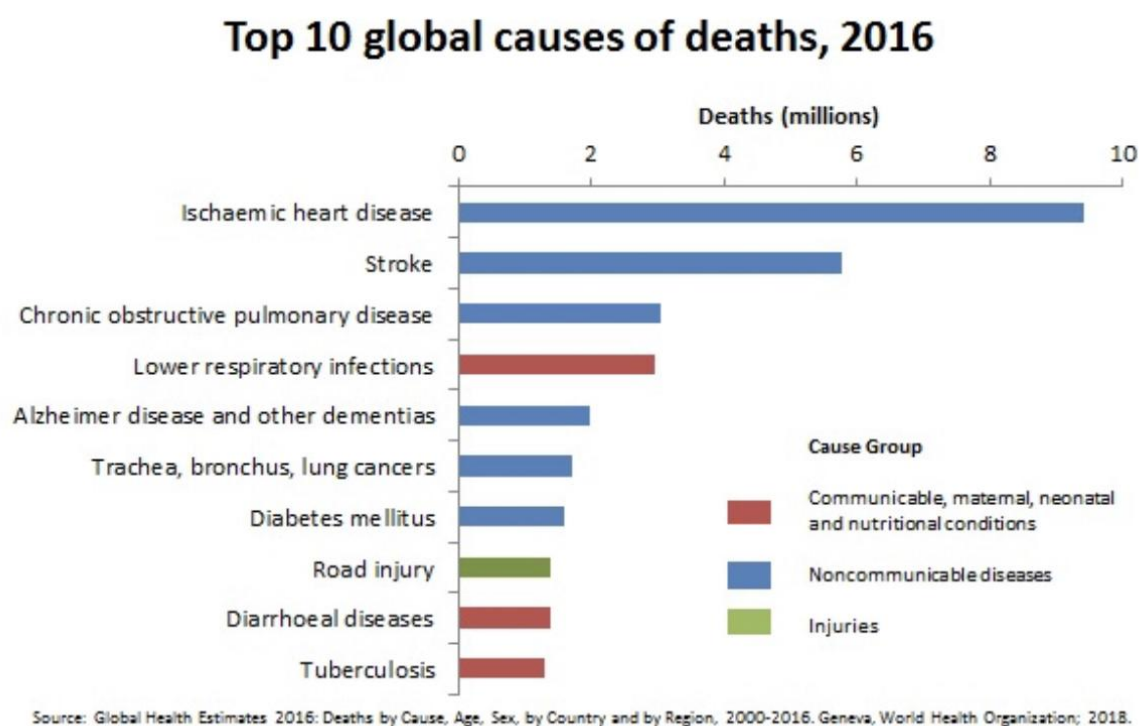


**Figure 1.1** Top 10 global causes of deaths, 2016

Remarkably, depsides, natural phenolic compounds, are reported to have wide range of biological activities.<sup>7,9,10</sup> However, limitations and challenges for the discovery of new compounds with various potent biological activities are difficulties chemists are facing. As depsides are well known for exhibiting diverse benefits toward human health, synthesis and modification of depside based compounds and tests for their biological performances are being conducted.

## 1.2 Research objectives

1. To synthesize and modify depside based compounds with similar structure to jaboticabin
2. To test anti  $\alpha$ -glucosidase and antioxidant properties of synthesized compounds
3. To characterize and elucidate structures of the synthesized compounds

## 1.3 Literature search

### 1.3.1 Phenolic compounds

Phenolic compounds, a broad class of phytochemicals with diverse structures are mainly found in plants, food and beverages. Their structure is composed of one or more aromatic rings, so-called polyphenol, with hydroxyl groups attached to it. Phenolic acids are phenolic compounds that comprise of one or more aromatic ring which are divided into two major groups, benzoic acid derivatives and cinnamic acid derivatives.<sup>1</sup> Moreover, polyphenols can also be characterized by the difference in the number and type of substituent groups, phenol moieties, and the linkage between aromatic rings, examples are flavonoids, lignans, curcumin, xanthones, depsides.<sup>2</sup> Due to the diverse structure, there are various natural phenolic compounds that contribute significantly to human health; commonly found in the form of polyphenols. Curcumin, an example of polyphenol, from turmeric is known to contain high antioxidant properties. Depsides, produced by lichens, are potential antioxidant and anti-glucosidase agents. Gallic acid, a benzoic acid derivative, found in tea and grape seed has antioxidant and anti-inflammatory activities. Chlorogenic acid and caffeic acid are cinnamic acid derivatives, found in coffee, are claimed to help reduce inflammation;<sup>3</sup> Parkinson's disease, cancer and diabetes.<sup>4</sup> Moreover, ferulic acid, which are found on the outer layer of cereal grains are reported to reduce risk of cancer and diabetes due to its high antioxidant properties.<sup>5</sup>

Therefore, many researches emphasize on long-term consumption of diets and the benefits of natural products as they are rich sources of polyphenol compounds which offers to minimize risks against diabetes, cancer, bacterial diseases, inflammation and many more.

### 1.3.2 Jaboticabin

Jaboticabin (Figure 1.2), a newly discovered depside was originally thought to be found in lichens. However, a report published in 2006 stated that jaboticabin can also be obtained by extraction and isolation from Jaboticaba (Figure 1.3), a fruit rich in phytochemicals including; anthocyanins, flavonoids, tannis and depsides. Based on the previous study reported by Reynertson and coworkers in 2006, jaboticabin possesses antiradical activity ( $IC_{50} = 51.4 \mu M$ ) and cytotoxicity against HT29 colon cancer cells ( $IC_{50} = 65 \mu M$ ) with  $IC_{50}$  value being the indication of drug potency or the

concentration of drug needed to inhibit 50% of the cell's growth. Moreover, it also inhibited the production of chemokine interleukin (IL)-8 in human small airway epithelial cells, both before and after cigarette smoke treatment which showed that jabolicabin displayed an anti-inflammatory activity. Therefore, jabolicabin can be considered a potent antiradical, anti-cytotoxicity and anti-inflammatory agent.<sup>6</sup> At the same time, it is also significant to further explore the study of other depsides along with their biological activities.

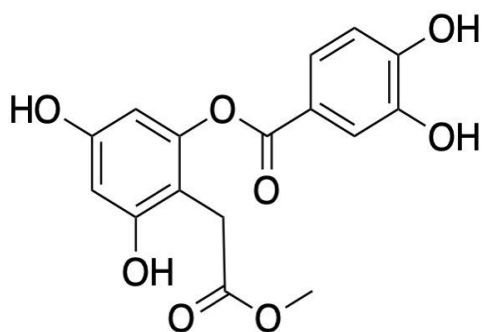


**Figure 1.2** Structure of jabolicabin

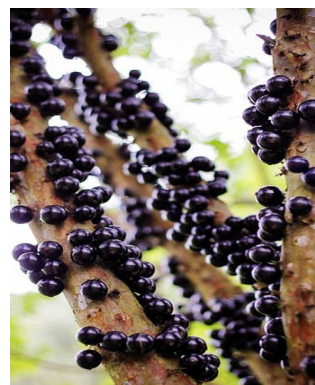


**Figure 1.2** Jaboticaba

### 1.3.3 Depsides

Currently, natural product classes are being studied and developed as therapeutic agents and new pharmacological drugs with promising biological activity, however, there are still many challenges and limitations in discovering new active compounds with multiple biological functions with least to no harm nor side effects. Depside (Figure 1.4) is a class of natural phenolic compounds, consisting of a phenolic ester linkage between two or more aromatic rings which originates from Lichens (Figure 1.5).<sup>7</sup> It is formed by a symbiotic association between a fungus and an alga.<sup>8</sup> In various researches, some depsides that were well-characterized and naturally isolated are reported to have numerous benefits to human health; exhibiting abundant biological properties, including, antibacterial, antioxidants, antiviral and anti-glucosidase.<sup>7,9,10</sup>

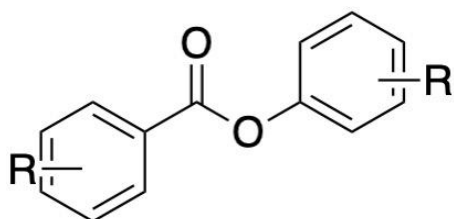


**Figure 1.4** Structure of depside



**Figure 1.5** Green lichen

### 1.3.4 Biological activities of depsides

#### 1.3.4.1 Antioxidant

As previously mentioned, antioxidant is one of the most common biological activity presence in phenolic compounds and well-characterized depsides. Due to the phenolic structure, depsides are able to perform a mechanism against the formation of free radicals and reactive oxygen species which are known as oxidative stress. In order to prevent oxidative stress, antioxidants are substances that prevent and/or slow down damages of cells, as excess of oxidative stress could further lead to several health problems such as ischemic disease, inflammatory disease and cancer.<sup>11</sup> Equally essential, a research reported that 1'-chloropannarin is a potential antioxidant with 66% protection against brain homogenate auto-oxidation at a concentration of 1.7 $\mu$ M in comparison to propylgallate, a reference antioxidant compound with 77% protection at 1.3 $\mu$ M.<sup>12</sup> Later on, a study on antioxidant activity of isolated compounds from *Salvia miltiorrhiza* was performed and two potential antioxidant compounds were salvianolic acid A (IC<sub>50</sub> = 2.62  $\mu$ M) and salvianolic acid B (IC<sub>50</sub> = 3.10  $\mu$ M).<sup>13</sup>

#### 1.3.4.2 Antibacterial

According to the prior study, a structure similar to depside jaboticabin was synthesized and characterized with further antibacterial testing on Gram-positive and Gram-negative bacteria. It is reported that 2-(2-methoxy-2-oxoethyl)phenyl 3-nitrobenzoate and 2-(2-ethoxy-2-oxoethyl)phenyl 3-nitrobenzoate both having an MIC value of 0.78  $\mu$ g/mL against *Bacillus subtilis* ATCC 6633, a type of Gram-positive bacteria. In addition, 2-(2-ethoxy-2-oxoethyl)phenyl 2-(3,4-diethoxyphenyl) acetate and 2-(2-ethoxy-2-oxoethyl)phenyl 2-(3,4-diethoxyphenyl) acetate displayed an MIC value of 1.562  $\mu$ g/mL against *Escherichia coli* ATCC, a type of Gram-negative bacteria.<sup>10</sup>

#### 1.3.4.3 Anti $\alpha$ -glucosidase

Furthermore, a well-characterized depside compound also functions as an inhibitory therapeutic agent towards  $\alpha$ -glucosidase which is an enzyme involved in the hydrolysis of polysaccharides into glucose, increasing blood sugar levels. This significantly affects patients especially those with Type 2 diabetes. The synthesized atranorin analogs which were *N*-substituted hydrazide derivatives were studied for anti-glucosidase inhibitory activity. Methyl (*E*)-4-((3-((2-benzoylhydrazineylidene)methyl)-2,4-dihydroxybenzoyl)oxy)-2-hydroxy-3,6-dimethylbenzoate exhibited an IC<sub>50</sub> value of 6.67 $\mu$ M which showed the most promising ability as glucosidase inhibitors when compared to acarbose which is a commercial antidiabetic drug (IC<sub>50</sub> value of 93.6 $\mu$ M).<sup>9</sup>



#### 1.3.4.4 Antiviral

In addition, depsides also act as an antiviral agent. Researches reported that atronorin, a natural depside and two synthetic depsides, 3-hydroxy-4-(methoxycarbonyl)-2,5-dimethylphenyl 2,4-dihydroxy-3-(hydroxymethyl)-6-methylbenzoate and 3-hydroxy-4-(methoxycarbonyl)-2,5-dimethylphenyl 2,4-dihydroxy-3,6-dimethylbenzoate displayed an anti-Hepatitis C Virus (HCV) activity. HCV can be transmitted through the bloodstream, it is known to cause liver complications such as inflammation and leads to severe damages. After performing a test against the Huh-7.5.1 cell line, with Telaprevir and Erlotinib as a control, atronorin and the above two synthetic compounds exhibited an  $IC_{50}$  of 22.3, 11.8 and 13.3  $\mu$ M.<sup>14</sup>

Therefore, discovering new depside-based compounds, structurally similar to jaboticabin with a lower  $IC_{50}$  value will enhance the ability to increase the degree of success in the process of treatment. The aim of this study is to synthesize depside-based compounds with a core structure similar to jaboticabin and discover the most suitable and effective compound with promising antibacterial, antioxidant and anti-glucosidase properties along with a high degree of safety towards human health.

## Chapter 2 Experimental

### 2.1 Equipment and Instrument

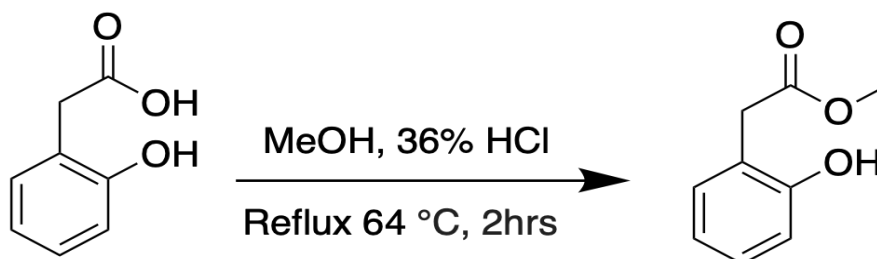
All  $^1\text{H}$ - and  $^{13}\text{C}$ -NMR spectra were recorded on JEOL (500 and 125 MHz) in  $\text{DMSO-d}_6$ , acetone- $\text{d}_4$  and  $\text{CDCl}_3$  as the solvent. The chemical shifts recorded were in parts per million (ppm). The MS was recorded on Bruker microOTOF Q-II. Thin layer chromatography was performed using a UV lamp. A pH meter was used to measure the pH of the buffer and incubator MB100-4A was used for anti-glucosidase test. Both biological test absorbance values were recorded on the AMR-100 Microplate reader.

### 2.2 Chemicals and Materials

3-Nitrobenzoic acid, homoveratric acid, monomethyl isophthalate, isophthalic acid, 3-cyanobenzoic acid, 2,6-dichlorophenylacetic acid, (*E*)-3-(3-nitrophenyl)acrylic acid, 3-(trifluoromethyl) benzaldehyde, 3-nitrophenylacetic acid, 2,6-dichlorocinnamic acid, 4-nitrocinnamic acid, 3-(4-nitrophenyl)propionic acid, and isophthalic acid were purchased from TCI. 4-Nitrobenzoic acid, disodium hydrogen phosphate heptahydrate and sodium dihydrogen phosphate monohydrate were purchased from Merck. 3-Methoxybenzoic acid, 3-chlorobenzoic acid, veratric acid, 3-fluorobenzoic acid and 3,4,5-trimethoxybenzoic acid were purchased from Fluka.  $\alpha$ -Methylcinnamic acid and 2,2-diphenyl-1-picrylhydrazyl were purchased from Aldrich. 3,5-Dinitrobenzoic acid and 2,4-dinitrobenzoic acid were purchased from BDH Chemical and Chemika, respectively. All chemicals were used without further purification. Materials used in the experiment include vials, magnetic stirrer, hot plate, 10, 100 and 1,000 mL graduated cylinder, 75 mm funnel, qualitative filter paper, 10 x 10 cm weighing paper, electronic balance, spatula, Eppendorf, 100 mL separatory funnel, column, condenser, dropper, ring stand, rubber stopper, utility clamp, 5-50  $\mu\text{L}$  and 50-300  $\mu\text{L}$  micropipettes, 10-100  $\mu\text{L}$ , 20-200  $\mu\text{L}$  and 100-1,000  $\mu\text{L}$  autopipette, forceps, TLC Silica gel 60 F<sub>254</sub>, silica gel, ice bath, 500 mL beaker, 500 mL reagent bottle, round bottom flask, needle, balloon, capillary tube, Erlenmeyer flask and metal rod.

## 2.3 Experimental procedure

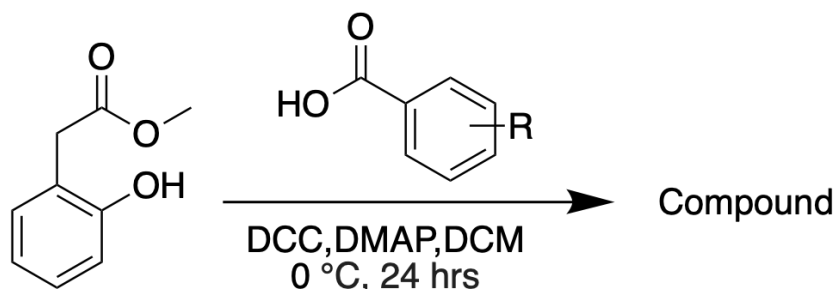
### 2.3.1 Synthesis of methyl 2-(2-hydroxyphenyl) acetate (NT0)



The reaction was carried out in a two neck round bottom flask where 2-hydroxyphenylacetic acid (2.x g, 13 mmol) was dissolved in 20 mL of methanol, then after 20 minutes, 2.4 mL of 36% concentrated HCl were added. The mixture was refluxed for 2 hours. After the reaction was completed, the mixture was placed into a rotary evaporator to remove remaining solvents. The product was isolated and purified by washing for 3 times with  $\text{NaHCO}_3$ . A white powder product was obtained and further used as one of the starting materials for esterification reaction.

Methyl 2-(2-hydroxyphenyl) acetate (90% isolated yield)  $^1\text{H}$  NMR (500 MHz,  $\text{DMSO-d}_6$ ):  $\delta$  9.45 (s, 1H), 7.06-7.02 (m, 2H), 6.76 (d,  $J = 8.0$  Hz, 1H), 6.70 (t,  $J = 7.0$  Hz, 1H), 3.54 (s, 3H) and 3.51 (s, 2H) ppm.  $^{13}\text{C}$  NMR (125 MHz,  $\text{DMSO-d}_6$ ):  $\delta$  171.9, 155.5, 131.1, 128.2, 121.3, 118.9, 114.9, 51.2 and 35.2 ppm.

### 2.3.2 General esterification reaction procedure for the synthesis of NT1-NT22



A solution of methyl 2-(2-hydroxyphenyl) acetate (100 mg, 0.602 mmol) with various substituted benzoic acid [phenylacetic acid, cinnamic acid and propionic acid (1.0 equiv)] in 4 mL of DCM was placed into ice bath for 15 minutes. Another vial consisting of DCC (1.1 equiv) and DMAP (0.2 equiv) with 2 mL of DCM was also placed into ice bath. After the mixture in both vials had

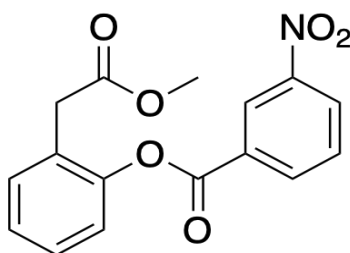
reached 0 °C, both solutions were added into the same vial and were stirred at 0 °C for 1 hour and continued at room temperature for overnight. Once the reaction was completed, the unwanted urea was filtered out by vacuum filtration. The vial was placed in the fume hood for 24 hours allowing the remaining solvents to evaporate before testing with TLC in order to determine the impurities and progress of the reaction.

### 2.3.3 General purification for NT3-NT6, NT8-NT13, NT15, NT19-NT21 and NT23

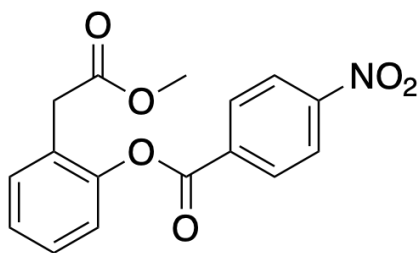
A mixture of distilled water: EtOAc: 1 N HCl (1:3:1) was added into the separatory funnel to remove excess base from the system. The remaining starting material, acid, was eliminated by adding 1 equiv of 1 N NaOH. The aqueous layer was removed and to acquire the pure product, the vial, containing the organic phase, was placed in the fume hood for 2 hours.

### 2.3.4 Purification by silica gel column chromatography

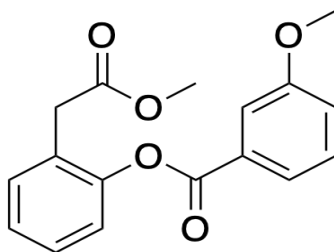
Compounds NT1, NT2, NT7, NT14, NT16-NT18, NT22, NT24 and NT25 were purified by silica gel column chromatography using an eluent of hexane: EtOAc (8:2).



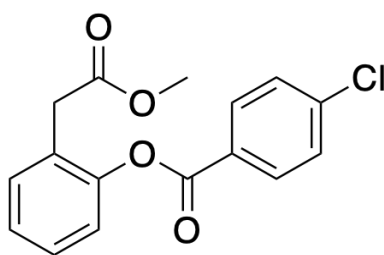
**2.3.4.1 2-(2-methoxy-2-oxoethyl)phenyl 3-nitrobenzoate (NT1)** (71.8% isolated yield)  $^1\text{H}$  NMR (500 MHz,  $\text{CDCl}_3$ ):  $\delta$  9.00 (s, 1H), 8.52-8.47 (m, 2H), 7.73 (t,  $J = 8.0$  Hz, 1H), 7.37 (d,  $J = 7.0$  Hz, 1H), 7.37 (t,  $J = 7.0$  Hz, 1H), 7.29-7.24 (m, 2H), 3.63 (s, 2H) and 3.61 (s, 3H) ppm.  $^{13}\text{C}$  NMR (125 MHz,  $\text{CDCl}_3$ ):  $\delta$  171.0, 162.8, 149.0, 148.5, 135.9, 131.8, 131.2, 130.1, 128.9, 128.2, 126.9, 126.6, 125.8, 122.6, 52.3 and 36.6 ppm.



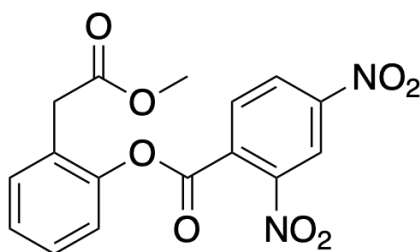
**2.3.4.2 2-(2-methoxy-2-oxoethyl)phenyl 4-nitrobenzoate (NT2)** (40.0% isolated yield)  $^1\text{H}$  NMR (500 MHz,  $\text{CDCl}_3$ ):  $\delta$  8.38-8.34 (m, 4H), 7.40-7.37 (m, 2H), 7.26 (t,  $J = 7.0$  Hz, 1H), 7.26 (d,  $J = 9.0$  Hz, 1H), 3.62 (s, 2H) and 3.58 (s, 3H) ppm.  $^{13}\text{C}$  NMR (125 MHz,  $\text{CDCl}_3$ ):  $\delta$  171.0, 163.0, 151.1, 149.0, 134.8, 131.8, 131.4, 131.4, 129.0, 126.9, 126.6, 123.9, 123.9, 122.6, 52.3 and 37.0 ppm. HR-MS (ESI) for  $\text{C}_{16}\text{H}_{13}\text{NO}_6$   $[\text{M}+\text{Na}]^+$  requires 338.0641 found 338.0677.



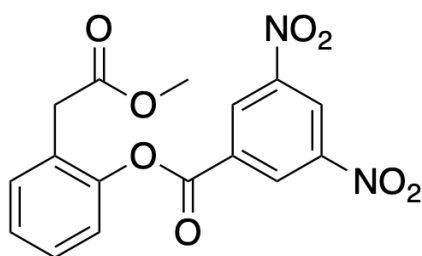
**2.3.4.3 2-(2-methoxy-2-oxoethyl)phenyl 3-methoxybenzoate (NT3)** (54.3% isolated yield)  $^1\text{H}$  NMR (500 MHz,  $\text{CDCl}_3$ ):  $\delta$  7.80 (d,  $J = 7.5$  Hz, 1H), 7.70 (s, 1H), 7.40 (t,  $J = 8.0$  Hz, 1H), 7.35 (d,  $J = 7.0$  Hz, 1H), 7.35 (t,  $J = 7.0$  Hz, 1H), 7.25-7.22 (m, 2H), 7.17 (dd,  $J = 8.0$  and 2.5 Hz, 1H), 3.86 (s, 3H), 3.63 (s, 2H) and 3.58 (s, 3H) ppm.  $^{13}\text{C}$  NMR (125 MHz,  $\text{CDCl}_3$ ):  $\delta$  171.1, 164.6, 159.8, 149.0, 131.4, 130.5, 129.7, 128.6, 126.7, 126.3, 122.7, 122.6, 120.3, 114.6, 55.5, 52.1 and 36.3 ppm. HR-MS (ESI) for  $\text{C}_{17}\text{H}_{16}\text{O}_5$   $[\text{M}+\text{Na}]^+$  requires 323.0896 found 323.0887.



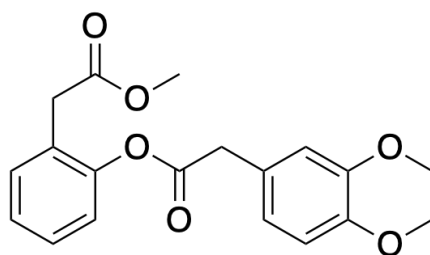
**2.3.4.4 2-(2-methoxy-2-oxoethyl)phenyl 4-chlorobenzoate (NT4)** (54.3% isolated yield)  $^1\text{H}$  NMR (500 MHz,  $\text{CDCl}_3$ ):  $\delta$  8.12 (d,  $J = 9.0$  Hz, 2H), 7.47 (d,  $J = 9.0$  Hz, 2H), 7.35 (d,  $J = 8.0$ , 1H), 7.35 (t,  $J = 8.5$ , 1H), 7.24 (d,  $J = 8.0$ , 1H), 7.24 (t,  $J = 8.5$ , 1H), 3.62 (s, 2H) and 3.57 (s, 3H) ppm.  $^{13}\text{C}$  NMR (125 MHz,  $\text{CDCl}_3$ ):  $\delta$  171.0, 163.8, 149.1, 140.2, 131.5, 131.5, 131.4, 129.0, 128.6, 127.7, 126.6, 126.3, 122.6 53.0 and 36.3 ppm.



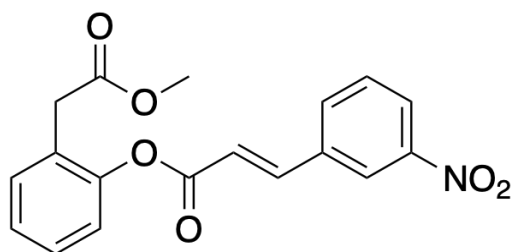
**2.3.4.5 2-(2-methoxy-2-oxoethyl)phenyl 2,4-dinitrobenzoate (NT5)** (41.4% isolated yield)  $^1\text{H}$  NMR (500 MHz,  $\text{CDCl}_3$ ):  $\delta$  8.92 (s, 1H), 8.62 (dd,  $J = 8.5$  and 2.0 Hz, 1H), 8.19 (d,  $J = 8.5$  Hz, 1H), 7.41 (t,  $J = 7.0$  Hz, 1H), 7.37 (d,  $J = 7.0$  Hz, 2H) and 7.30 (t,  $J = 7.5$  Hz, 1H) ppm.  $^{13}\text{C}$  NMR (125 MHz,  $\text{CDCl}_3$ ):  $\delta$  171.0, 163.7, 149.2, 148.6, 147.6, 132.9, 131.9, 131.6, 129.2, 128.2, 127.3, 126.4, 122.1, 119.9, 52.4 and 36.6 ppm. HR-MS (ESI) for  $\text{C}_{16}\text{H}_{12}\text{N}_2\text{O}_8$   $[\text{M}+\text{Na}]^+$  requires 383.0492 found 383.0516.



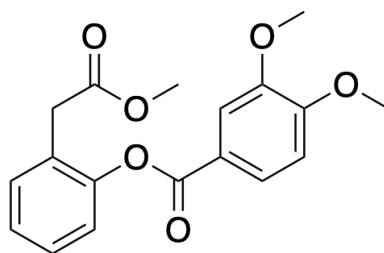
**2.3.4.6 2-(2-methoxy-2-oxoethyl)phenyl 3,5-dinitrobenzoate (NT6)** (46.0% isolated yield)  $^1\text{H}$  NMR (500 MHz,  $\text{CDCl}_3$ ):  $\delta$  9.29 (d,  $J = 2.5$  Hz, 1H), 9.27 (t,  $J = 2.5$  Hz, 1H), 7.41-7.38 (m, 2H), 7.31 (t,  $J = 8.5$  Hz, 1H), 7.26 (d,  $J = 8.5$  Hz, 1H), 3.63 (s, 2H) and 3.62 (s, 3H) ppm.  $^{13}\text{C}$  NMR (125 MHz,  $\text{CDCl}_3$ ):  $\delta$  170.8, 161.0, 148.9, 148.9, 148.7, 133.14, 132.0, 132.0, 130.0, 129.1, 127.3, 126.4, 123.1, 122.3, 52.4 and 36.8 ppm.



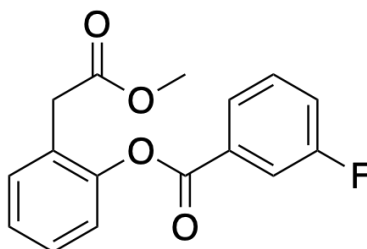
**2.3.4.7 2-(2-methoxy-2-oxoethyl)phenyl 2-(3,4-dimethoxyphenyl)acetate (NT7)** (68.6% isolated yield)  $^1\text{H}$  NMR (500 MHz,  $\text{CDCl}_3$ ):  $\delta$  7.27-7.24 (m, 2H), 7.16 (t,  $J = 7.5$  Hz, 1H), 7.05 (t,  $J = 8.0$  Hz, 1H), 6.91 (d,  $J = 10.0$  Hz, 2H), 6.83 (d,  $J = 8.0$  Hz, 1H), 3.87 (s, 3H), 3.85 (s, 3H), 3.78 (s, 2H), 3.58 (s, 3H) and 3.44 (s, 2H) ppm.  $^{13}\text{C}$  NMR (125 MHz,  $\text{CDCl}_3$ ):  $\delta$  171.0, 149.1, 149.0, 148.4, 131.3, 128.5, 126.5, 126.2, 125.8, 122.4, 121.6, 111.3, 112.5, 55.9, 55.9, 55.9, 52.0, 40.8 and 36.0 ppm.



**2.3.4.8 2-(2-methoxy-2-oxoethyl)phenyl (*E*)-3-(3-nitrophenyl)acrylate (NT8)** (52.7% isolated yield)  $^1\text{H}$  NMR (500 MHz,  $\text{CDCl}_3$ ):  $\delta$  8.41 (s, 1H), 8.23 (dd,  $J = 8.0$  and 2.0 Hz, 1H), 7.89 (d,  $J = 16.0$  Hz, 1H), 7.87 (s,  $J = 5.5$  Hz, 1H), 7.59 (t,  $J = 8.0$  Hz, 1H), 7.34 (d,  $J = 7.5$  Hz, 1H), 7.34 (t,  $J = 7.5$  Hz, 1H), 7.23-7.15 (m, 2H), 6.75 (d,  $J = 16.0$  Hz, 1H), 3.64 (s, 3H) and 3.62 (s, 2H) ppm.  $^{13}\text{C}$  NMR (125 MHz,  $\text{CDCl}_3$ ):  $\delta$  171.1, 164.1, 149.0, 148.7, 143.9, 135.6, 133.9, 131.4, 130.1, 128.6, 126.5, 126.3, 124.9, 122.6, 122.4, 120.0, 52.1 and 36.2 ppm.

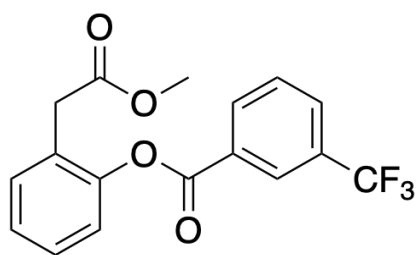


**2.3.4.9 2-(2-methoxy-2-oxoethyl)phenyl 3,4-dimethoxybenzoate (NT9)** (82.7% isolated yield)  $^1\text{H}$  NMR (500 MHz,  $\text{CDCl}_3$ ):  $\delta$  7.84 (dd,  $J = 8$  and 2 Hz, 1H), 7.66 (d,  $J = 2$  Hz, 1H), 7.33 (t,  $J = 7.5$  Hz, 1H), 7.22 (d,  $J = 7.5$  Hz, 1H), 7.22 (t,  $J = 7.5$  Hz, 1H), 7.33 (d,  $J = 7.5$  Hz, 1H), 6.94 (d,  $J = 8.5$  Hz, 1H), 3.94 (s, 6 H), 3.57 (s, 3H) and 3.62 (s, 2H) ppm.  $^{13}\text{C}$  NMR (125 MHz,  $\text{CDCl}_3$ ):  $\delta$  171.2, 164.4, 153.7, 149.4, 148.8, 132.5, 128.6, 126.7, 126.1, 124.5, 122.7, 122.4, 121.6, 110.5, 56.1, 56.1, 52.0 and 35.8 ppm.

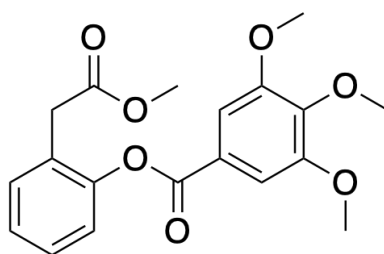


**2.3.4.10 2-(2-methoxy-2-oxoethyl)phenyl 3-fluorobenzoate (NT10)** (85.2% isolated yield)  $^1\text{H}$  NMR (500 MHz,  $\text{CDCl}_3$ ):  $\delta$  8.02 (d,  $J = 7.5$  Hz, 1H), 7.90 (d,  $J = 9.0$  Hz, 1H), 7.52 (dd,  $J = 13.5$  and 8.0 Hz, 1H), 7.39 (t,  $J = 7.0$  Hz, 1H), 7.39 (t,  $J = 7.0$  Hz, 1H), 7.35 (d,  $J = 8.5$  Hz, 1H), 7.28 (t,  $J = 8.5$  Hz, 1H), 7.28 (d,  $J = 8.5$  Hz, 1H), 3.66 (s, 2H) and 3.62 (s, 3H) ppm.  $^{13}\text{C}$  NMR (125 MHz,  $\text{CDCl}_3$ ):  $\delta$  171.2, 163.6, 149.2, 131.5, 130.4, 128.7, 126.5, 126.6, 126.0, 122.6, 121.0, 120.8, 117.1, 116.9, 52.1 and 36.4 ppm.

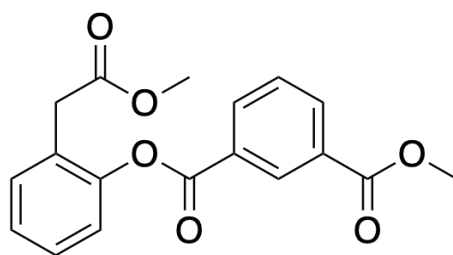




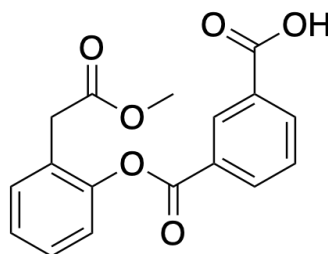
**2.3.4.11 2-(2-methoxy-2-oxoethyl)phenyl 3-(trifluoromethyl)benzoate (NT11)** (31.0% isolated yield)  $^1\text{H}$  NMR (500 MHz,  $\text{CDCl}_3$ ):  $\delta$  8.45 (s, 1H), 8.39 (d,  $J = 8.0$  Hz, 1H), 7.91 (d,  $J = 7.5$  Hz, 1H), 7.68 (t,  $J = 8.0$  Hz, 1H), 7.40-7.37 (m, 2H), 7.26 (t,  $J = 7.5$  Hz, 1H), 7.26 (d,  $J = 7.5$  Hz, 1H), 3.63 (s, 2H) and 3.60 (s, 3H) ppm.  $^{13}\text{C}$  NMR (125 MHz,  $\text{CDCl}_3$ ):  $\delta$  171.2, 163.6, 149.2, 133.5, 131.7, 131.7, 131.7, 130.4, 129.5, 129.5, 128.9, 127.2, 126.7, 122.7, 52.2 and 36.5 ppm.



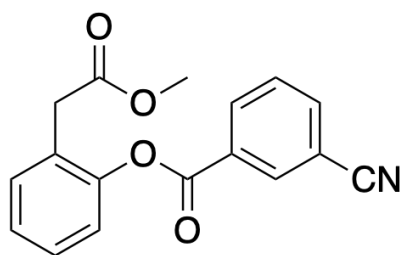
**2.3.4.12 2-(2-methoxy-2-oxoethyl)phenyl 3,4,5-trimethoxybenzoate (NT12)** (48.9% isolated yield)  $^1\text{H}$  NMR (500 MHz,  $\text{CDCl}_3$ ):  $\delta$  7.45 (s, 2H), 7.34 (t,  $J = 7.5$  Hz, 1H), 7.34 (d,  $J = 7.5$  Hz, 1H), 7.23 (d,  $J = 7.5$  Hz, 1H), 7.23 (t,  $J = 7.5$  Hz, 1H), 3.56 (s, 3H), 3.93 (s, 3H), 3.92 (s, 6H) and 3.62 (s, 2H) ppm.  $^{13}\text{C}$  NMR (125 MHz,  $\text{CDCl}_3$ ):  $\delta$  171.2, 164.3, 153.1, 153.1, 149.3, 143.3, 131.4, 128.6, 126.6, 126.2, 124.1, 122.6, 107.5, 107.5, 60.5, 56.2, 56.2, 52.1 and 36.3 ppm.



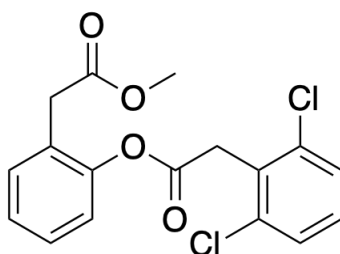
**2.3.4.13 2-(2-methoxy-2-oxoethyl)phenyl methyl isophthalate (NT13)** (78.8% isolated yield)  $^1\text{H}$  NMR (500 MHz,  $\text{CDCl}_3$ ):  $\delta$  8.82 (s, 1H), 8.35 (d,  $J = 7.5$  Hz, 1H), 8.29 (d,  $J = 8$  Hz, 1H), 7.59 (t,  $J = 8$  Hz, 1H), 7.34 (t,  $J = 7.5$  Hz, 1H), 7.34 (d,  $J = 7.5$  Hz, 1H), 7.23 (d,  $J = 7.5$  Hz, 1H), 7.23 (t,  $J = 7.5$  Hz, 1H), 3.93 (s, 3H), 3.57 (s, 3H) and 3.62 (s, 2H) ppm.  $^{13}\text{C}$  NMR (125 MHz,  $\text{CDCl}_3$ ):  $\delta$  171.0, 163.9, 166.1, 149.2, 134.6, 134.3, 131.5, 131.2, 130.1, 129.8, 129.0, 128.7, 126.7, 126.5, 122.6, 52.4, 52.1 and 36.4 ppm.



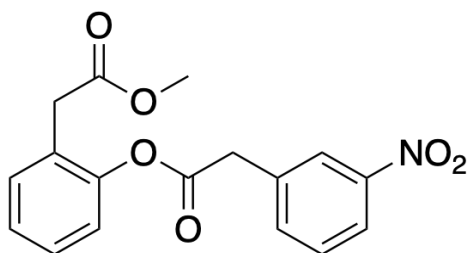
**2.3.4.14 3-((2-(2-methoxy-2-oxoethyl)phenoxy)carbonyl)benzoic acid (NT14)** (12% isolated yield)  $^1\text{H}$  NMR (500 MHz,  $\text{CDCl}_3$ ):  $\delta$  8.62 (s, 1H), 8.29 (d,  $J = 7.5$  Hz, 2H), 7.74 (t,  $J = 7.5$  Hz, 1H), 7.44 (d,  $J = 7.5$  Hz, 1H), 7.40 (d,  $J = 7.5$  Hz, 1H), 7.33 (d,  $J = 8.0$  Hz, 1 H), 7.30 (t,  $J = 7.5$  Hz, 1H), 3.68 (s, 1H) and 3.48 (s, 1H) ppm.  $^{13}\text{C}$  NMR (125 MHz,  $\text{CDCl}_3$ ):  $\delta$  170.8, 166.8, 163.5, 149.0, 134.5, 133.4, 131.7, 130.4, 129.5, 129.1, 128.5, 127.1, 126.3, 126.3, 122.8, 51.7 and 35.7 ppm.



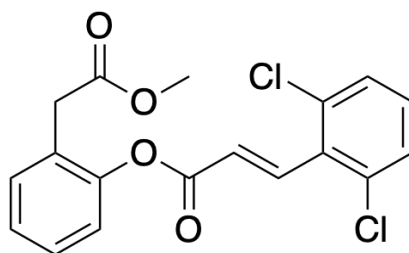
**2.3.4.15 2-(2-methoxy-2-oxoethyl)phenyl 3-cyanobenzoate (NT15)** (42.0% isolated yield)  $^1\text{H}$  NMR (500 MHz,  $\text{CDCl}_3$ ):  $\delta$  8.46 (s, 1H), 8.40 (d,  $J = 8.0$  Hz, 1H), 7.90 (d,  $J = 7.5$  Hz, 1H), 7.65 (t,  $J = 7.5$  Hz, 1H), 7.36 (d,  $J = 7.5$  Hz, 1H), 7.36 (t,  $J = 7.5$  Hz, 1H), 7.26 (t,  $J = 7.5$  Hz, 1H), 7.23 (d,  $J = 8.0$  Hz, 1H), 3.59 (s, 3H) and 3.62 (s, 2H) ppm.  $^{13}\text{C}$  NMR (125 MHz,  $\text{CDCl}_3$ ):  $\delta$  171.0, 171.0, 149.0, 136.7, 134.2, 133.8, 131.7, 130.7, 129.9, 128.8, 126.8, 126.6, 122.5, 117.8, 113.4, 52.2 and 36.5 ppm.



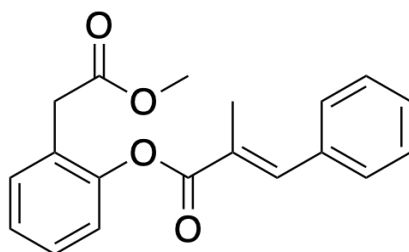
**2.3.4.16 2-(2-methoxy-2-oxoethyl)phenyl 2-(2,6-dichlorophenyl)acetate (NT16)** (51.5% isolated yield)  $^1\text{H}$  NMR (500 MHz,  $\text{CDCl}_3$ ):  $\delta$  4.27 (s, 2H), 7.34 (d,  $J = 8.0$  Hz, 2H), 7.28 (d,  $J = 7.0$  Hz, 1H), 7.28 (t,  $J = 7.0$  Hz, 1H), 7.19-7.13 (m, 3H), 3.64 (s, 3H) and 3.57 (s, 2H) ppm.  $^{13}\text{C}$  NMR (125 MHz,  $\text{CDCl}_3$ ):  $\delta$  171.0, 167.6, 149.1, 136.2, 136.2, 131.3, 130.7, 129.3, 128.5, 128.1, 128.1, 126.4, 126.3, 122.5, 52.1, 36.8 and 35.9 ppm.



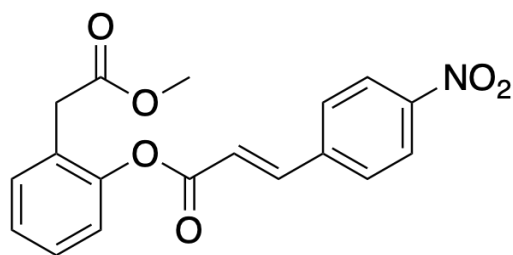
**2.3.4.17 2-(2-methoxy-2-oxoethyl)phenyl 2-(3-nitrophenyl)acetate (NT17)** (40.6% isolated yield)  $^1\text{H}$  NMR (500 MHz,  $\text{CDCl}_3$ ):  $\delta$  8.29 (s, 1H), 8.18 (dd,  $J = 8.0$  and 2.0 Hz, 1H), 7.74 (d,  $J = 8.0$  Hz, 1H), 7.55 (t,  $J = 8.0$  Hz, 1H), 7.29 (t,  $J = 7.5$  Hz, 2H), 7.21 (t,  $J = 7.5$  Hz, 1H), 7.08 (d,  $J = 8.0$  Hz, 1H), 4.00 (s, 2H), 3.61 (s, 3H) and 3.49 (s, 2H) ppm.  $^{13}\text{C}$  NMR (125 MHz,  $\text{CDCl}_3$ ):  $\delta$  171.0, 168.7, 149.0, 148.5, 135.9, 135.3, 131.6, 129.7, 128.7, 126.6, 126.4, 124.7, 122.6, 122.5, 52.2, 40.6 and 36.4 ppm.



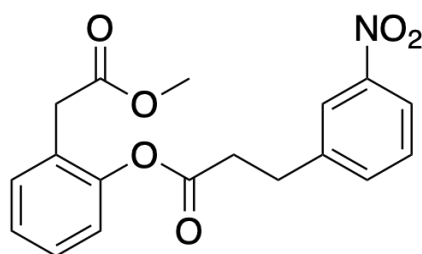
**2.3.4.18 2-(2-methoxy-2-oxoethyl)phenyl (*E*)-3-(2,6-dichlorophenyl)acrylate (NT18)** (44.8% isolated yield)  $^1\text{H}$  NMR (500 MHz,  $\text{CDCl}_3$ ):  $\delta$  7.99 (d,  $J = 16.0$  Hz, 1H), 7.38 (d,  $J = 8.0$  Hz, 2H), 7.32 (d,  $J = 7.0$  Hz, 1H), 7.32 (t,  $J = 7.0$  Hz, 1H), 7.25-7.22 (m, 3H), 6.81 (d,  $J = 16.0$  Hz, 1H), 3.66 (s, 3H) and 3.63 (s, 2H) ppm.  $^{13}\text{C}$  NMR (125 MHz,  $\text{CDCl}_3$ ):  $\delta$  171.2, 164.3, 149.2, 140.2, 135.3, 131.7, 131.7, 131.5, 130.4, 130.4, 129.1, 129.1, 128.7, 126.7, 126.4, 125.8, 122.7, 52.3 and 36.4 ppm.



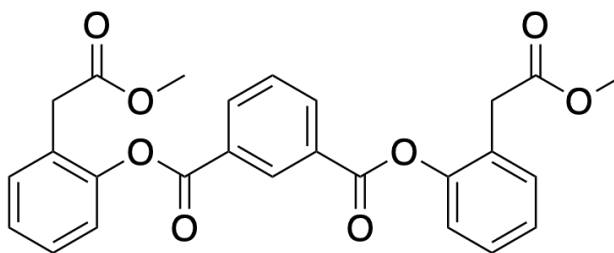
**2.3.4.19 2-(2-methoxy-2-oxoethyl)phenyl (*E*)-2-methyl-3-phenylacrylate (NT19)** (49.2% isolated yield)  $^1\text{H}$  NMR (500 MHz,  $\text{CDCl}_3$ ):  $\delta$  7.92 (s, 1H), 7.47 (d,  $J = 7.5$  Hz, 2H), 7.42 (t,  $J = 7.5$  Hz, 2H), 7.37 (d,  $J = 7.0$  Hz, 1H), 7.35-7.34 (m, 2H), 7.24 (d,  $J = 7.5$  Hz, 1H), 7.21 (t,  $J = 7.5$  Hz, 1H), 3.65 (s, 3H), 3.62 (s, 2H) and 2.25 (2, 3H) ppm.  $^{13}\text{C}$  NMR (125 MHz,  $\text{CDCl}_3$ ):  $\delta$  171.3, 166.8, 149.7, 141.0, 141.0, 135.7, 131.4, 130.0, 128.9, 128.6, 128.6, 128.6, 127.6, 126.8, 126.2, 122.8, 52.2, 36.5 and 14.31 ppm.



**2.3.4.20 2-(2-methoxy-2-oxoethyl)phenyl (*E*)-3-(4-nitrophenyl)acrylate (NT20)** (41.2% isolated yield)  $^1\text{H}$  NMR (500 MHz,  $\text{CDCl}_3$ ):  $\delta$  8.24 (d,  $J = 9.0$  Hz, 2H), 7.88 (d,  $J = 16.0$  Hz, 1H), 7.71 (d,  $J = 8.5$  Hz, 2H), 7.34-7.30 (m, 2H), 7.21 (dd,  $J = 7.5$  and 1.5 Hz, 1H), 7.17 (d,  $J = 8.0$  Hz, 1H), 3.63 (s, 3H) and 3.61 (s, 2.0H) ppm.  $^{13}\text{C}$  NMR (125 MHz,  $\text{CDCl}_3$ ):  $\delta$  171.1, 164.1, 149.0, 148.8, 143.8, 140.1, 131.5, 129.0, 128.7, 126.5, 126.5, 124.3, 122.5, 121.2, 52.2 and 36.3 ppm.



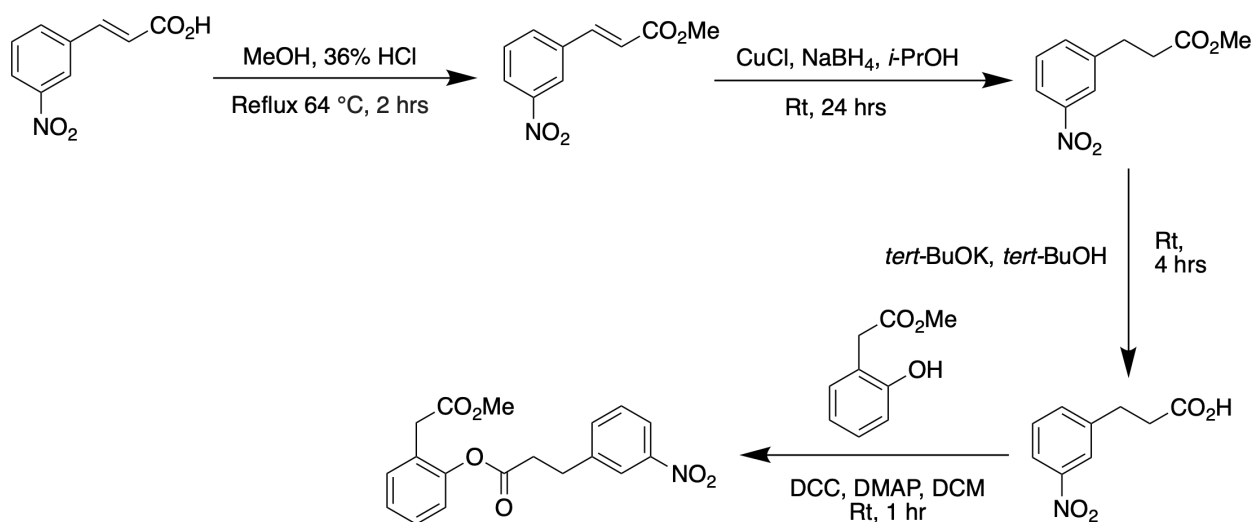
**2.3.4.21 2-(2-methoxy-2-oxoethyl)phenyl 3-(3-nitrophenyl)propanoate (NT21)** (53.6% isolated yield)  $^1\text{H}$  NMR (500 MHz,  $\text{CDCl}_3$ ):  $\delta$  8.14 (d,  $J = 9.0$  Hz, 2H), 7.42 (d,  $J = 8.5$  Hz, 2H), 7.27 (t,  $J = 9.5$  Hz, 1H), 7.27 (d,  $J = 9.5$  Hz, 1H), 7.18 (t,  $J = 7.5$  Hz, 1H), 7.00 (d,  $J = 8$  Hz, 1H), 3.60 (s, 3H), 3.46 (s, 2H), 3.15 (t,  $J = 7.5$  Hz, 2H) and 2.94 (t,  $J = 7.5$  Hz, 2H) ppm.  $^{13}\text{C}$  NMR (125 MHz,  $\text{CDCl}_3$ ):  $\delta$  171.0, 170.4, 148.9, 147.9, 146.7, 131.3, 129.4, 128.6, 126.4, 126.4, 123.8, 122.4, 52.1, 36.2, 34.8 and 30.4 ppm.



**2.3.4.20 Bis(2-(2-methoxy-2-oxoethyl)phenyl) isophthalate (NT22)** (46.4% isolated yield)  $^1\text{H}$  NMR (500 MHz,  $\text{CDCl}_3$ ):  $\delta$  8.99 (s, 1H), 8.46 (dd,  $J = 8.0$  and  $2.0$  Hz, 2H), 7.70 (t,  $J = 7.5$  Hz, 1H), 7.36-7.35 (m, 4H), 7.28-7.25 (m, 4H), 3.65 (s, 4H) and 3.59 (s, 6H) ppm.  $^{13}\text{C}$  NMR (125 MHz,  $\text{CDCl}_3$ ):  $\delta$  171.1, 163.8, 149.2, 135.1, 131.9, 131.6, 130.2, 129.3, 129.9, 126.7, 126.6, 122.7, 52.2 and 36.7 ppm.

### 2.3.5 Synthesis and purification of 2-(2-methoxy-2-oxoethyl)phenyl 3-(3-nitrophenyl)propanoate (NT23)

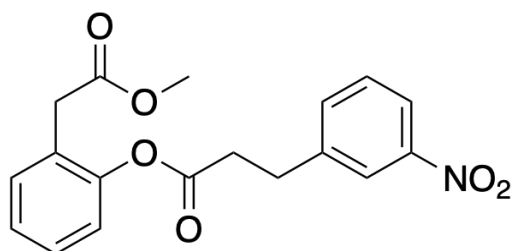
The synthesis of **NT23** was carried out according to the plan described in Scheme 2.1.



**Scheme 2.1** Synthesis pathway of 2-(2-methoxy-2-oxoethyl)phenyl 3-(3-nitrophenyl)propanoate (**NT23**)

3-(3-Nitrophenyl)propanoic acid was obtained by methylation of (*E*)-3-(3-nitrophenyl)acrylic acid (100 g, 0.52 mmol) under reflux for 2 hours with 20 mL of methanol and 2.4 mL of 36% concentrated HCl. The reduction reaction was carried out using 0.2 equiv CuCl, 1.2 equiv NaBH<sub>4</sub> and 10 mL of *i*-PrOH. The mixture was stirred at room temperature for 24 hours. 10 Equiv of *tert*-BuOK in 5 mL *tert*-BuOH was added to the mixture and the reaction was stirred at room temperature

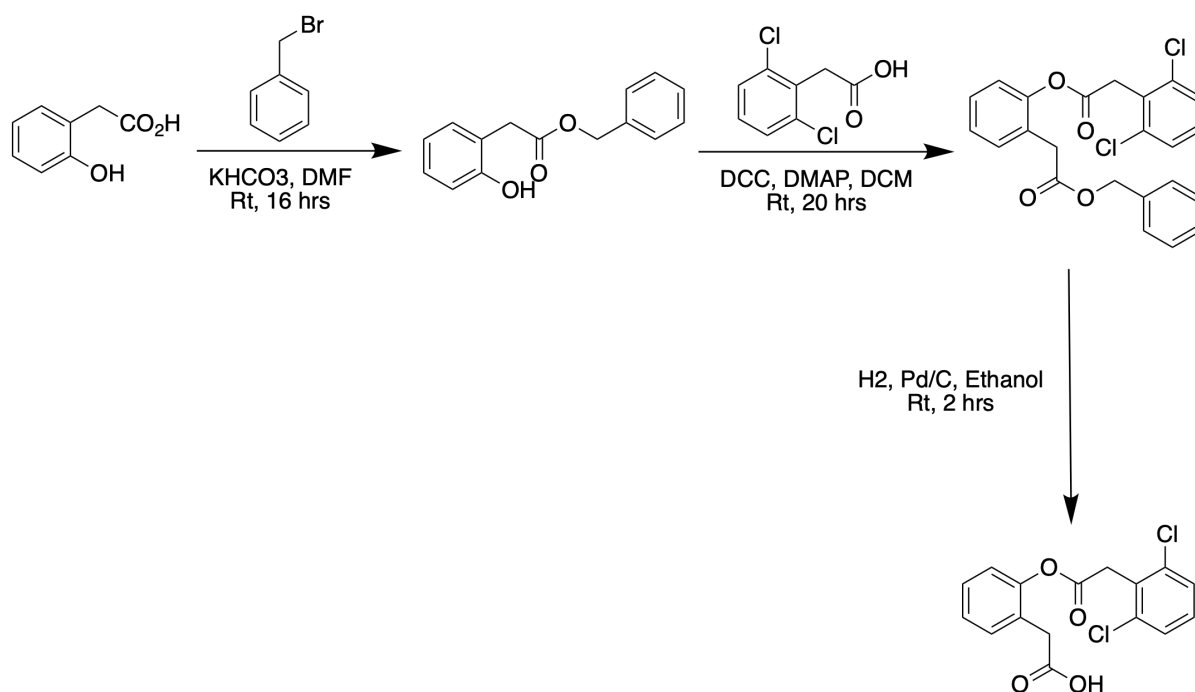
for another 4 hours. After obtaining 3-(3-nitrophenyl)propanoic acid, the esterification and purification was carried out according to the general procedure specified in 2.3.2 and 2.3.3, respectively.



**2-(2-methoxy-2-oxoethyl)phenyl 3-(3-nitrophenyl)propanoate (NT23)** (71.0% isolated yield)  $^1\text{H}$  NMR (500 MHz,  $\text{CDCl}_3$ ):  $\delta$  8.16 (s, 1H), 8.10 (d,  $J = 8.0$  Hz, 1H), 7.63 (d,  $J = 7.5$  Hz, 1H), 7.49 (t,  $J = 8.0$  Hz, 1H), 7.30 (d,  $J = 8.0$  Hz, 1H), 7.30 (t,  $J = 8.0$  Hz, 1H), 7.20 (t,  $J = 8.0$  Hz, 1H), 7.03 (d,  $J = 8.0$  Hz, 1H), 3.63 (s, 3H), 3.48 (s, 2H), 3.19 (t,  $J = 7.5$  Hz, 2H) and 2.97 (t,  $J = 7.5$  Hz, 2H) ppm.  $^{13}\text{C}$  NMR (125 MHz,  $\text{CDCl}_3$ ):  $\delta$  171.0, 170.6, 149.0, 143.8, 142.2, 135.0, 131.6, 129.7, 128.8, 126.6, 126.5, 123.4, 122.6, 121.8, 52.7, 36.4, 35.1 and 29.5 ppm.

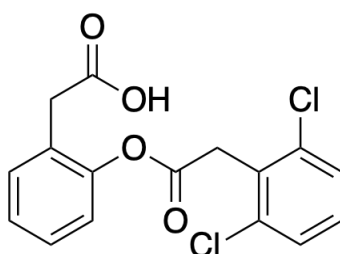
### 2.3.6 Synthesis and purification of 2-(2-(2-(2,6-dichlorophenyl)acetoxy)phenyl)acetic acid (NT24)

The synthesis of **NT24** was carried out according to the plan described in Scheme 2.3.



**Scheme 2.2** Synthesis pathway of 2-(2-(2-(2,6-dichlorophenyl)acetoxy)phenyl)acetic acid (**NT24**)

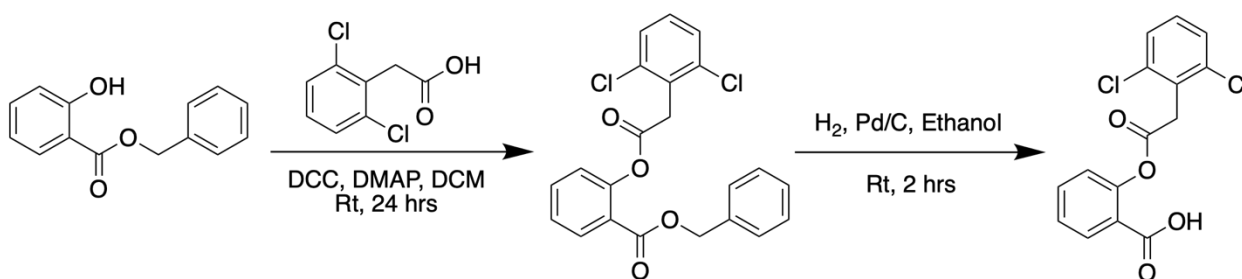
Firstly, 2-hydroxyphenylacetic acid (200 mg, 1.31 mmol) and  $\text{KHCO}_3$  (196.7 mg, 1.97 mmol) was dissolved in 4 mL of DMF. The reaction was stirred at room temperature for 15 minutes, then 246  $\mu\text{L}$  of benzyl bromide was added to the reaction and was stirred at room temperature for 16 hours. Secondly, after obtaining the protected product, the mixture was extracted with 10 mL of EtOAc and several times with 50 mL of water. Anhydrous  $\text{Na}_2\text{SO}_4$  was then added to the washed product before filtering with a filter paper. After obtaining the purified product, esterification was conducted as detailed in 2.3.2 but the reaction time was 20 hours. The esterified product (200 mg, 0.46 mmol) was deprotected by dissolving 2 mL EtOH along with 20 mg of Pd/C catalyst fitted with  $\text{H}_2$  balloon. The reaction was then stirred at room temperature for another 2 hours. However, in order to obtain a pure product, column chromatography was performed as stated in 2.3.3.



**2-(2-(2-(2,6-dichlorophenyl)acetoxy)phenyl)acetic acid (NT24)** (21.3% isolated yield)  $^1\text{H}$  NMR (500 MHz,  $\text{CDCl}_3$ ):  $\delta$  7.34-7.29 (m, 4H), 7.21-7.13 (m, 3H), 4.29 (s, 2H) and 3.58 (s, 2H) ppm.  $^{13}\text{C}$  NMR (125 MHz,  $\text{CDCl}_3$ ):  $\delta$  176.1, 167.7, 149.2, 136.3, 136.3, 131.5, 130.8, 129.4, 128.7, 128.3, 128.3, 126.3, 126.1, 122.5, 36.9 and 35.9 ppm.

### 2.3.7 Synthesis and purification of 2-(2-(2,6-dichlorophenyl)acetoxy)benzoic acid (NT25)

The synthesis of **NT25** was carried out according to the plan described in Scheme 2.3.

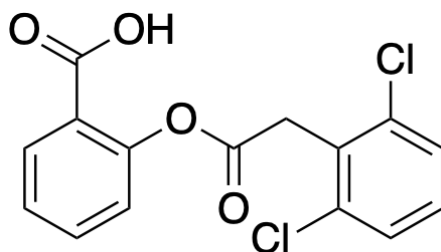


**Scheme 2.3** Synthesis pathway of 2-(2-(2,6-dichlorophenyl)acetoxy)benzoic acid (**NT25**)

Benzyl salicylate (500 mg, 2.190 mmol) and 2,6-dichlorophenylacetic acid (449 mg, 2.190 mmol) were used as the starting materials. Esterification reaction was carried out as mentioned in the general synthesis procedure with the same amount of DCC and DMAP, but 8 mL DCM was added



to dissolve the mixture and the reaction was stirred at room temperature for 24 hours. After the product was formed, the deprotection was conducted under H<sub>2</sub> in 4.5 mL EtOH and 50 mg of Pd/C catalyst. The reaction was stirred at room temperature for 2 hours. In order to obtain a pure product, a purification method was performed as stated in 2.3.4.



**2-(2-(2,6-dichlorophenyl)acetoxy)benzoic acid (NT25)** (11.0% isolated yield) <sup>1</sup>H NMR (500 MHz, Acetone-d<sub>6</sub>): δ 8.20 (dd, J<sub>1</sub> = 8.0, J<sub>2</sub> = 7.5 Hz, 1H), 7.66 (td, J<sub>1</sub> = 7.5 Hz, J<sub>2</sub> = 2.0, 1H), 7.47 (d, J = 8.0 Hz, 1H), 7.47 (d, J = 8.0 Hz, 1H), 7.41 (t, J = 7.5 Hz, 1H), 7.36 (d, J = 7.5 Hz, 1H) and 7.21 (d, J = 8.0 Hz, 1H) ppm. <sup>13</sup>C NMR (125 MHz, Acetone-d<sub>6</sub>): δ 168.5, 165.7, 151.5, 136.8, 136.8, 134.6, 131.8, 130.5, 130.5, 128.9, 128.9, 126.9, 124.6 and 124.6 ppm.

### 2.3.8 Biological activity tests of synthesized compounds

#### 2.3.8.1 Anti α-glucosidase activity

α-Glucosidase inhibition assay of each synthesized compounds was performed with yeast glucosidase and the assay was conducted on a 96-well plate. A buffer was prepared by mixing hydrogen phosphate heptahydrate (3.576 g, 0.0534 M) and sodium dihydrogen phosphate monohydrate (1.609 g, 0.0466 M with 200 mL of distilled water). The pH of the buffer was measured and monitored using a pH meter with the addition of dropwise NaOH and/or HCl. Each sample compound (4 mM) was made ready by dissolving the compound with 500 μL DMSO and 500 μL of buffer. Different aliquots (200, 100, 50, 25, 12.5 mM) contained 10 μL of buffer and 10 μL of synthesized sample were tested along with a reference compound, acarbose. 40 μL of enzymatic solution was then added and the incubation were performed at 37 °C for 10 minutes. The reaction started when 50 μL of 4-nitrophenyl α-D-glucopyranoside (substrate) was mixed into each well and incubated at 37 °C for 20 minutes. To stop the reaction, Na<sub>2</sub>CO<sub>3</sub> solution was added into the wells. Lastly, the absorbance value and inhibition activity were measured using a microplate reader at a wavelength of 405 nm. The % inhibition and IC<sub>50</sub> value was calculated from the obtained data.

The % inhibition was calculated by the following equation:

$$\text{Abs}_{\text{Mixture}} - \text{Abs}_{\text{Blank sample}} = A$$

$$\% \text{ Inhibition} = [(A - B) / B] \times 100$$

Where  $\text{Abs}_{\text{Mixture}}$  is the absorbance value of the reaction mixture containing sample and of  $\text{Abs}_{\text{Blank sample}}$  is the absorbance value of the reaction mixture without the enzyme and substrate. The calculated A value was then used to find the % inhibition and B is the average value of the negative control (without sample). The % inhibition was reported as the average value for each concentration.

The half maximal inhibitory concentration ( $\text{IC}_{50}$ ) value was calculated by the following equation:

$$\text{IC}_{50} = (50 - M) / C$$

Where M is the slope and C is the y-intercept obtained from the plot of average % inhibition at each concentration.

### 2.3.8.2 Antioxidant activity

DPPH assay was conducted in a 96-well plate with 3 mM in 1 mL MeOH solution of synthesized sample. The DPPH was prepared from 0.5 mg of 1,1-diphenyl-2-picrylhydrazyl in 10 mL MeOH. The test was performed among six different concentrations (1.0, 0.5, 0.25, 0.125, 0.0625, 0.03125 mM) along with ascorbic acid (standard control). For each concentration, 50  $\mu\text{L}$  sample and 100  $\mu\text{L}$  of 0.05 mM DPPH were mixed and incubated for 30 minutes in the dark at room temperature. The absorbance of radical scavenging activity was measured using a microplate reader at 520 nm. The percent DPPH scavenging effect inhibition was calculated using the formula below:

$$\text{DPPH scavenging effect (\%)} = [(A_0 - A_1) \div A_0] \times 100$$

Where  $A_0$  is the absorbance value of the control and  $A_1$  is the absorbance of the sample.

## CHAPTER 3

### RESULTS AND DISCUSSION

#### 3.1 Structural modification

A research on Jaboticabin showed that this compound exhibited several biological properties. Modification of Jaboticabin-based structure resulted in various desired depsides (Figure 1.3), which were subsequently subjected to biological evaluation to investigate their anti- $\alpha$ -glucosidase and antioxidant properties. This includes introduction of different substituent patterns along with varying the carbon linkage between the aromatic rings. In order to notice the influence of structures on the activity, first few synthesized compounds underwent anti- $\alpha$ -glucosidase and antioxidant assays. Moreover, further modification was taken place for structures that showed highest potential as inhibitors.

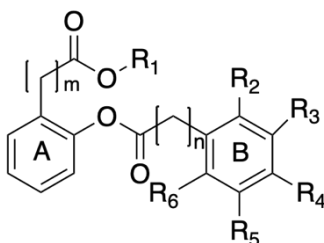


**Figure 3.1** Synthesized depside based structure

The key step of the synthesis was carried out through the esterification reaction between the hydroxy group of the A ring and carboxylic acid group of the B ring. This reaction generated the desired depsides with structure based on Jaboticabin. The reaction involved DCC and DMAP as the catalysts required to activate the carboxylic group and DCM as a solvent at 0 °C for 24 hours. The filtration was then done to remove unwanted urea along with extraction and purification with ethyl acetate, HCl, NaOH and silica gel. The modification of the R group lead to 25 synthesized compounds with % yield ranging from 11 to 85.2% and the selected R group was chosen based on a report stating that nitro, chlorine and some methoxy substituents exhibit antibacterial properties. However, as the result did not come back in time, the synthesized compounds were tested for its anti  $\alpha$ -glucosidase activity and antioxidant properties due to the availability of the machine and limited reports were conducted on these activities.

#### 3.2 Tentative $^1\text{H}$ and $^{13}\text{C}$ -NMR spectroscopic data of synthesized depsides

After synthesis, it is necessary to confirm the identity and purity of synthesized compounds with  $^1\text{H}$  and  $^{13}\text{C}$ -NMR technique before performing biological assays. As shown below are the  $^1\text{H}$

and  $^{13}\text{C}$ -NMR spectrum of NT0 in DMSO. The hydroxyl group exhibit the most downfield chemical shift which is 9.45 ppm as well as appearing as a clear singlet due to no neighboring hydrogens. The second most downfield chemical shift appears as a multiplet which belongs to hydrogen at position 3 and 5 which are meta to the hydroxyl group. Hydrogen at position 4 and 6 which are para to the hydroxyl group (electron donating group), with position 4 containing 2 neighboring hydrogen and position 6 containing 1 neighboring hydrogen which resulted in a triplet and a doublet splitting pattern.

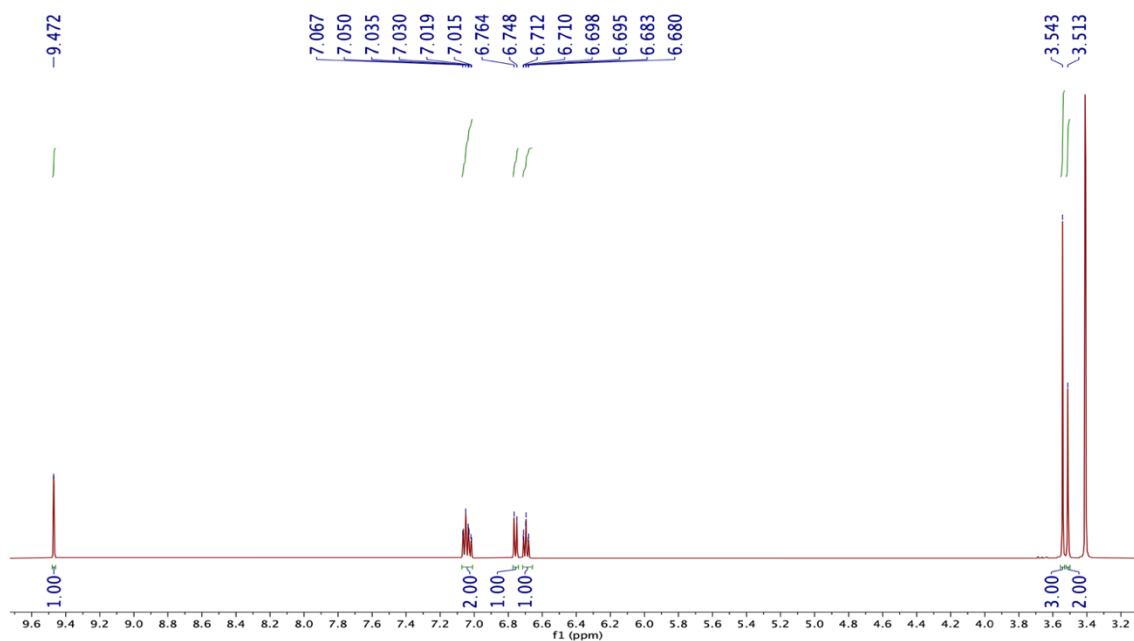


**Figure 3.2** The  $^1\text{H}$  NMR spectrum of NT0

The  $^{13}\text{C}$ -NMR spectrum were also analyzed according to the electron-withdrawing ability of atoms connected to carbon. It can be seen that carbon atom at position number 8 (171.9 ppm) is directly double-bonded to an oxygen atom which is the most electron-withdrawing when compared to other bonds in the structure. The second most downfield carbon is the carbon atom at position 1 that is attached to a hydroxyl group which is also a strong electron withdrawing group. Moreover, carbon position 3 and 5 exhibit similar chemical shift which was 128.2 and 131.1 ppm and carbon position 2, 4 and 6 which exhibited the most upfield chemical shift as of carbons that belongs to the aromatic ring with chemical shifts of 118.9, 121.3 and 114.9 ppm. With the last two remaining carbons which are carbon position 7 and 9, appearing at the upfield chemical shift of 35.2 and 51.2 as it is singled-bonded to carbon 8 and 2 and also directly attached to oxygen which is an electron-withdrawing atom.

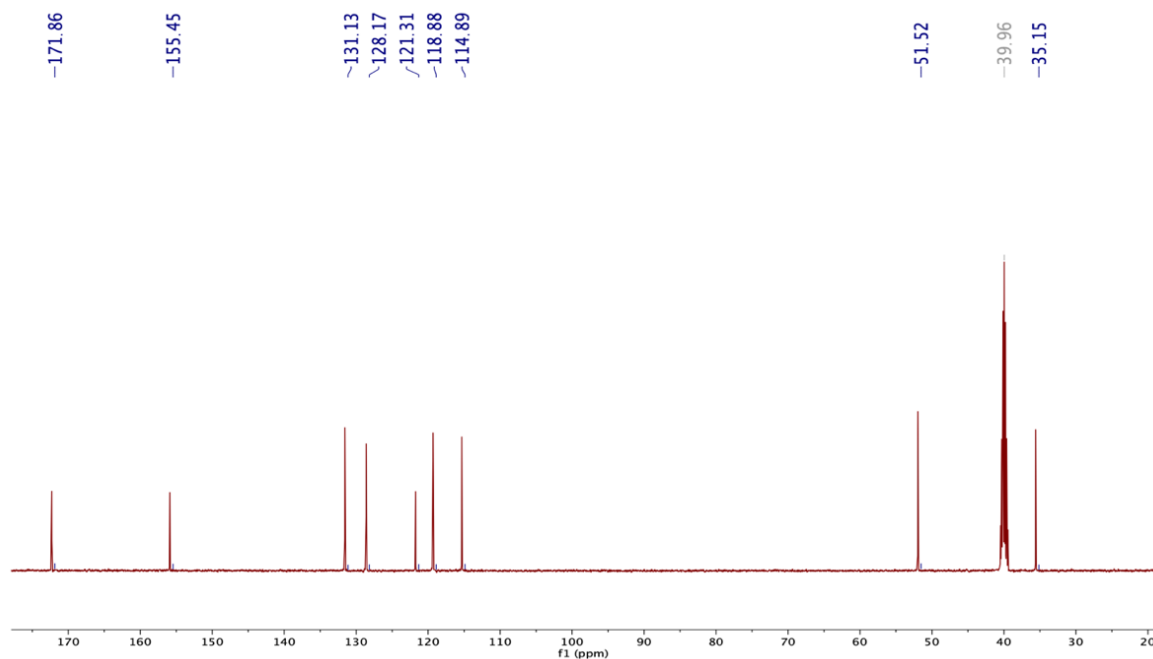


**Figure 3.3** The  $^{13}\text{C}$  NMR spectrum of NT0

**Table 3.1** The  $^1\text{H}$  and  $^{13}\text{C}$  NMR spectral assignment of NT0 in  $\text{CDCl}_3$  and reference compound in  $\text{DMSO-d}_6$

NT0		Methyl 2-(2-hydroxyphenyl) acetate (Lv et al, 1995)		
Position	Chemical shift (ppm)		Chemical shift (ppm)	
	$^{13}\text{C}$	$^1\text{H}$	$^{13}\text{C}$	$^1\text{H}$
1	155.5	-	155.4	-
6	114.9	6.76 (d, $J = 8.0$ Hz, 1H)	115	6.78 (m, 2H)
4	121.3	6.70 (t, $J = 7.0$ Hz, 1H)	121.4	
3	128.2	7.06-7.02 (m, 2H)	128.2	7.06 (m, 2H)
5	131.1		131.2	
7	35.2	3.51 (s, 2H)	35.2	3.54 (s, 2H)
9	51.2	3.54 (s, 3H)	51.6	3.58 (s, 3H)

2	118.9	-	118.9	-
8	171.9	-	171.9	-
OH		9.45 (s, 1H)		9.47 (s, 1H)

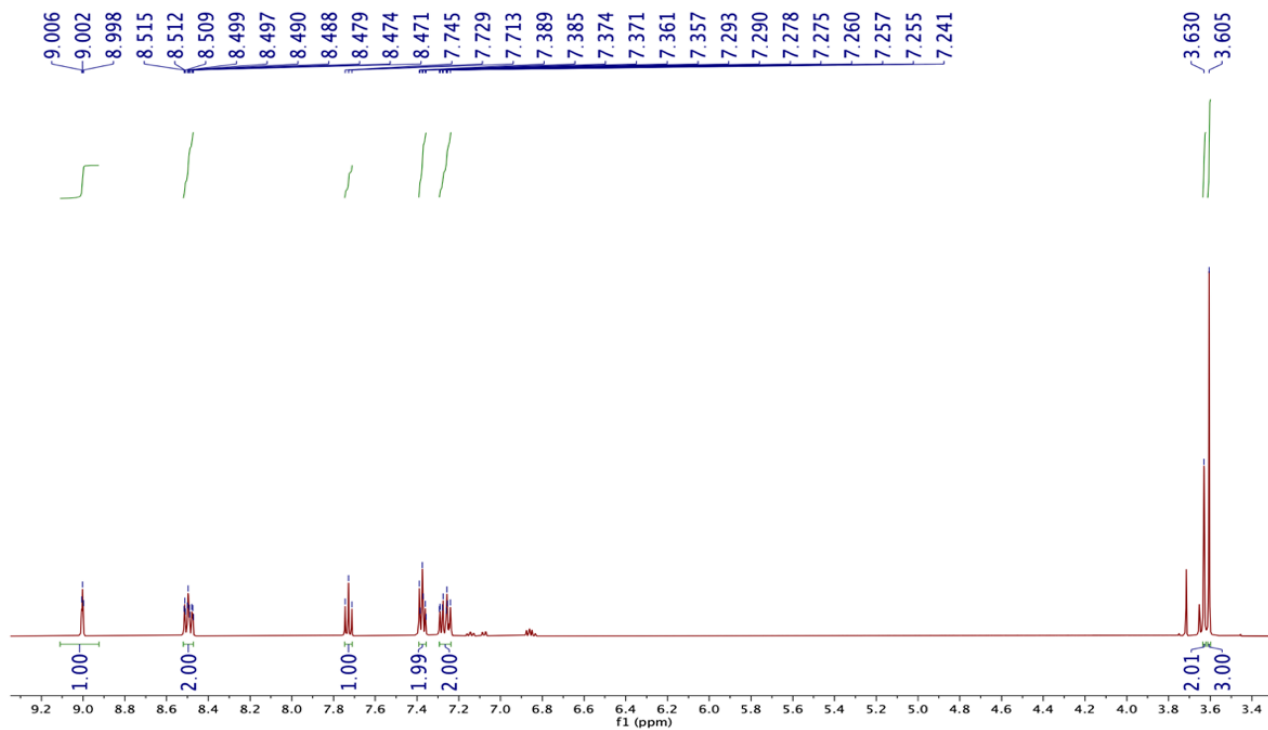


Figure 3.4 The <sup>1</sup>H NMR spectrum of NT1

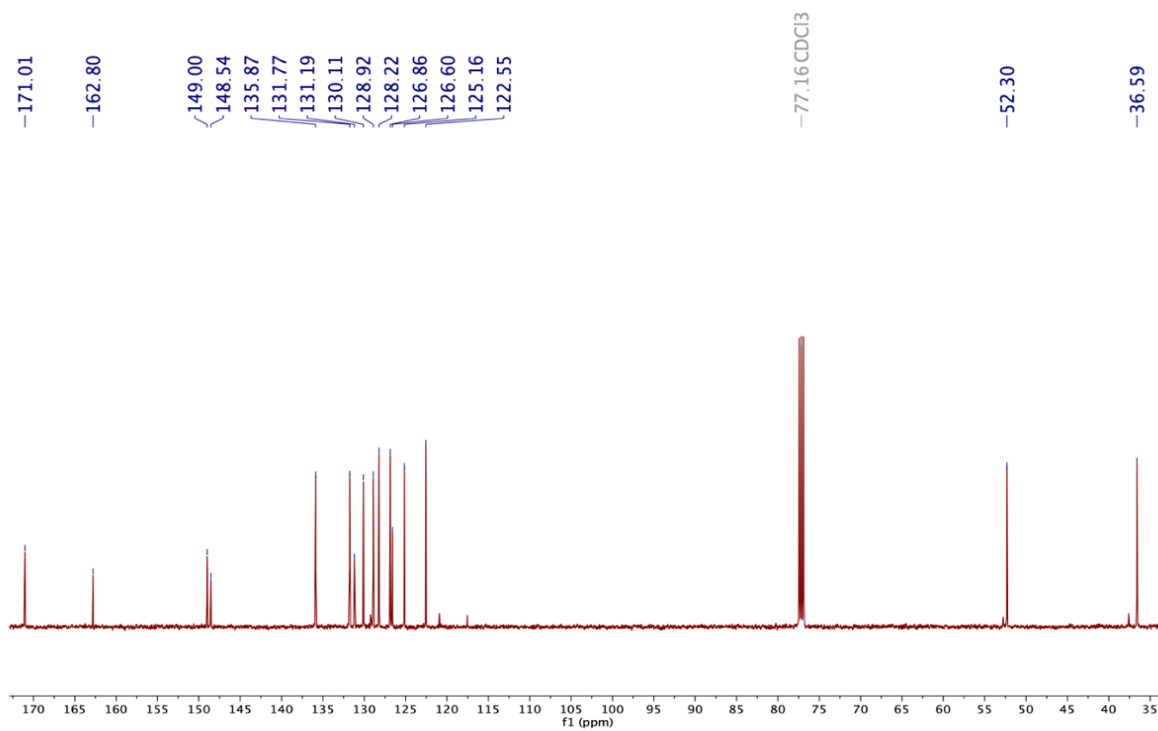
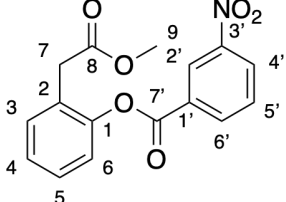
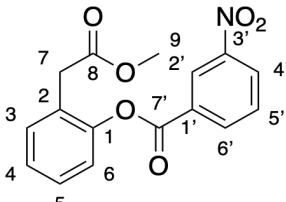


Figure 3.5 The <sup>13</sup>C NMR spectrum of NT1

**Table 3.2** The  $^1\text{H}$  and  $^{13}\text{C}$  NMR spectral assignment of **NT1** and reference compound in  $\text{DMSO-d}_6$ 

NT1		2-(2-methoxy-2-oxoethyl)phenyl 3-nitrobenzoate (Lv <i>et al</i> , 1995)		
				
Position	Chemical shift (ppm)		Chemical shift (ppm)	
	$^{13}\text{C}$	$^1\text{H}$	$^{13}\text{C}$	$^1\text{H}$
1	149.0	-	148.9	-
2	126.6	-	126.6	-
3	128.9	7.37 (d, $J = 7.0$ Hz, 1H)	127.1	7.43 (m, 3H)
5	131.8	7.37 (t, $J = 7.0$ Hz, 1H)	131.9	
4	126.9	7.29-7.24 (m, 2H)	126.6	
6	122.6		122.7	7.31 (m, 1H)
7	36.6	3.63 (s, 2H)	35.2	3.73 (s, 2H)
8	171.0	-	170.8	-
9	52.3	3.61 (s, 3H)	51.7	3.52 (s, 3H)
1'	131.2	-	131.1	-
2'	125.2	9.00 (s, 1H)	124.2	8.76 (m, 1H)
3'	148.5	-	148.2	-
4'	130.1	8.52-8.47 (m, 2H)	130.6	8.51 (m, 1H)
6'	135.9		135.7	8.58 (m, 1H)
5'	128.2	7.73 (t, $J = 8.0$ Hz, 1H)	126.6	7.94 (t, $J = 8.62$ Hz, 1H)
7'	162.8	-	162.4	-

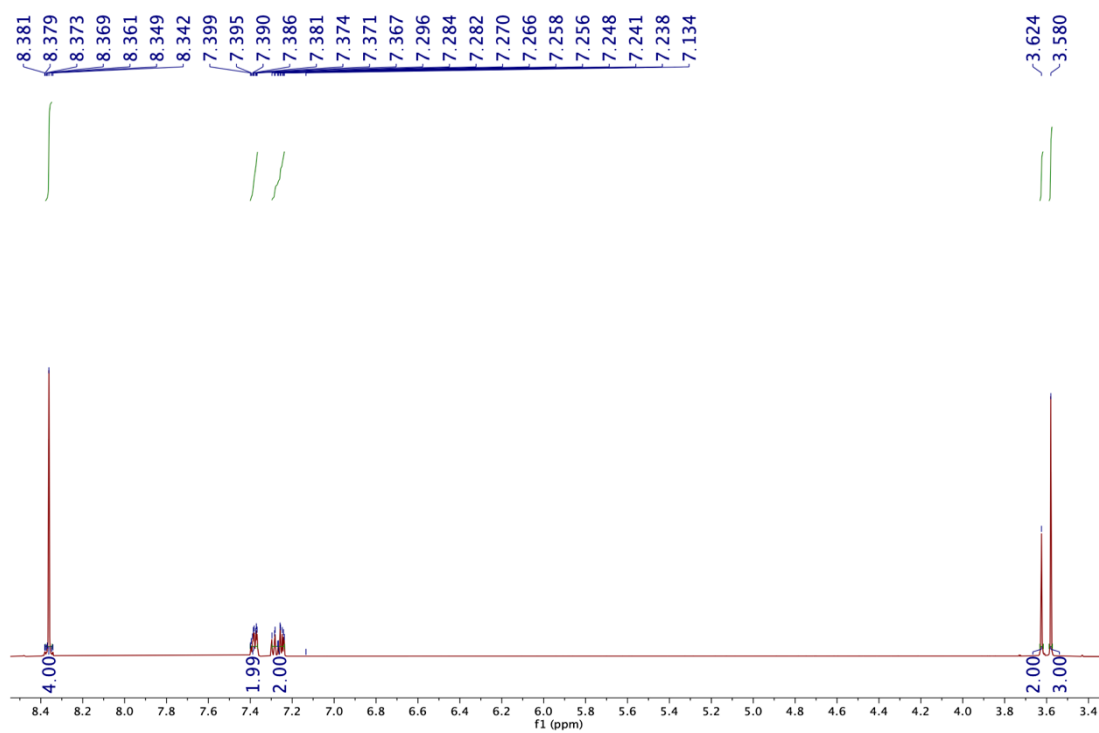


Figure 3.6 The <sup>1</sup>H NMR spectrum of NT2

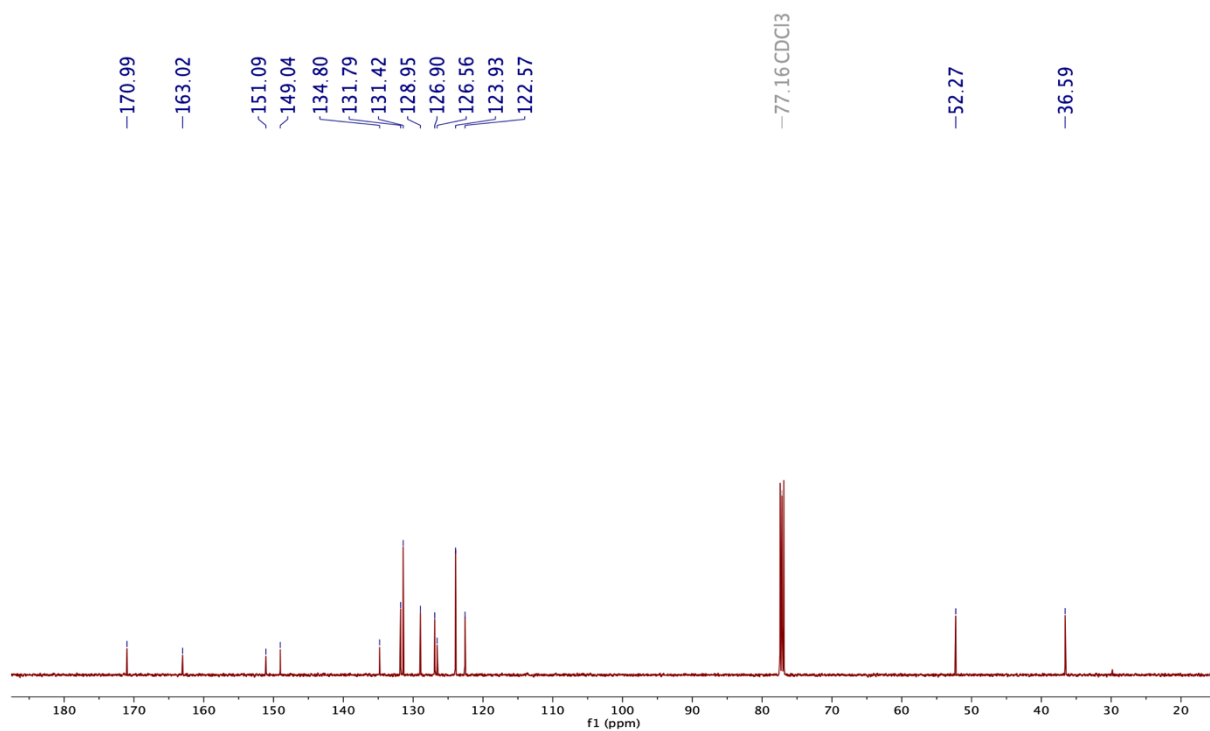


Figure 3.7 The <sup>13</sup>C NMR spectrum of NT2



**Table 3.3** The  $^1\text{H}$  and  $^{13}\text{C}$  NMR spectral assignment of **NT2**

<b>NT2</b>		
Position	Chemical shift (ppm)	
	$^{13}\text{C}$	$^1\text{H}$
1	149.0	-
2	126.6	-
3	129.0	7.40-7.37 (m, 2H)
5	131.8	
4	126.9	7.26 (t, $J = 7.0$ Hz, 1H)
6	122.6	7.26 (d, $J = 9.0$ Hz, 1H)
7	37.0	3.62 (s, 2H)
8	171.0	-
9	52.3	3.58 (s, 3H)
1'	134.8	-
2'	131.4	8.38-8.34 (m, 4H)
3'	123.9	
5'	123.9	
6'	131.4	
4'	151.1	-
7'	163.0	-

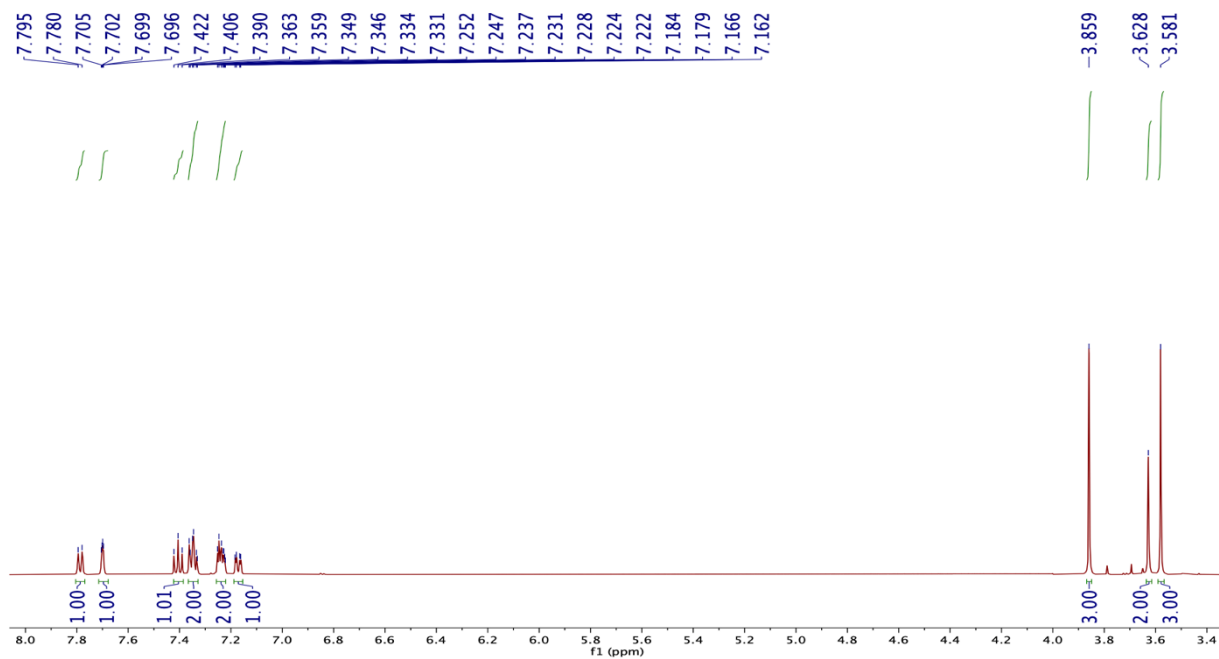


Figure 3.8 The  $^1\text{H}$  NMR spectrum of NT3

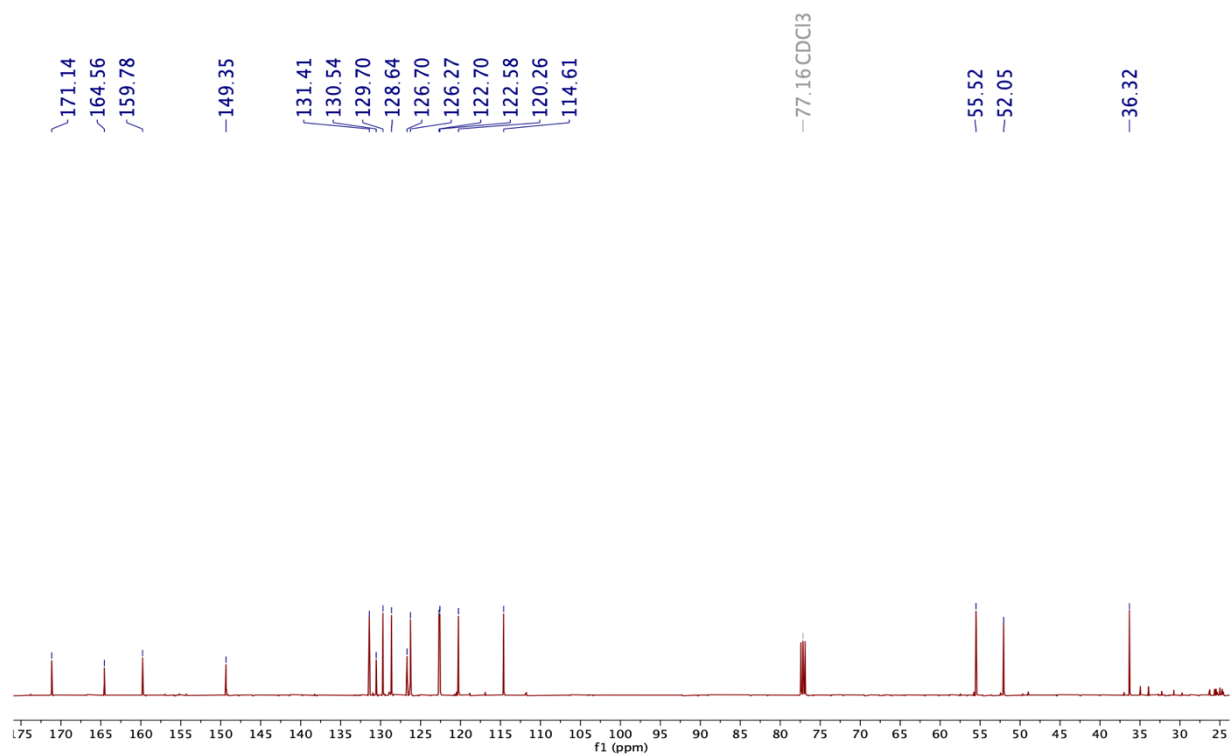
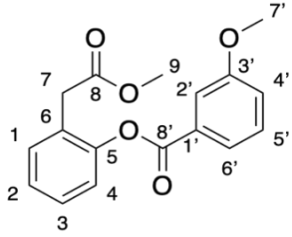
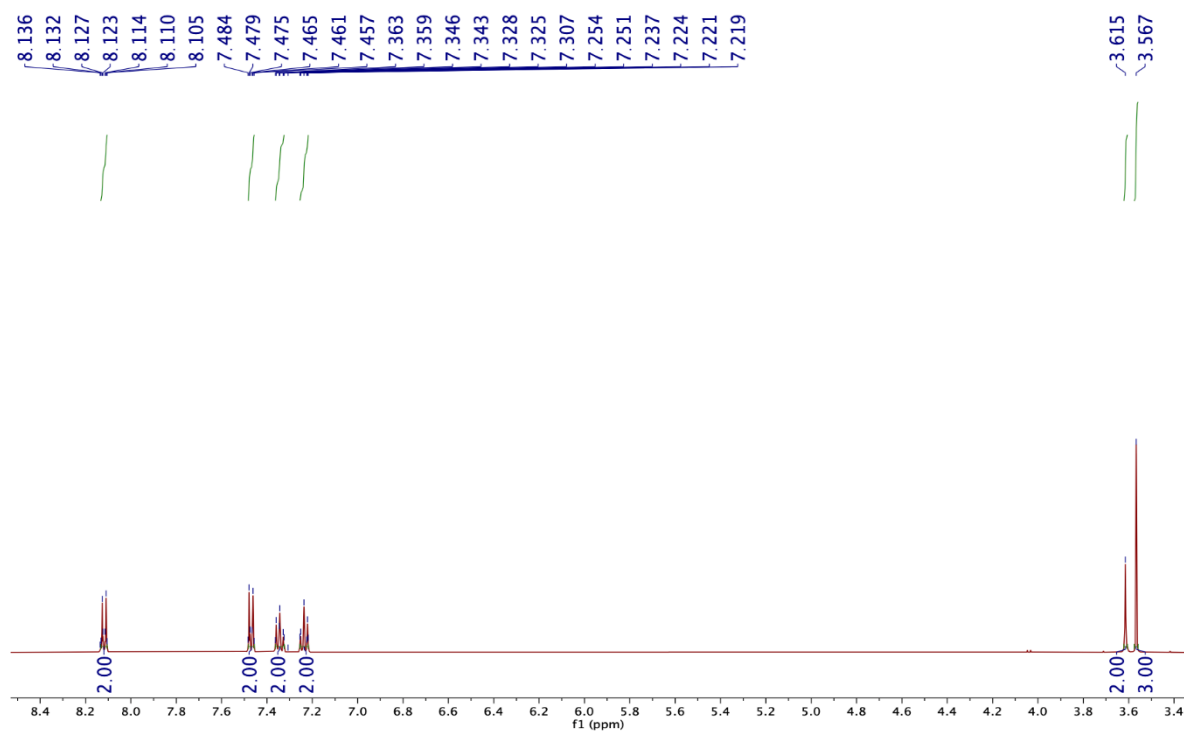


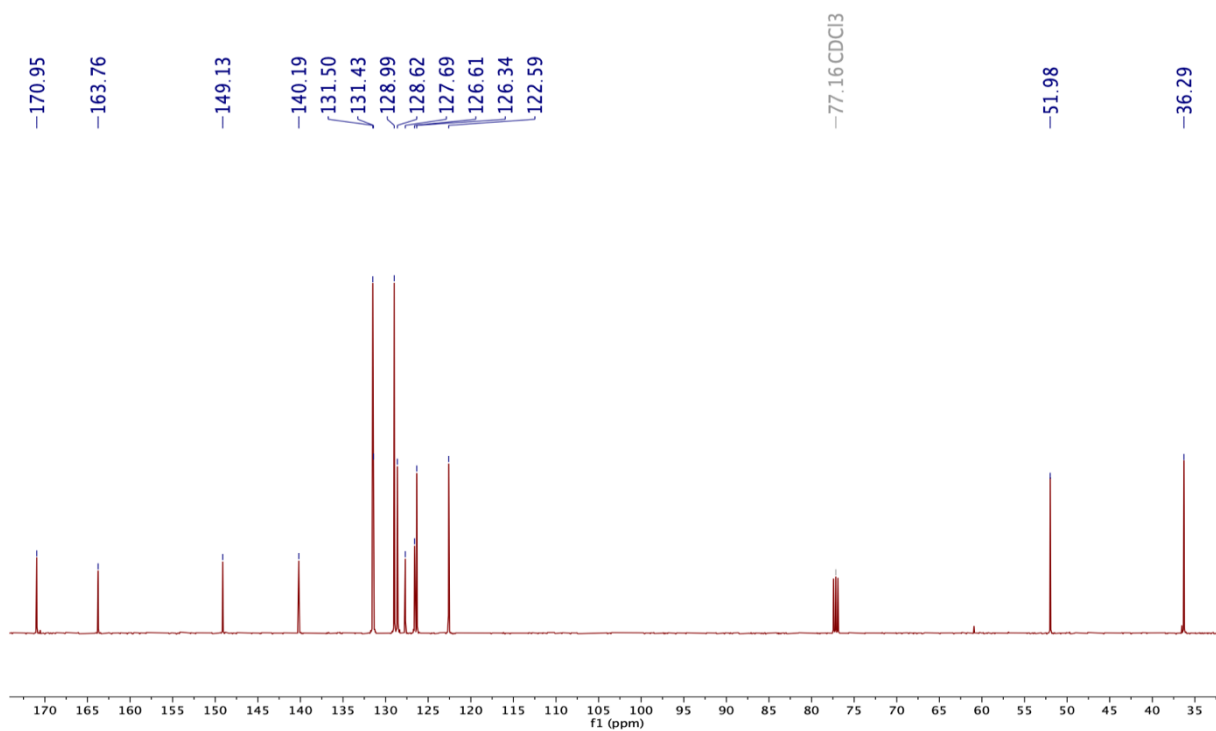
Figure 3.9 The  $^{13}\text{C}$  NMR spectrum of NT3

**Table 3.4** The  $^1\text{H}$  and  $^{13}\text{C}$  NMR spectral assignment of **NT3** in  $\text{CDCl}_3$ 

<b>NT3</b>		
		
Position	Chemical shift (ppm)	
	$^{13}\text{C}$	$^1\text{H}$
1	149.0	-
2	126.3	-
3	128.6	7.35 (d, $J = 7.0$ Hz, 1H)
5	131.4	7.35 (t, $J = 7.0$ Hz, 1H)
4	126.7	7.25-7.22 (m, 2H)
6	122.7	
7	36.3	3.63 (s, 2H)
8	171.1	-
9	52.1	3.58 (s, 3H)
1'	130.5	-
2'	114.6	7.70 (s, 1H)
3'	159.8	-
4'	120.3	7.17 (dd, $J = 8.0, 2.5$ Hz, 1H)
5'	129.7	7.40 (t, $J = 8.0$ Hz, 1H)
6'	122.6	7.80 (d, $J = 7.5$ Hz, 1H)
7'	164.6	-
8'	55.5	3.86 (s, 3H)

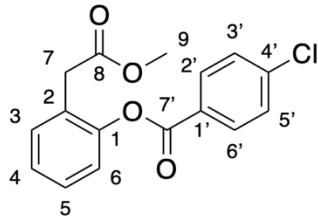
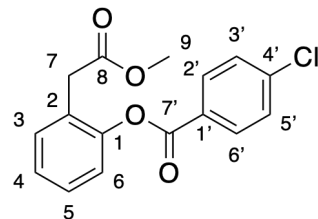


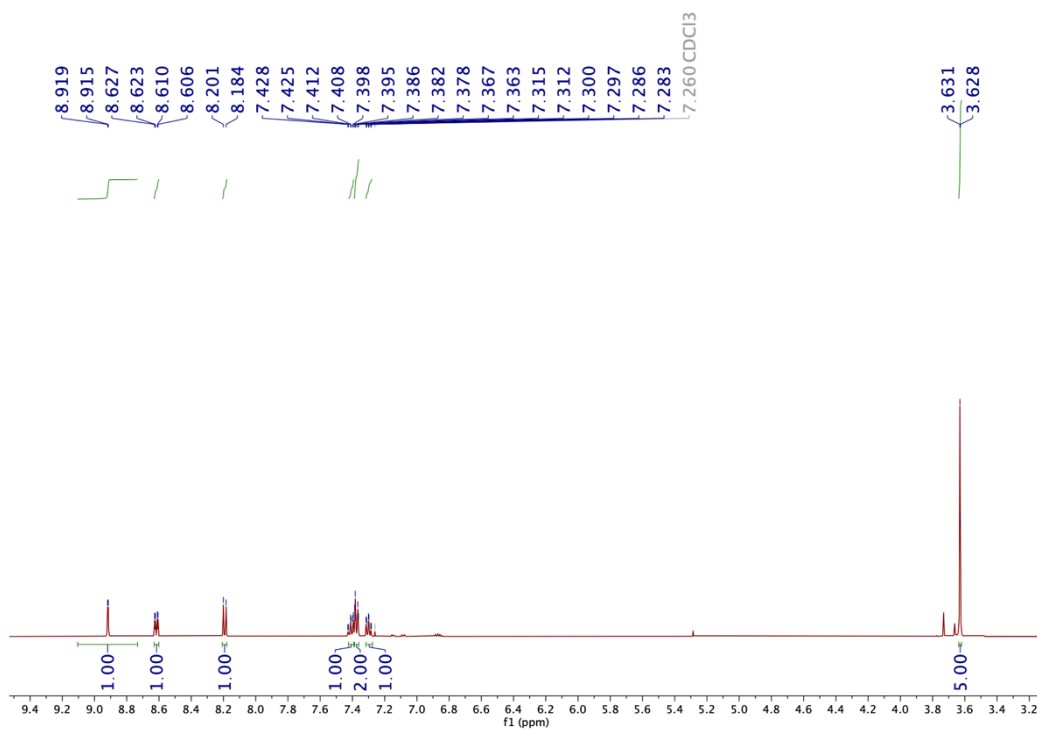
**Figure 3.10** The  $^1\text{H}$  NMR spectrum of NT4



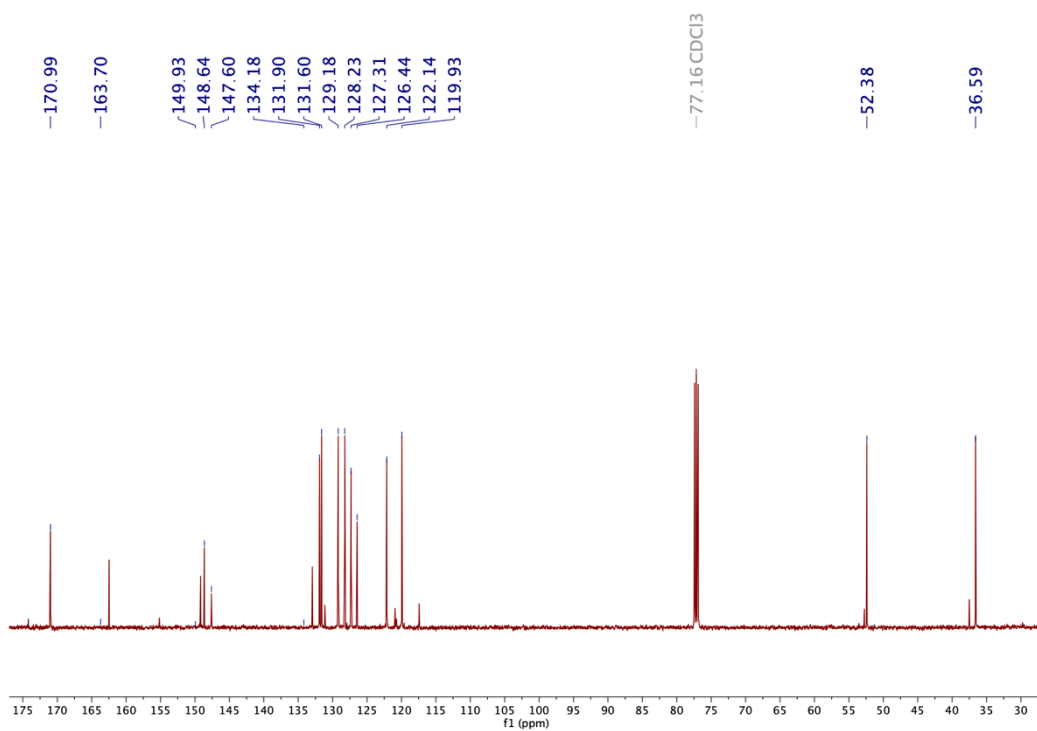
**Figure 3.11** The  $^{13}\text{C}$  NMR spectrum of NT4

**Table 3.5** The  $^1\text{H}$  and  $^{13}\text{C}$  NMR spectral assignment of NT4 and reference compound in DMSO- $d_6$ 

NT4		2-(2-methoxy-2-oxoethyl)phenyl 4-chlorobenzoate (Lv <i>et al</i> , 1995)		
				
Position	Chemical shift (ppm)		Chemical shift (ppm)	
	$^{13}\text{C}$	$^1\text{H}$	$^{13}\text{C}$	$^1\text{H}$
1	149.1	-	149.1	-
2	126.6	-	127.2	-
3	127.7	7.35 (d, $J = 8.0$ , 1H)	127.8	7.30 (m, 4H)
5	128.6	7.35 (t, $J = 8.5$ , 1H)	128.1	
4	126.3	7.24 (d, $J = 8.0$ , 1H)	126.4	
6	122.6	7.24 (t, $J = 8.5$ , 1H)	122.8	
7	36.3	3.62 (s, 2H)	35.9	3.69 (s, 2H)
8	171.0	-	170.8	-
9	53.0	3.57 (s, 3H)	51.8	3.47 (s, 3H)
1'	131.4	-	129.3	-
2'	131.5	8.12 (d, $J = 9.0$ Hz, 2H)	131.7	8.10 (d, $J = 8.4$ Hz, 2H)
6'	131.5		131.8	
3'	129.0	7.47 (d, $J = 9.0$ Hz, 2H)	129.1	7.41 (m, 2H)
5'	129.0		128.6	
4'	140.2	-	139.3	-
7'	163.8	-	163.3	-

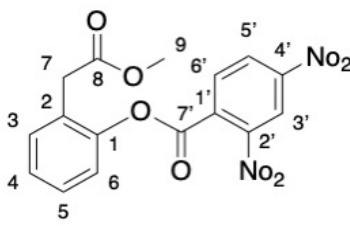


**Figure 3.12** The <sup>1</sup>H NMR spectrum of NT5



**Figure 3.13** The <sup>13</sup>C NMR spectrum of NT5

**Table 3.6** The  $^1\text{H}$  and  $^{13}\text{C}$  NMR spectral assignment of **NT5**

<b>NT5</b>		
		
Position	Chemical shift (ppm)	
	$^{13}\text{C}$	$^1\text{H}$
1	149.2	-
2	126.4	-
3	128.2	7.37 (d, $J = 7.0$ Hz, 2H)
6	122.1	
4	127.3	7.30 (t, $J = 7.5$ Hz, 1H)
5	131.6	7.41 (t, $J = 7.0$ Hz, 1H)
7	36.6	-
9	52.4	-
8	171.0	-
1'	132.9	-
2'	147.6	-
3'	119.9	8.92 (s, 1H)
4'	148.6	-
5'	129.2	8.62 (dd, $J = 8.5, 2.0$ Hz, 1H)
6'	131.9	8.19 (d, $J = 8.5$ Hz, 1H)
7'	163.7	-

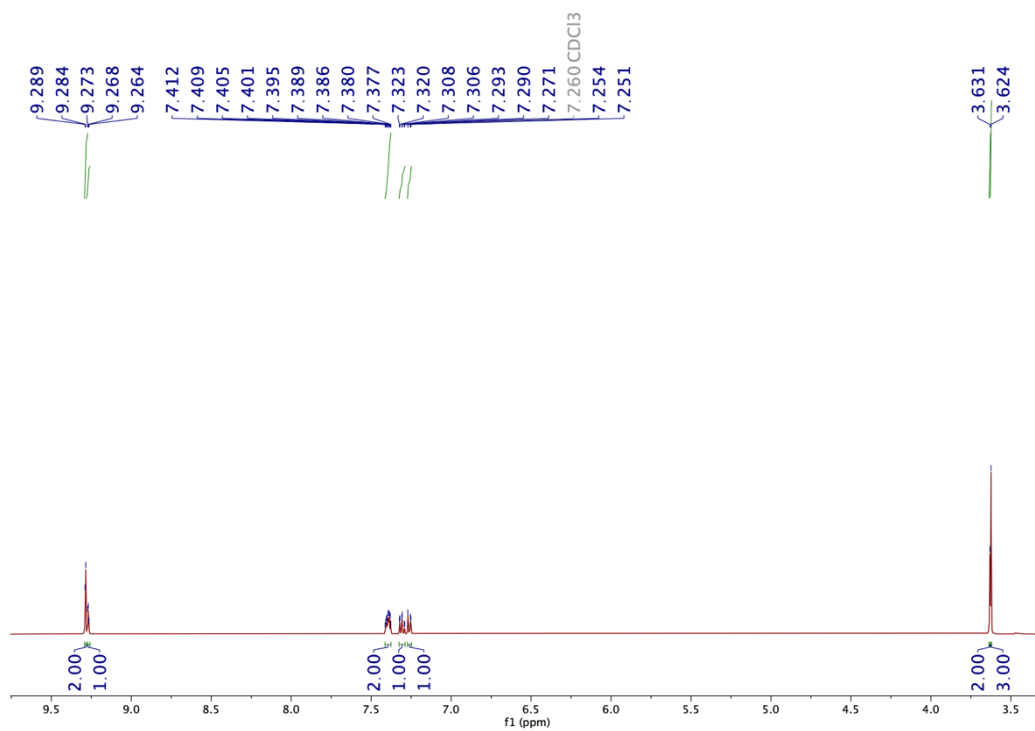


**Figure 3.14** The <sup>1</sup>H NMR spectrum of NT6

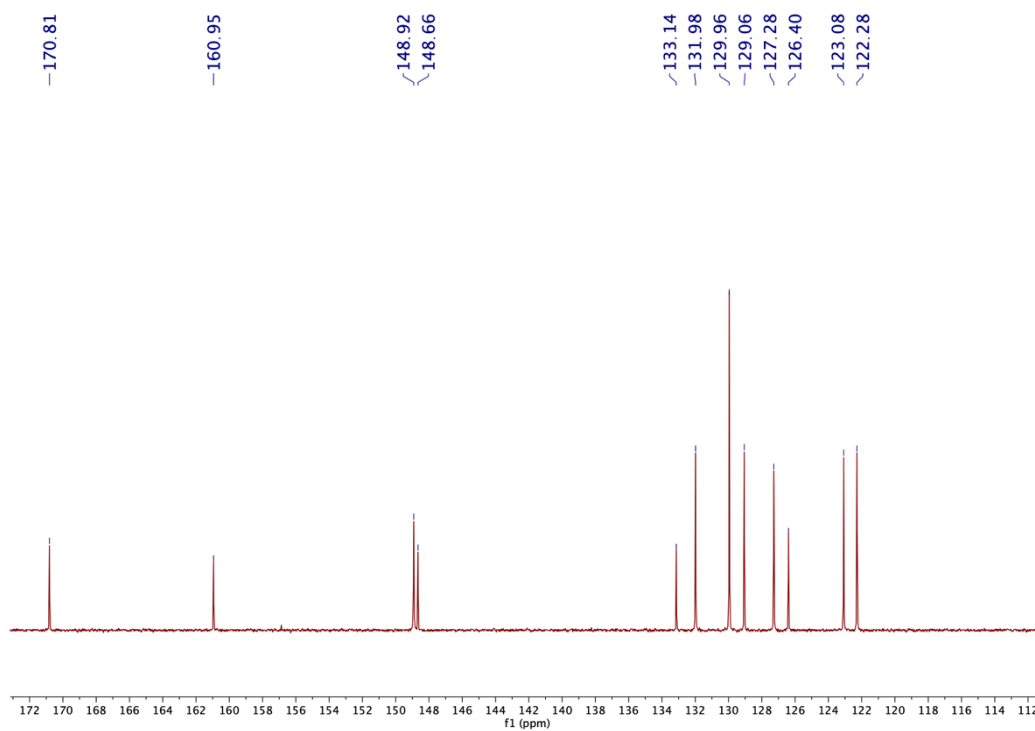
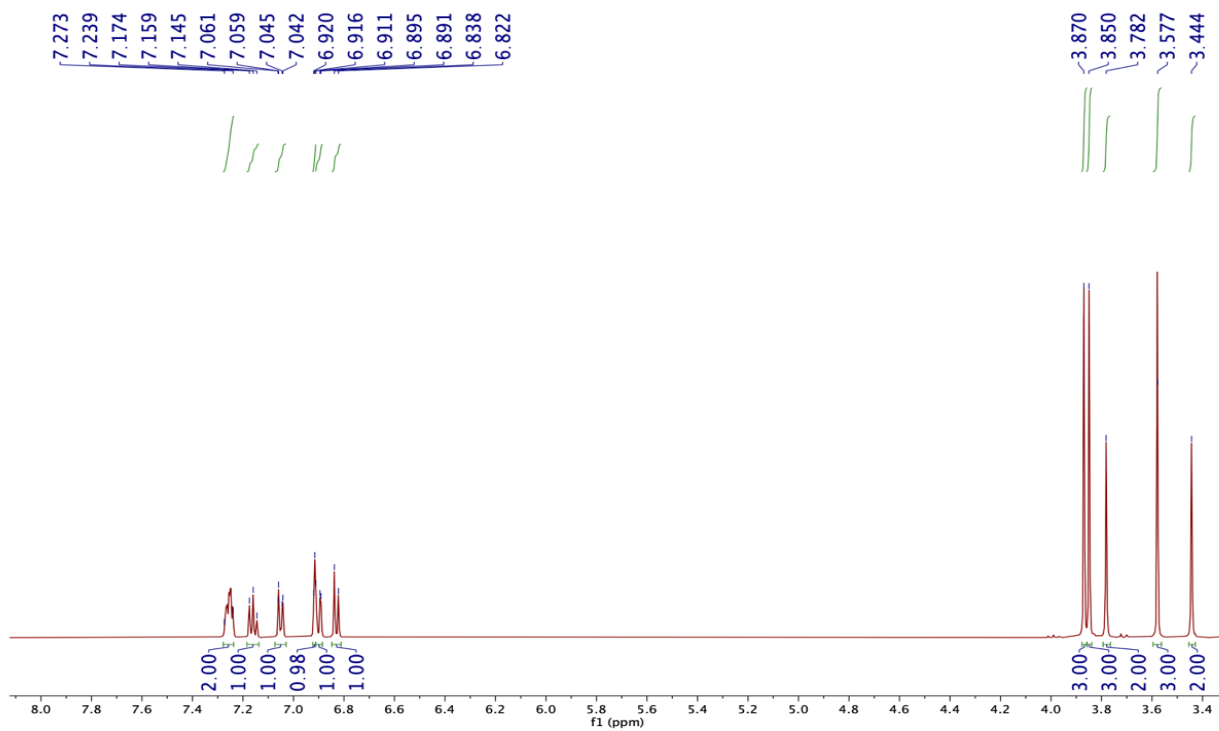


**Figure 3.15** The <sup>13</sup>C NMR spectrum of NT6

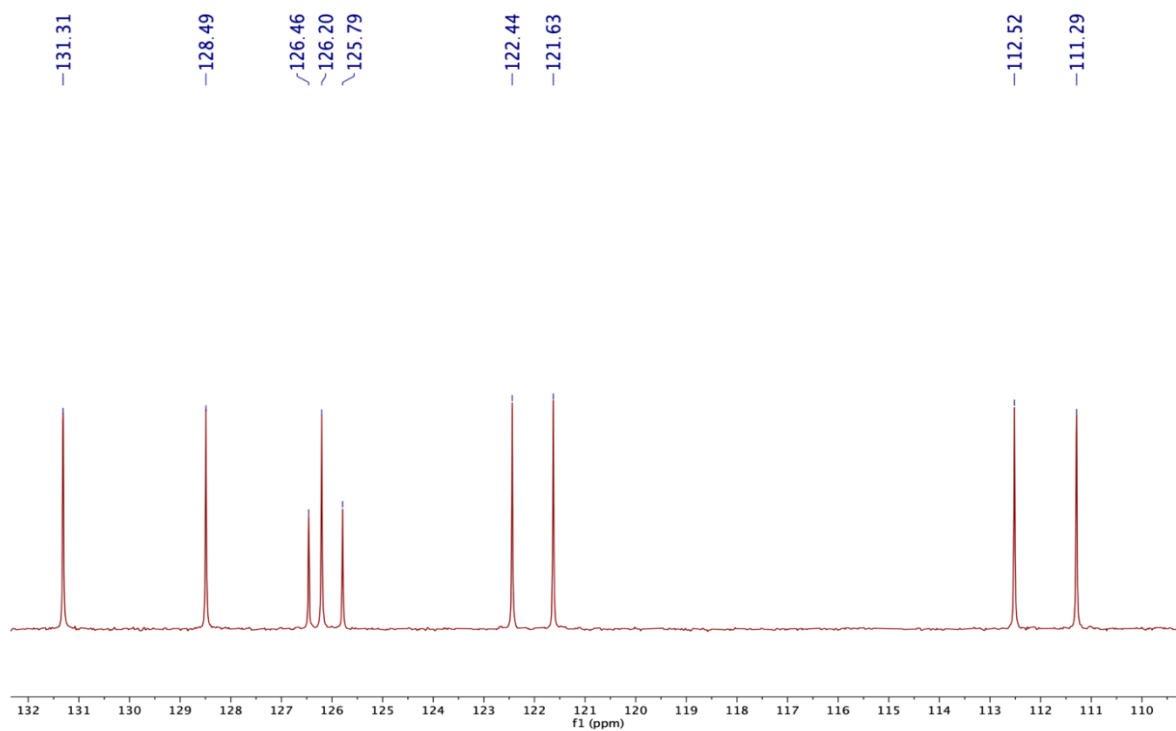


**Table 3.7** The  $^1\text{H}$  and  $^{13}\text{C}$  NMR spectral assignment of NT6

<b>NT6</b>		
Position	Chemical shift (ppm)	
	$^{13}\text{C}$	$^1\text{H}$
1	148.7	-
2	126.4	-
3	127.3	7.41-7.38 (m, 2H)
5	129.1	
4	123.1	7.31 (t, $J = 8.5$ Hz, 1H)
6	122.3	7.26 (d, $J = 8.5$ Hz, 1H)
7	36.8	3.63 (s, 2H)
8	170.8	-
9	52.4	3.62 (s, 3H)
1'	133.1	-
2'	132.0	9.29 (d, $J = 2.5$ Hz, 1H)
6'	132.0	
4'	130.0	9.27 (t, $J = 2.5$ Hz, 1H)
3'	148.9	-
5'	148.9	-
7'	161.0	-

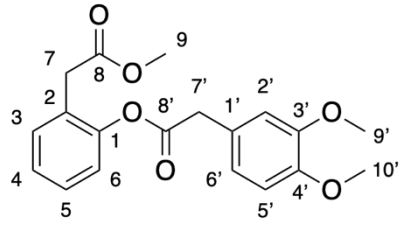
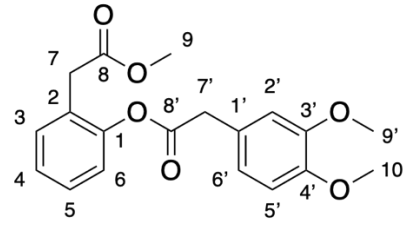


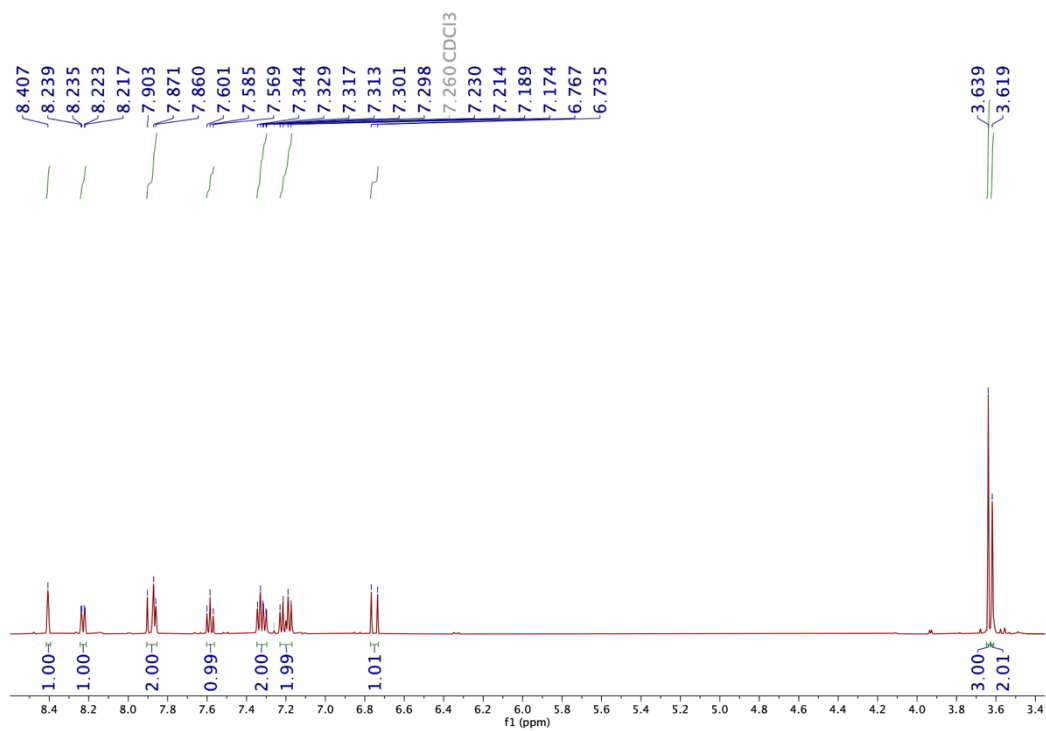
**Figure 3.16** The  $^1\text{H}$  NMR spectrum of NT7



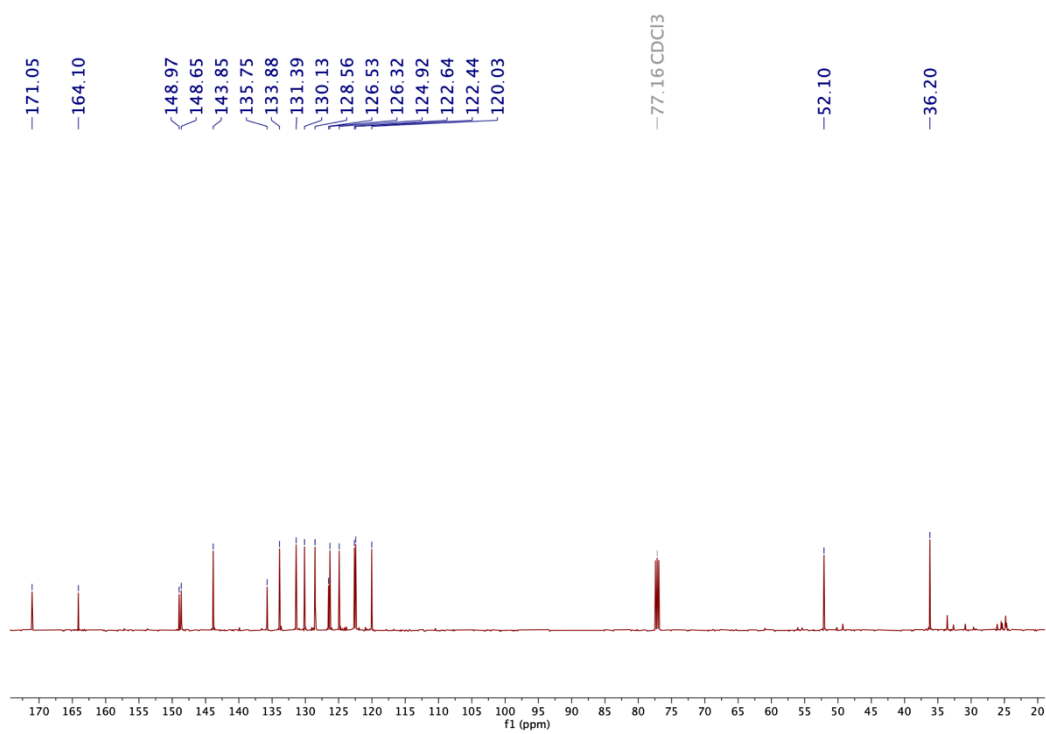
**Figure 3.17** The  $^{13}\text{C}$  NMR spectrum of NT7

**Table 3.8** The  $^1\text{H}$  and  $^{13}\text{C}$  NMR spectral assignment of NT7 reference compound in  $\text{DMSO-d}_6$ 

NT7		2-(2-methoxy-2-oxoethyl)phenyl 2-(3,4-dimethoxyphenyl)acetate (Lv <i>et al</i> , 1995)		
				
Position	Chemical shift (ppm)		Chemical shift (ppm)	
	$^{13}\text{C}$	$^1\text{H}$	$^{13}\text{C}$	$^1\text{H}$
1	148.4	-	148.2	-
2	125.8	-	126.1	-
3	126.2	7.27-7.24 (m, 2H)	126.1	7.30 (m, 2H)
5	128.5		128.4	
4	122.4	6.91 (d, $J = 10.0$ Hz, 2H)	122.6	6.89 (m, 1H)
6	121.6		121.8	6.94 (m, 1H)
7	40.8	3.44 (s, 2H)	35.2	3.49 (s, 2H)
8	171.0	-	170.8	-
9	36.0	3.58 (s, 3H)	35.2	3.51 (s, 3H)
1'	126.5	-	126.3	-
2'	112.5	7.05 (t, $J = 8.0$ Hz, 1H)	127.0	7.08 (m, 1H)
3'	149.1	-	149.1	-
4'	149.0	-	149.1	-
5'	111.3	6.83 (d, $J = 8.0$ Hz, 1H)	113.5	6.84 (m, 1H)
6'	131.3	7.16 (t, $J = 7.5$ Hz, 1H)	131.6	7.18 (m, 1H)
7'	52.0	3.78 (s, 2H)	51.8	3.82 (s, 2H)
8'	55.9	-	55.6	-
9'	55.9	3.87 (s, 3H)	55.6	3.73 (s, 2H)
10'	55.9	3.85 (s, 3H)	55.6	3.72 (s, 3H)



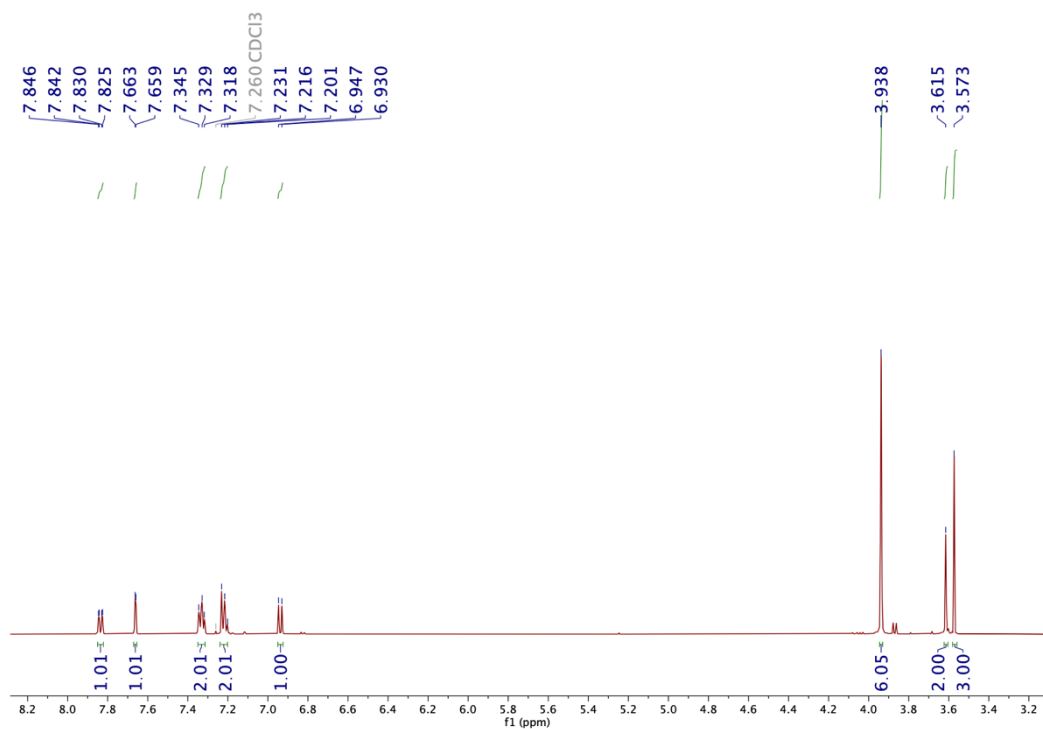
**Figure 3.18** The  $^1\text{H}$  NMR spectrum of NT8



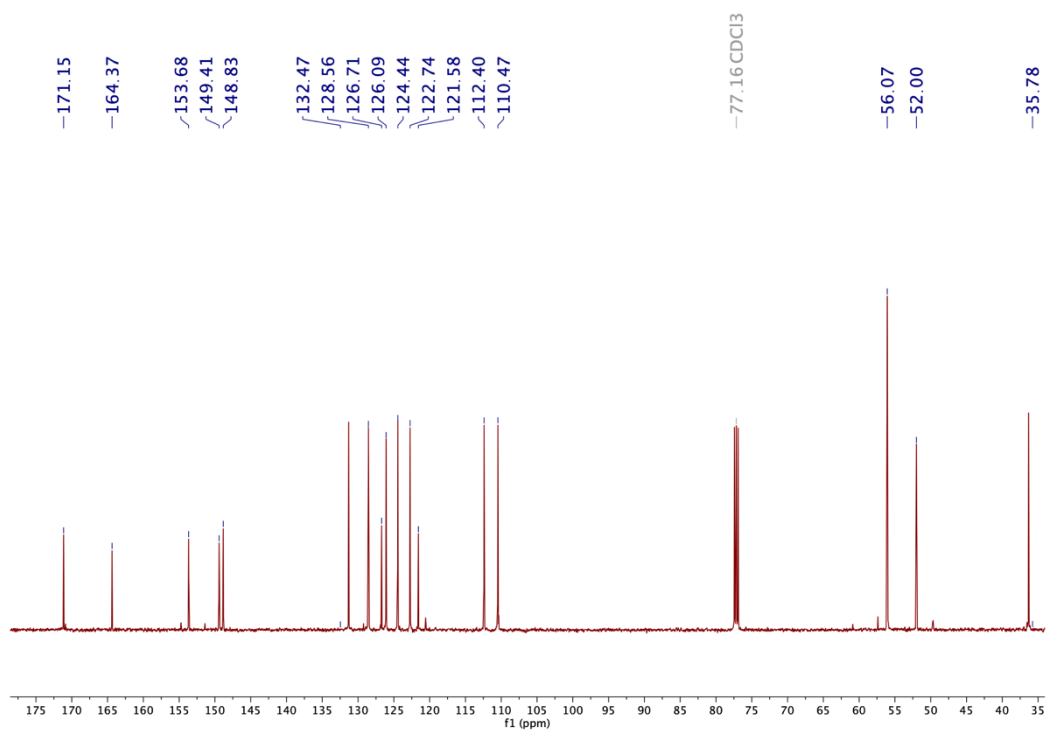
**Figure 3.19** The  $^{13}\text{C}$  NMR spectrum of NT8

**Table 3.9** The  $^1\text{H}$  and  $^{13}\text{C}$  NMR spectral assignment of **NT8**

<b>NT8</b>		
Position	Chemical shift (ppm)	
	$^{13}\text{C}$	$^1\text{H}$
1	149.0	-
2	126.5	-
3	128.6	7.34 (d, $J = 7.5$ Hz, 1H)
5	131.4	7.34 (t, $J = 7.5$ Hz, 1H)
4	126.3	7.23-7.15 (m, 2H)
6	122.4	
7	36.2	3.62 (s, 2H)
8	171.1	-
9	52.1	3.64 (s, 3H)
1'	135.6	-
2'	122.6	8.41 (s, 1H)
3'	148.7	-
4'	133.9	8.23 (dd, $J = 8.0, 2.0$ Hz, 1H)
5'	130.1	7.89 (d, $J = 16.0$ Hz, 1H)
6'	120.0	7.59 (t, $J = 8.0$ Hz, 1H)
7'	143.9	7.87 (s, $J = 5.5$ Hz, 1H)
8'	124.9	6.75 (d, $J = 16.0$ Hz, 1H)
9'	164.1	-

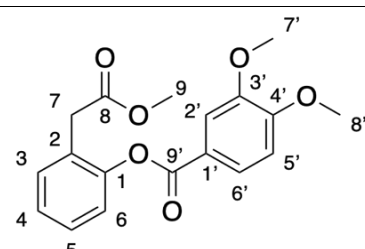


**Figure 3.20** The <sup>1</sup>H NMR spectrum of NT9



**Figure 3.21** The <sup>13</sup>C NMR spectrum of NT9

**Table 3.10** The  $^1\text{H}$  and  $^{13}\text{C}$  NMR spectral assignment of NT9

NT9		
		
Position	Chemical shift (ppm)	
	$^{13}\text{C}$	$^1\text{H}$
1	149.4	-
2	128.6	-
3	126.7	7.22 (d, $J = 7.5$ Hz, 1 H)
4	126.1	7.33 (t, $J = 7.5$ Hz, 1H)
5	132.5	7.22 (t, $J = 7.5$ Hz, 1 H)
6	122.7	7.33 (d, $J = 7.5$ Hz, 1H)
7	35.8	3.62 (s, 2H)
8	171.2	-
9	52.0	3.57 (s, 3H)
1'	153.7	-
2'	122.4	7.66 (d, $J = 2$ Hz, 1H)
3'	121.6	-
4'	148.8	-
5'	110.5	6.94 (d, $J = 8.5$ Hz, 1H)
6'	124.5	7.84 (dd, $J = 8$ and 2 Hz, 1H)
7'	56.1	3.94 (s, 6 H)
8'	56.1	
9'	164.4	-

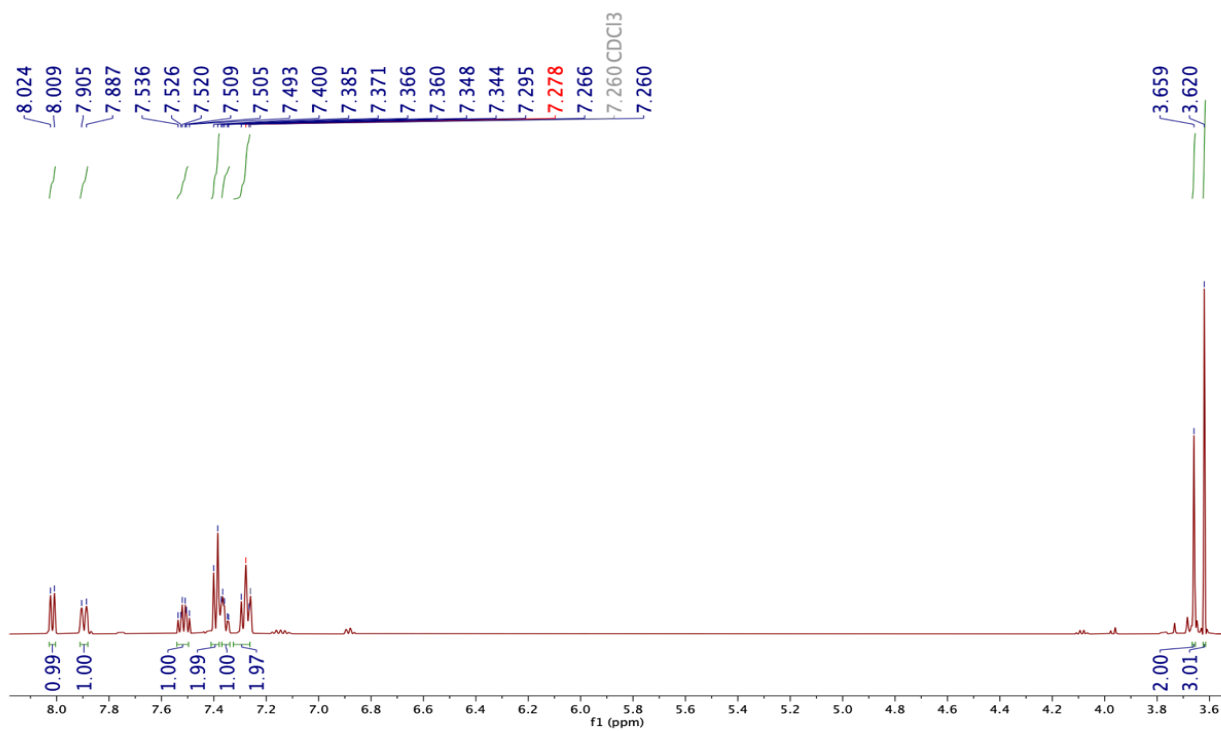


Figure 3.22 The  $^1\text{H}$  NMR spectrum of NT10

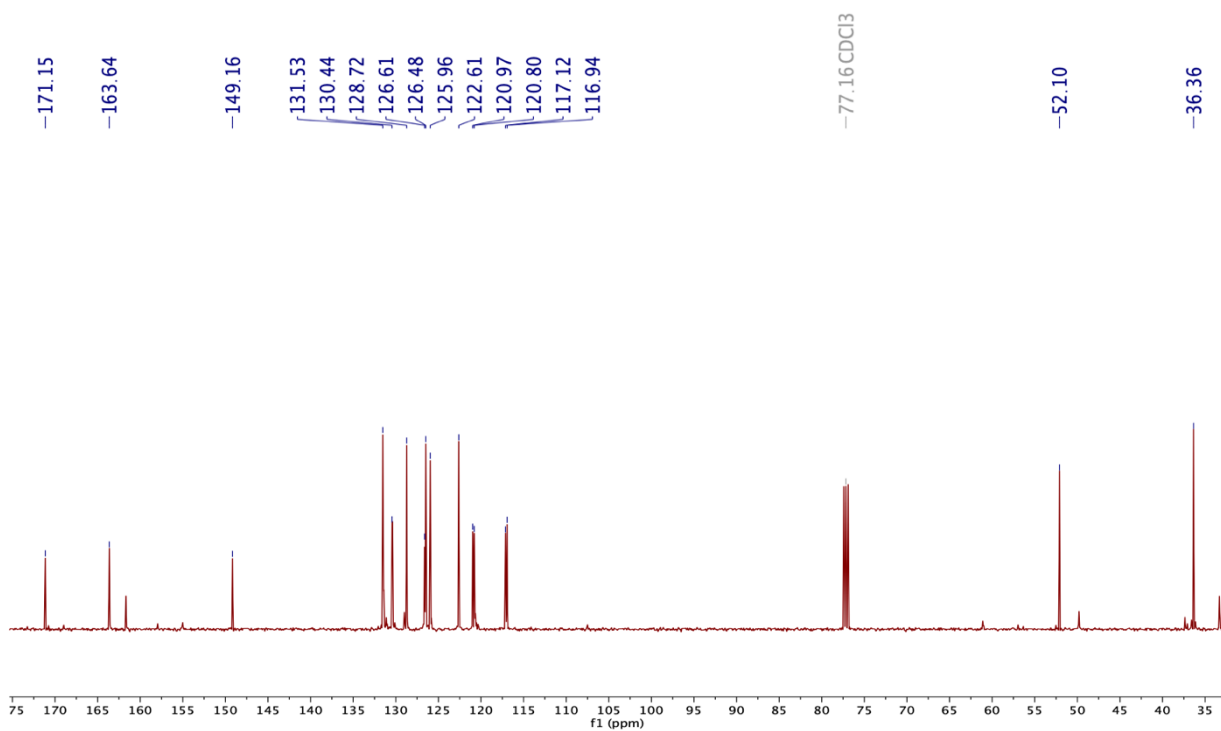


Figure 3.23 The  $^{13}\text{C}$  NMR spectrum of NT10



**Table 3.11** The  $^1\text{H}$  and  $^{13}\text{C}$  NMR spectral assignment of **NT10**

<b>NT10</b>		
Position	Chemical shift (ppm)	
	$^{13}\text{C}$	$^1\text{H}$
1	149.2	-
2	117.1	-
3	121.0	7.35 (d, $J = 8.5$ Hz, 1H)
5	122.6	7.39 (t, $J = 7.0$ Hz, 1H)
5'	126.0	7.39 (t, $J = 7.0$ Hz, 1H)
4	120.8	7.28 (t, $J = 8.5$ Hz, 1H)
6	116.9	7.28 (d, $J = 8.5$ Hz, 1H)
7	36.4	3.66 (s, 2H)
8	171.2	-
9	52.1	3.62 (s, 3H)
1'	130.4	-
2'	128.7	8.02 (d, $J = 7.5$ Hz, 1H)
3'	131.5	-
4'	126.5	7.90 (d, $J = 9.0$ Hz, 1H)
6'	126.6	7.52 (dd, $J = 13.5, 8$ Hz, 1H)
7'	163.6	-

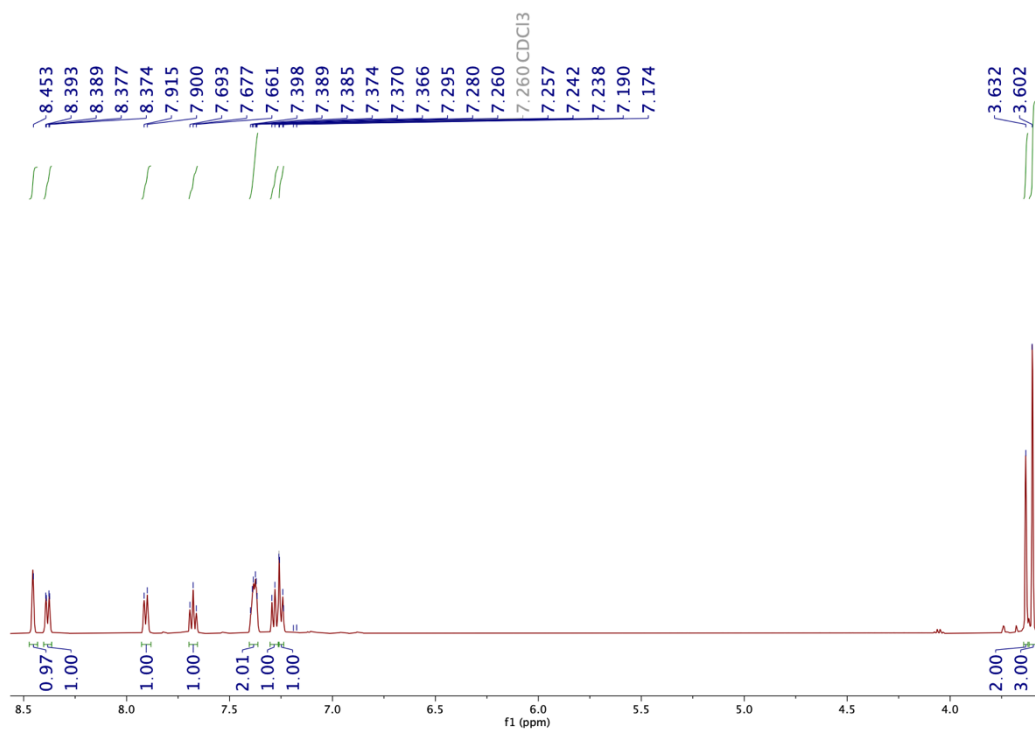


Figure 3.24 The  $^1\text{H}$  NMR spectrum of NT11

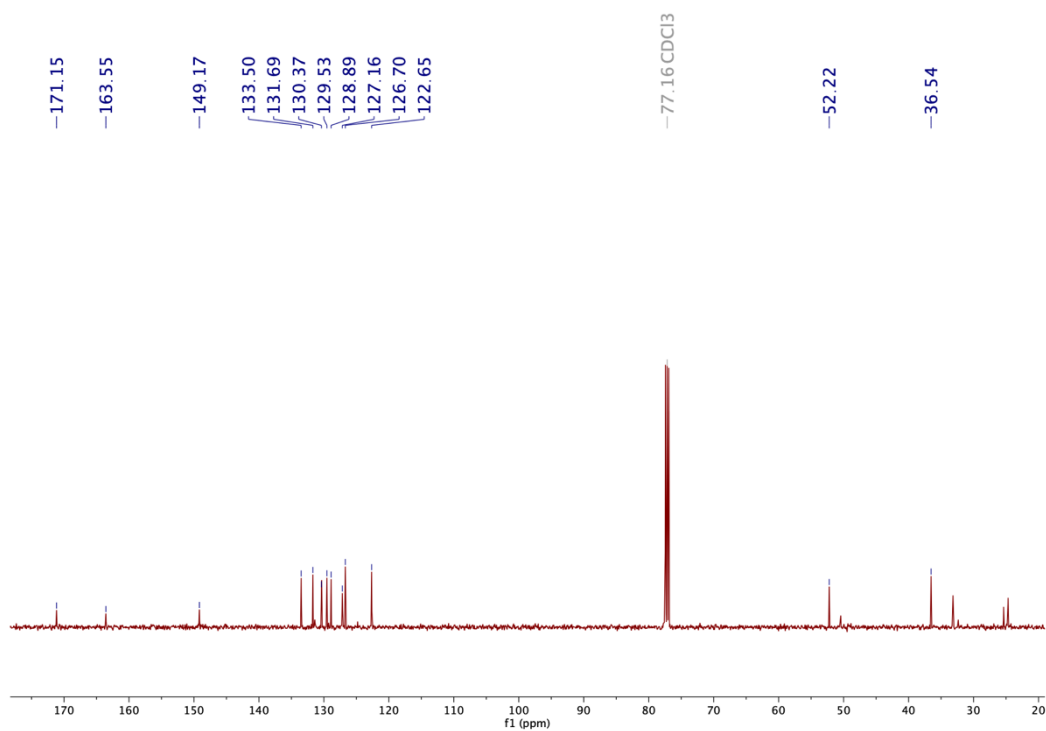
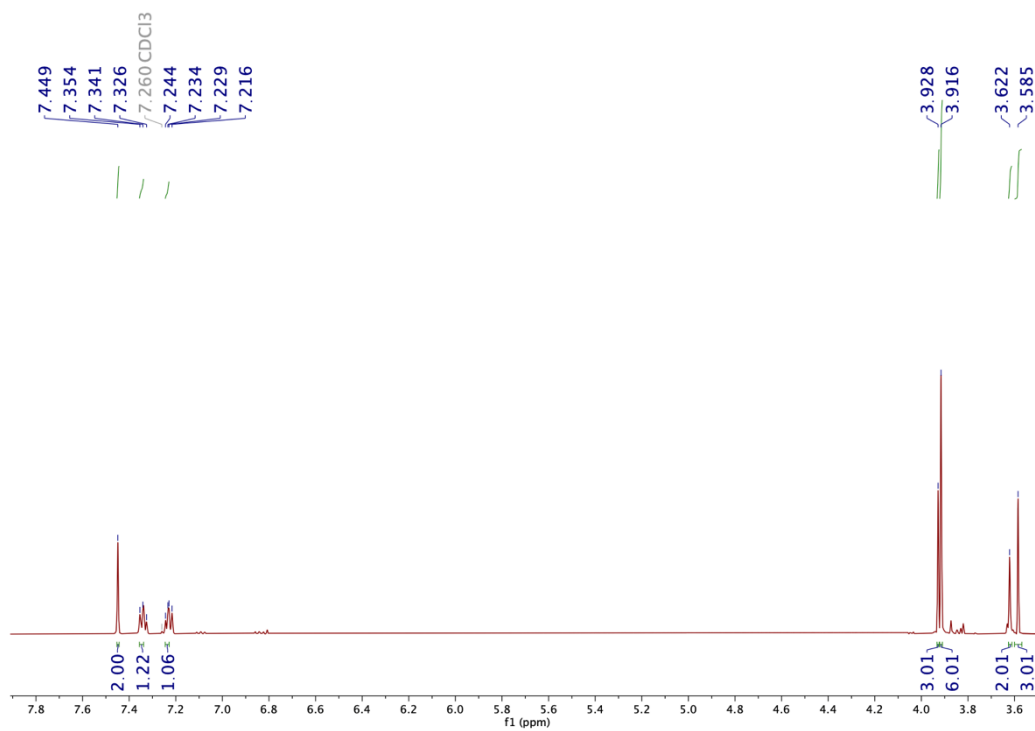


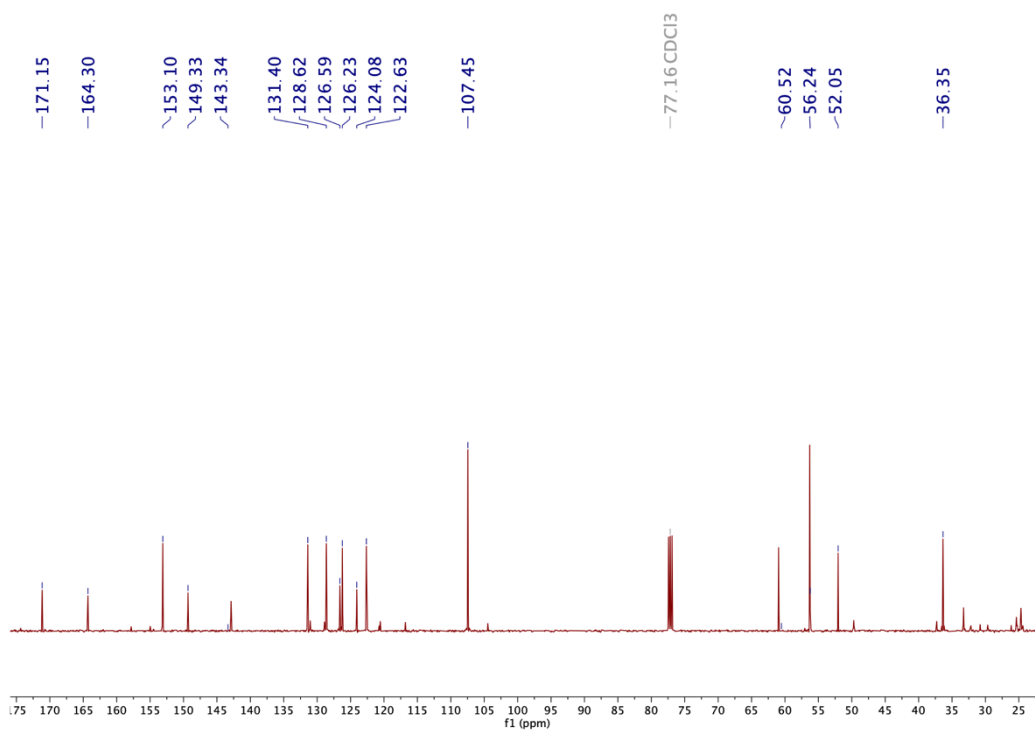
Figure 3.25 The  $^{13}\text{C}$  NMR spectrum of NT11

**Table 3.12** The  $^1\text{H}$  and  $^{13}\text{C}$  NMR spectral assignment of **NT11**

<b>NT11</b>		
Position	Chemical shift (ppm)	
	$^{13}\text{C}$	$^1\text{H}$
1	149.2	-
2	127.2	-
3	128.9	7.40-7.37 (m, 2H)
5	129.5	
4	126.7	7.26 (t, $J = 7.5$ Hz, 1H)
6	122.7	7.26 (d, $J = 7.5$ Hz, 1H)
7	36.5	3.63 (s, 2H)
8	171.2	-
9	52.2	3.60 (s, 3H)
1'	133.5	-
2'	129.5	8.45 (s, 1H)
3'	131.7	-
4'	131.7	7.91 (d, $J = 7.5$ Hz, 1H)
5'	130.4	7.68 (t, $J = 8.0$ Hz, 1H)
6'	131.7	8.39 (d, $J = 8.0$ Hz, 1H)
7'	-	-
8'	163.6	-



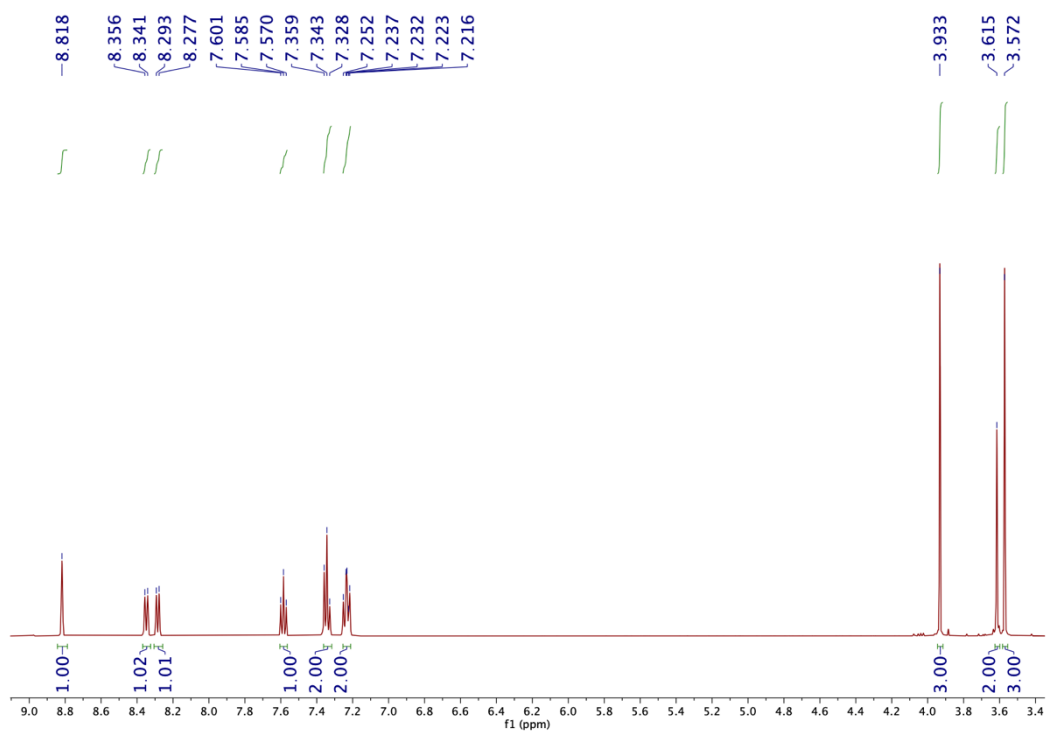
**Figure 3.26** The  $^1\text{H}$  NMR spectrum of NT12



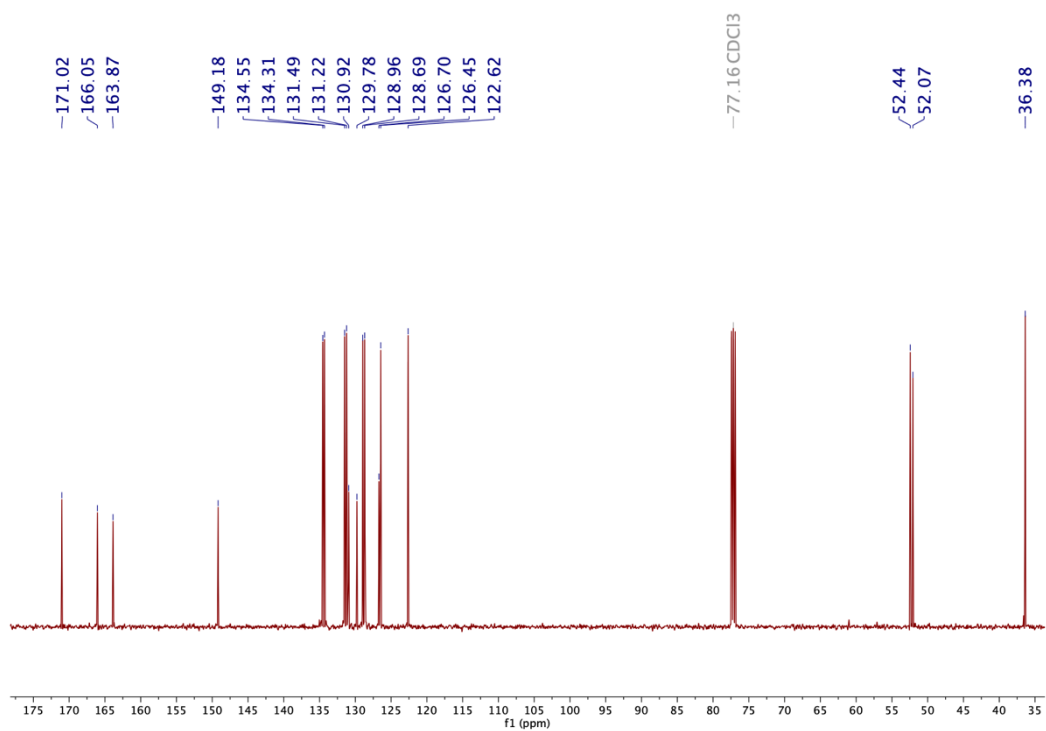
**Figure 3.27** The  $^{13}\text{C}$  NMR spectrum of NT12

**Table 3.13** The  $^1\text{H}$  and  $^{13}\text{C}$  NMR spectral assignment of **NT12**

<b>NT12</b>		
Position	Chemical shift (ppm)	
	C-NMR	H-NMR
1	149.3	-
2	126.6	-
3	128.6	7.23 (d, $J = 7.5$ Hz, 1H)
4	126.2	7.34 (t, $J = 7.5$ Hz, 1H)
5	131.4	7.23 (t, $J = 7.5$ Hz, 1H)
6	122.6	7.34 (d, $J = 7.5$ Hz, 1H)
7	36.3	3.62 (s, 2H)
8	171.2	-
9	52.1	3.56 (s, 3H)
1'	124.1	-
2'	107.5	7.45 (s, 2H)
6'	107.5	
3'	153.1	-
4'	143.3	-
5'	153.1	-
7'	56.2	3.92 (s, 6H)
9'	56.2	
8'	60.5	3.93 (s, 3H)
10'	164.3	-



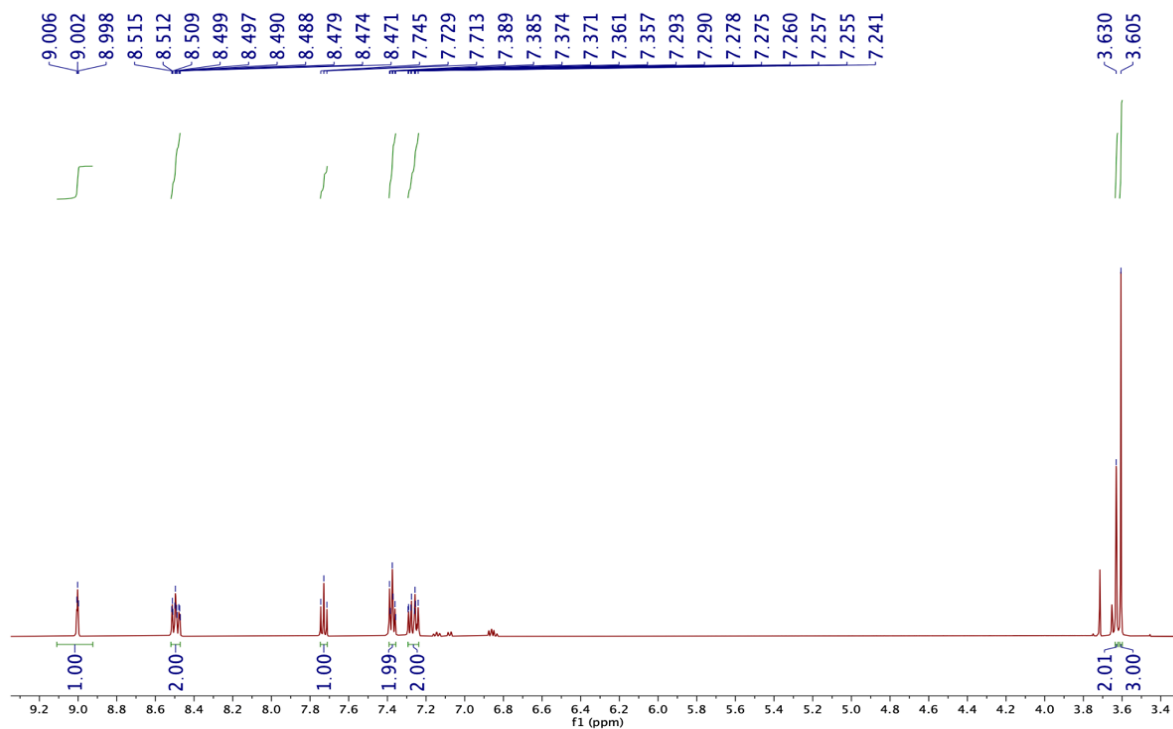
**Figure 3.28** The <sup>1</sup>H NMR spectrum of NT13



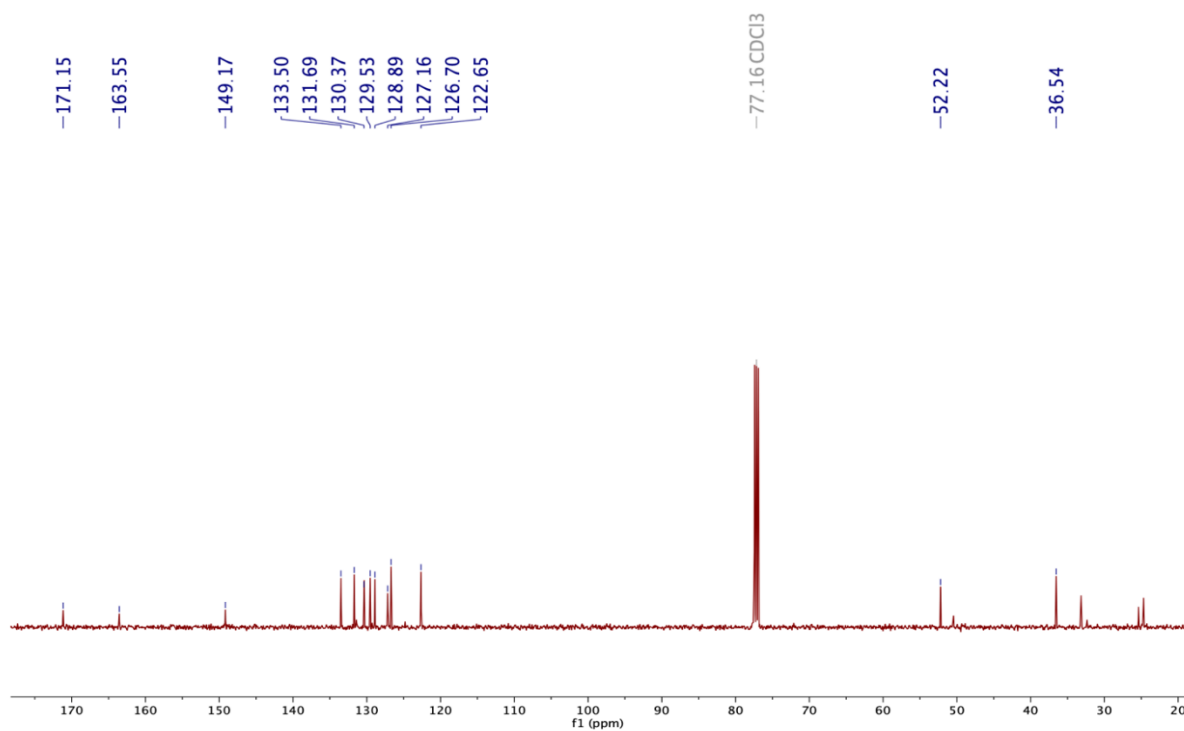
**Figure 3.29** The <sup>13</sup>C NMR spectrum of NT13

**Table 3.14** The  $^1\text{H}$  and  $^{13}\text{C}$  NMR spectral assignment of **NT13**

<b>NT13</b>		
Position	Chemical shift (ppm)	
	$^{13}\text{C}$	$^1\text{H}$
1	149.2	-
2	126.7	-
3	128.7	7.23 (d, $J = 7.5$ Hz, 1H)
4	126.5	7.34 (t, $J = 7.5$ Hz, 1H)
5	131.5	7.23 (t, $J = 7.5$ Hz, 1H)
6	122.6	7.34 (d, $J = 7.5$ Hz, 1H)
7	36.4	3.62 (s, 2H)
8	171.0	-
9	52.1	3.57 (s, 3H)
1'	129.8	-
2'	134.6	8.82 (s, 1H)
3'	130.1	-
4'	131.2	8.29 (d, $J = 8$ Hz, 1H)
5'	129.0	7.59 (t, $J = 8$ Hz, 1H)
6'	134.3	8.35 (d, $J = 7.5$ Hz, 1H)
7'	166.1	-
8'	52.4	3.93 (s, 3H)
9'	163.9	-



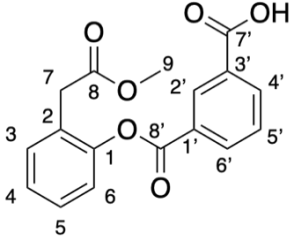
**Figure 3.30** The  $^1\text{H}$  NMR spectrum of NT14



**Figure 3.31** The  $^{13}\text{C}$  NMR spectrum of NT14



**Table 3.15** The  $^1\text{H}$  and  $^{13}\text{C}$  NMR spectral assignment of **NT14**

<b>NT14</b>		
		
Position	Chemical shift (ppm)	
	$^{13}\text{C}$	$^1\text{H}$
1	149.0	-
2	126.3	-
3	128.5	7.44 (d, $J = 7.5$ Hz, 1H)
4	126.3	7.30 (t, $J = 7.5$ Hz, 1H)
5	131.7	7.40 (d, $J = 7.5$ Hz, 1H)
6	122.8	7.33 (d, $J = 8.0$ Hz, 1 H)
7	35.7	3.68 (s, 1H)
8	170.8	-
9	51.7	3.48 (s, 1H)
1'	129.5	-
2'	129.1	8.62 (s, 1H)
3'	130.4	-
4'	133.4	8.29 (d, $J = 7.5$ Hz, 2H)
6'	134.5	
5'	127.1	7.74 (t, $J = 7.5$ Hz, 1H)
7'	166.8	-
8'	163.5	-

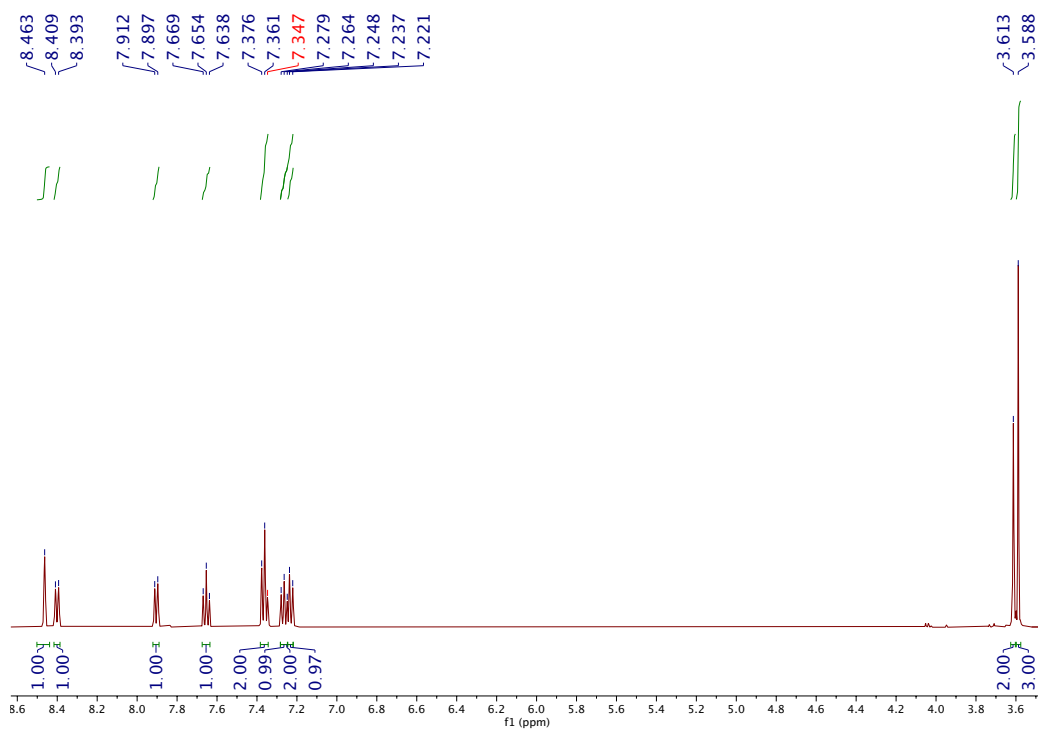


Figure 3.32 The <sup>1</sup>H NMR spectrum of NT15

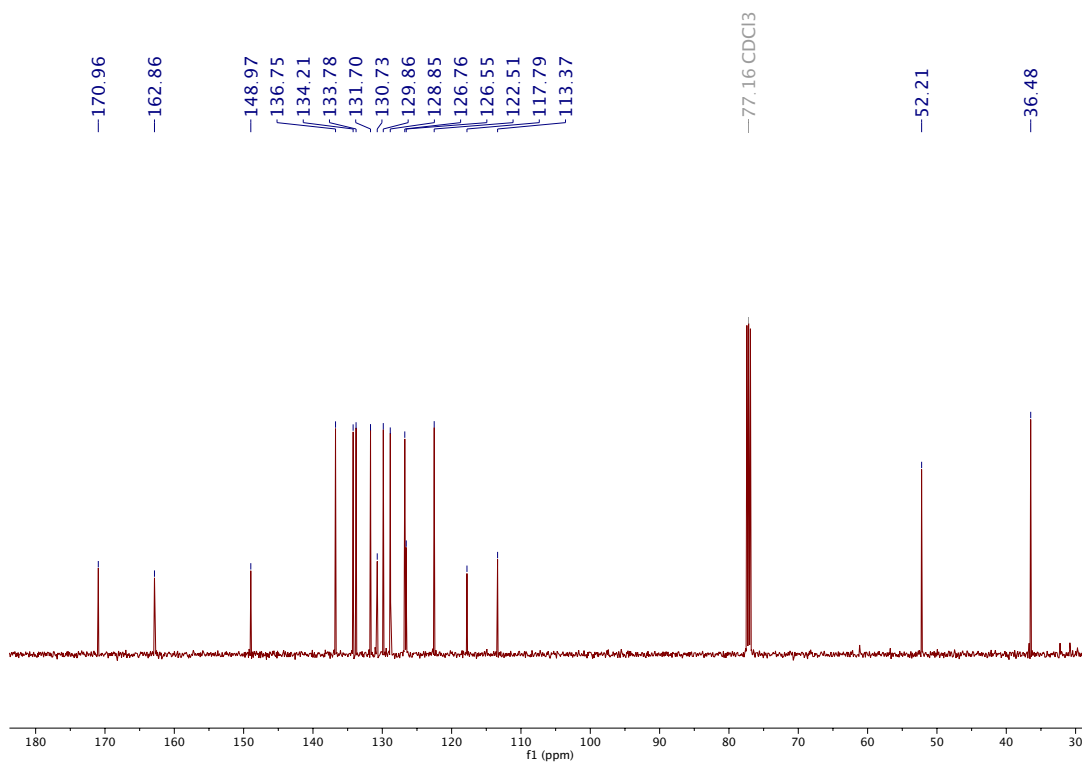


Figure 3.33 The <sup>13</sup>C NMR spectrum of NT15

**Table 3.16** The  $^1\text{H}$  and  $^{13}\text{C}$  NMR spectral assignment of **NT15**

<b>NT15</b>		
Position	Chemical shift (ppm)	
	$^{13}\text{C}$	$^1\text{H}$
1	149.0	-
2	126.6	-
3	128.8	7.36 (d, $J = 7.5$ Hz, 1H)
4	126.8	7.26 (t, $J = 7.5$ Hz, 1H)
5	131.7	7.36 (t, $J = 7.5$ Hz, 1H)
6	122.5	7.23 (d, $J = 8.0$ Hz, 1H)
7	36.5	3.62 (s, 2H)
8	171.0	-
9	52.2	3.59 (s, 3H)
1'	130.7	-
2'	136.7	8.46 (s, 1H)
3'	113.4	-
4'	134.2	8.40 (d, $J = 8.0$ Hz, 1H)
5'	129.9	7.65 (t, $J = 7.5$ Hz, 1H)
6'	133.8	7.90 (d, $J = 7.5$ Hz, 1H)
7'	117.8	-
8'	171.0	-

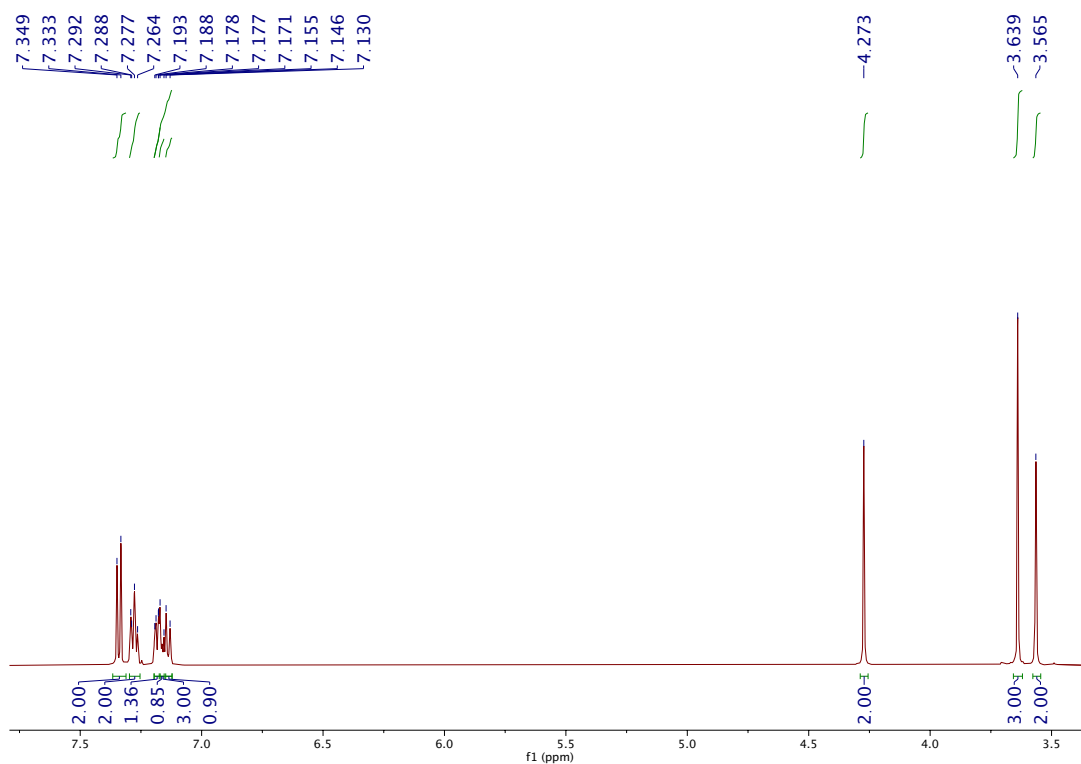


Figure 3.34 The <sup>1</sup>H NMR spectrum of NT16

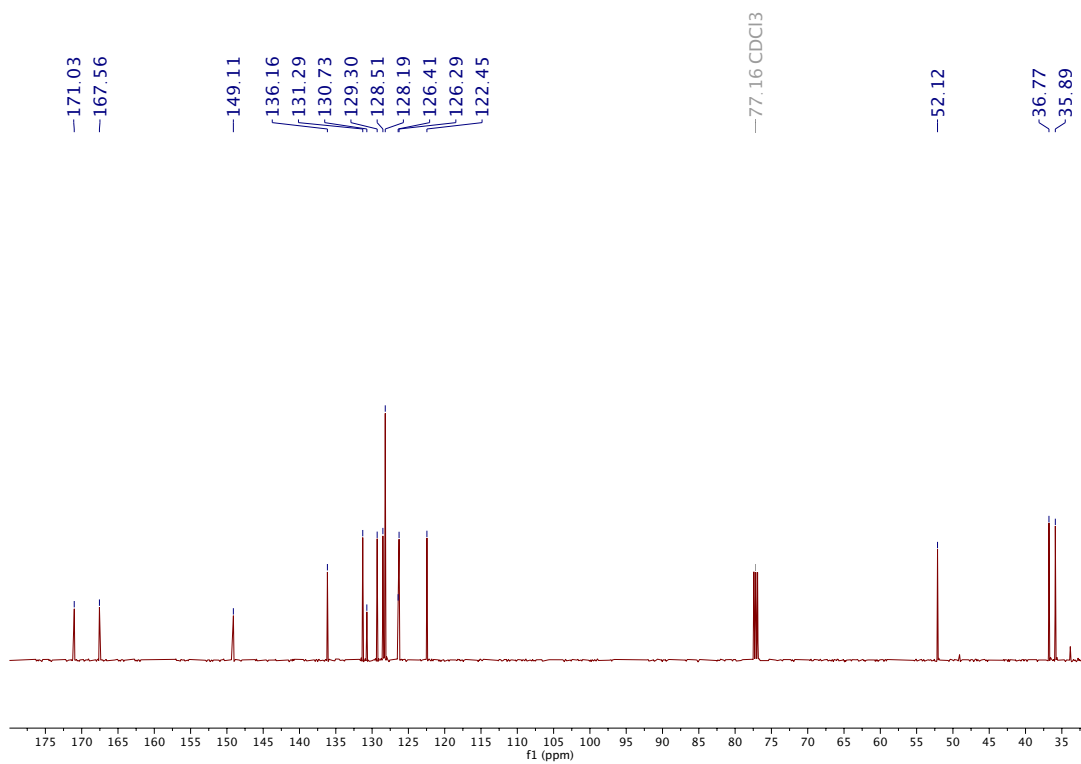
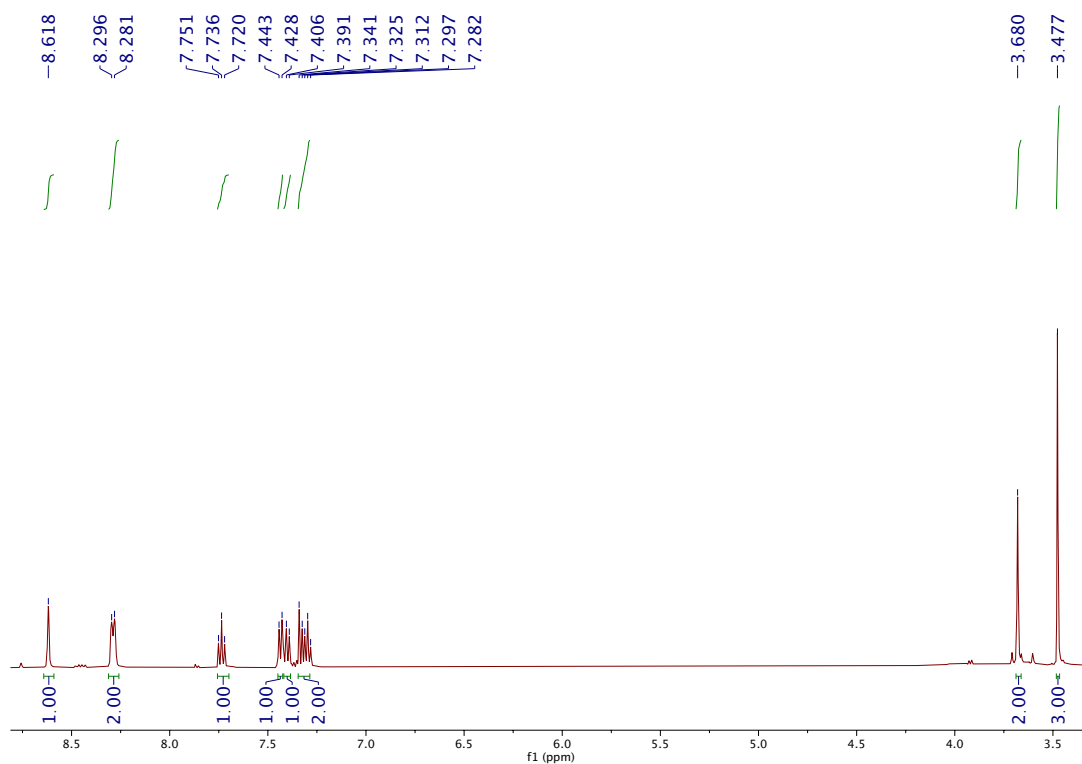


Figure 3.35 The <sup>13</sup>C NMR spectrum of NT16

**Table 3.17** The  $^1\text{H}$  and  $^{13}\text{C}$  NMR spectral assignment of **NT16**

<b>NT16</b>		
Position	Chemical shift (ppm)	
	$^{13}\text{C}$	$^1\text{H}$
1	149.1	-
2	126.4	-
3	128.5	7.28 (d, $J = 7.0$ Hz, 1H)
4	126.3	7.19-7.13 (m, 3H)
6	122.5	
4'	129.3	
5	131.3	7.28 (t, $J = 7.0$ Hz, 1H)
7	36.8	3.57 (s, 2H)
8	171.0	-
9	52.1	3.64 (s, 3H)
1'	130.7	-
2'	136.2	-
3'	128.1	7.34 (d, $J = 8.0$ Hz, 2H)
5'	128.1	
6'	136.2	-
7'	35.9	4.27 (s, 2H)
8'	167.6	-



**Figure 3.36** The <sup>1</sup>H NMR spectrum of NT17

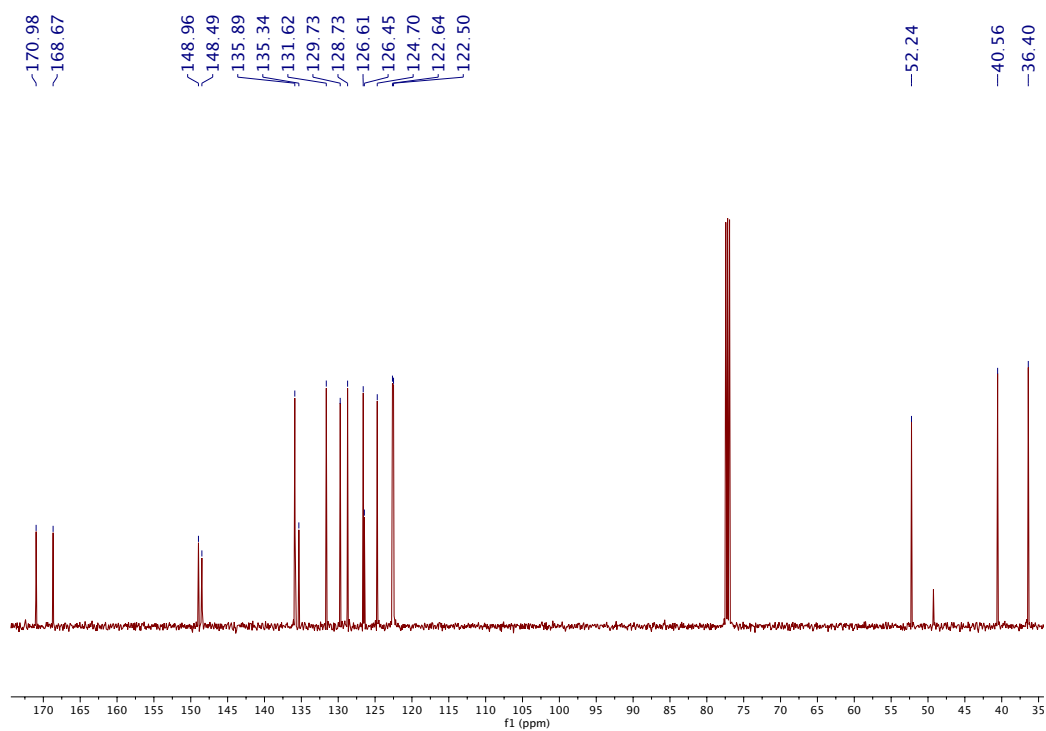


**Figure 3.37** The <sup>13</sup>C NMR spectrum of NT17

**Table 3.18** The  $^1\text{H}$  and  $^{13}\text{C}$  NMR spectral assignment of **NT17**

<b>NT17</b>		
Position	Chemical shift (ppm)	
	$^{13}\text{C}$	$^1\text{H}$
1	149.0	-
2	126.4	-
3	128.7	7.21 (t, $J = 7.5$ Hz, 1H)
4	126.6	7.29 (t, $J = 7.5$ Hz, 2H)
6	122.6	
5	131.6	7.55 (t, $J = 8.0$ Hz, 1H)
7	36.4	4.00 (s, 2H)
8	171.0	-
9	52.2	3.61 (s, 3H)
1'	135.3	-
2'	122.5	8.29 (s, 1H)
3'	148.5	-
4'	124.7	7.74 (d, $J = 8.0$ Hz, 1H)
5'	129.7	8.18 (dd, $J = 8.0, 2.0$ Hz, 1H)
6'	135.9	7.08 (d, $J = 8.0$ Hz, 1H)
7'	40.6	3.49 (s, 2H)
8'	168.7	-

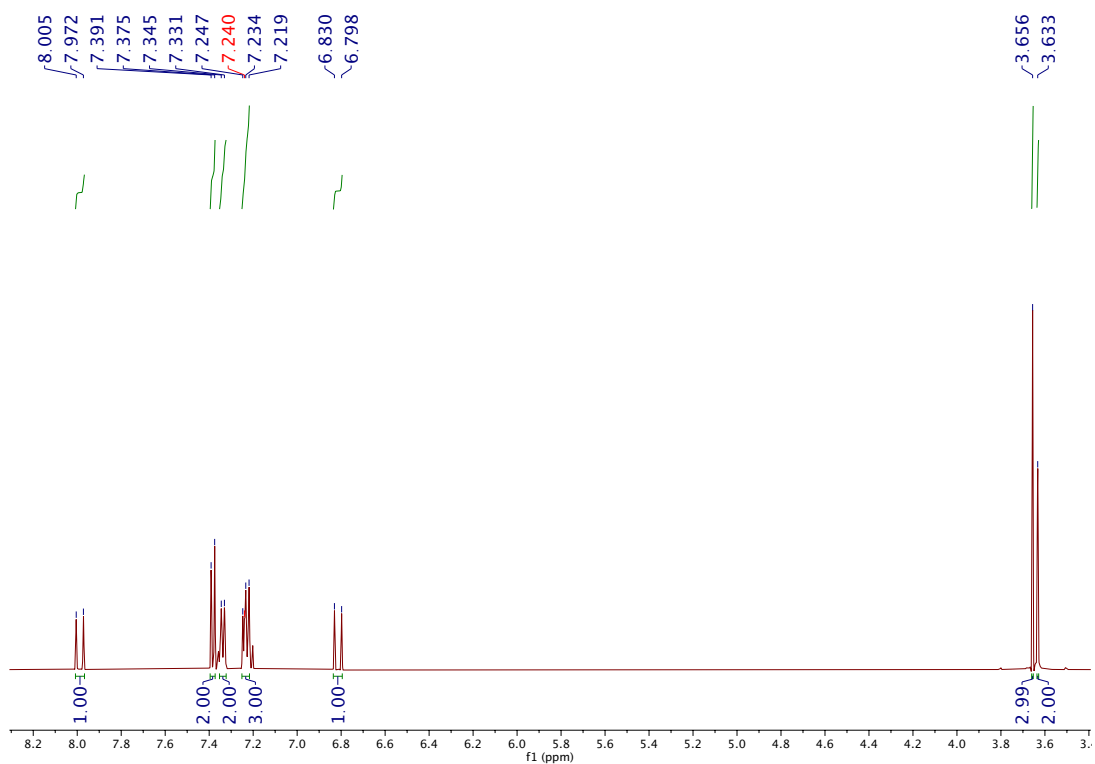


Figure 3.38 The  $^1\text{H}$  NMR spectrum of NT18

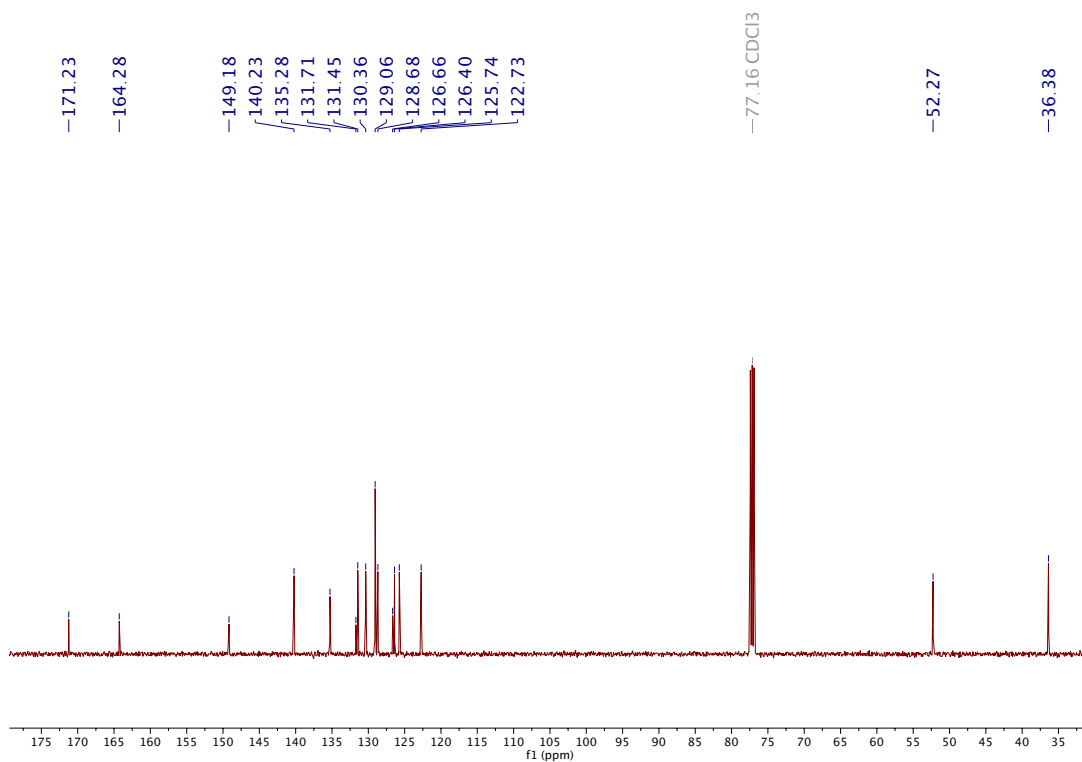


Figure 3.39 The  $^{13}\text{C}$  NMR spectrum of NT18



**Table 3.19** The  $^1\text{H}$  and  $^{13}\text{C}$  NMR spectral assignment of **NT18**

<b>NT18</b>		
Position	Chemical shift (ppm)	
	$^{13}\text{C}$	$^1\text{H}$
1	149.2	-
2	126.7	-
3	128.7	7.32 (d, $J = 7.0$ Hz, 1H)
4	126.4	7.25-7.22 (m, 3H)
6	122.7	
4'	130.4	
5	131.5	7.32 (t, $J = 7.0$ Hz, 1H)
7	36.4	3.63 (s, 2H)
8	171.2	-
9	52.3	3.66 (s, 3H)
1'	135.3	-
2'	131.7	-
3'	129.1	7.38 (d, $J = 8.0$ Hz, 2H)
4'	130.4	
5'	129.1	-
6'	131.7	-
7'	140.2	6.81 (d, $J = 16.0$ Hz, 1H)
8'	125.8	7.99 (d, $J = 16.0$ Hz, 1H)
9'	164.3	-

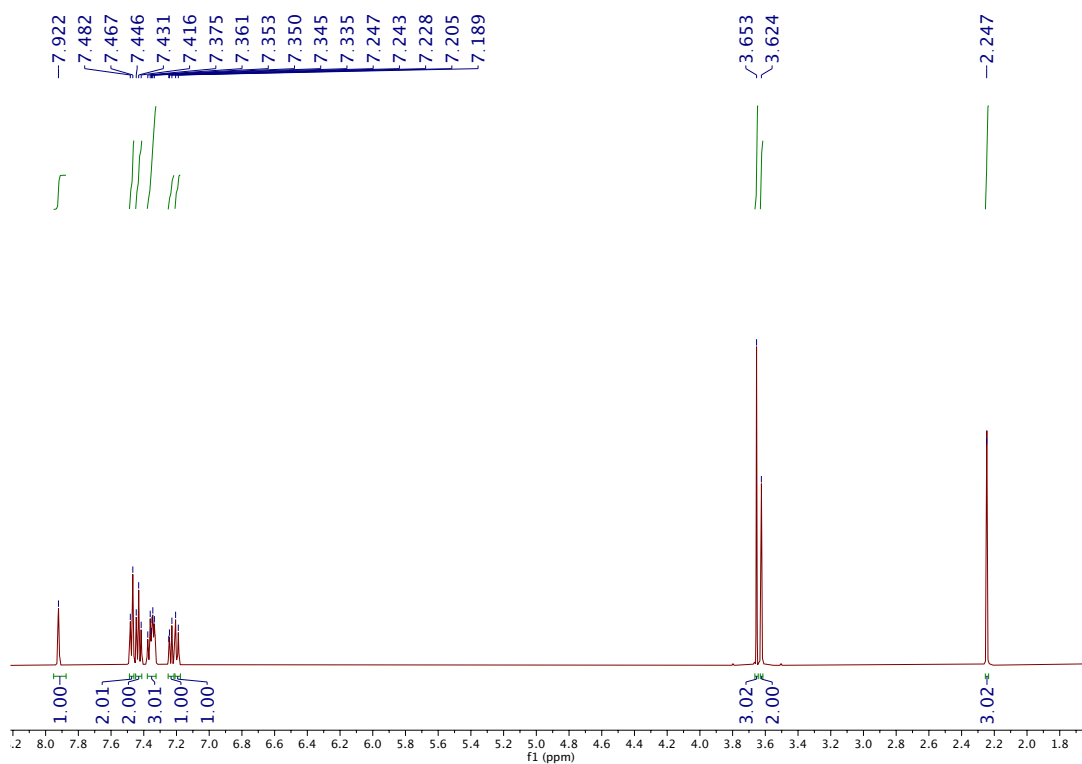


Figure 3.40 The  $^1\text{H}$  NMR spectrum of NT19

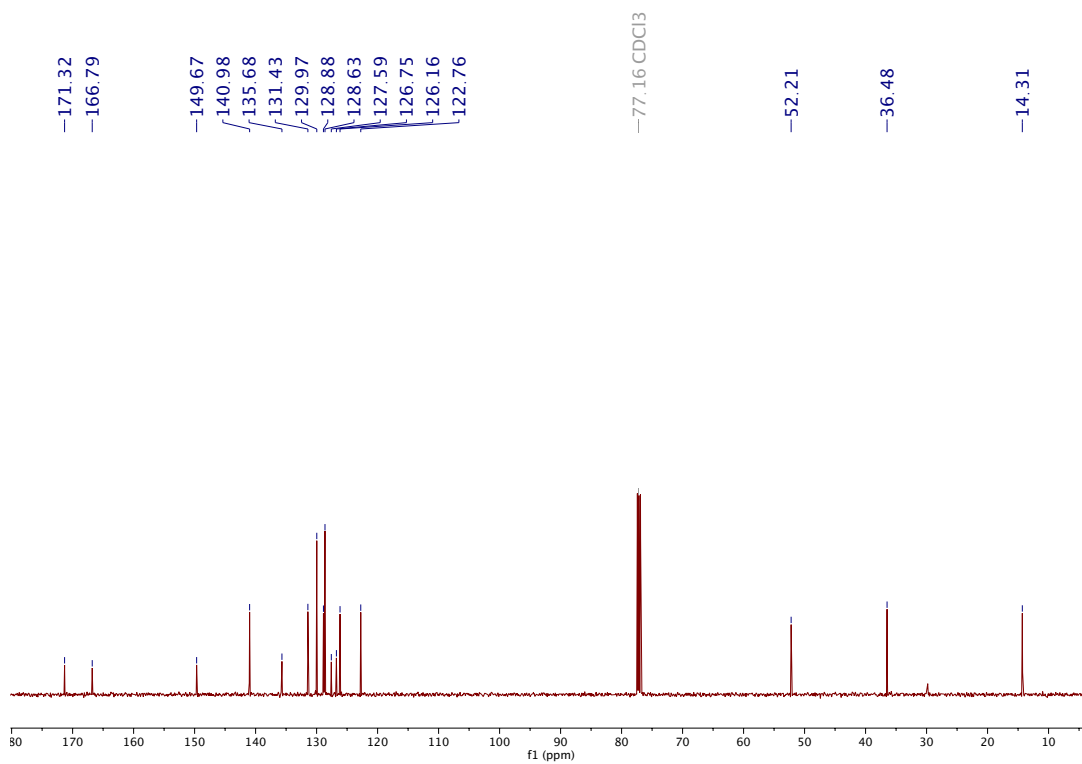
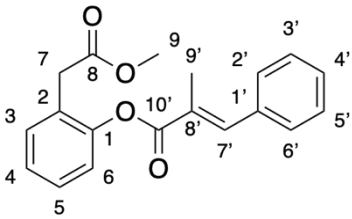


Figure 3.41 The  $^{13}\text{C}$  NMR spectrum of NT19

**Table 3.20** The  $^1\text{H}$  and  $^{13}\text{C}$  NMR spectral assignment of **NT19**

<b>NT19</b>		
		
Position	Chemical shift (ppm)	
	$^{13}\text{C}$	$^1\text{H}$
1	149.7	-
2	126.8	-
3	128.9	7.24 (d, $J = 7.5$ Hz, 1H)
5	131.4	7.21 (t, $J = 7.5$ Hz, 1H)
3'	141.0	7.42 (t, $J = 7.5$ Hz, 2H)
5'	141.0	
4	126.2	7.35-7.34 (m, 2H)
4'	130	
6	122.8	7.37 (d, $J = 7.0$ Hz, 1H)
7	36.5	3.62 (s, 2H)
8	171.3	-
9	52.2	3.65 (s, 3H)
1'	135.7	-
2'	128.6	7.47 (d, $J = 7.5$ Hz, 2H)
6'	128.6	
7'	128.6	7.92 (s, 1H)
8'	127.6	-
9'	14.31	2.25 (2, 3H)
10'	166.8	-

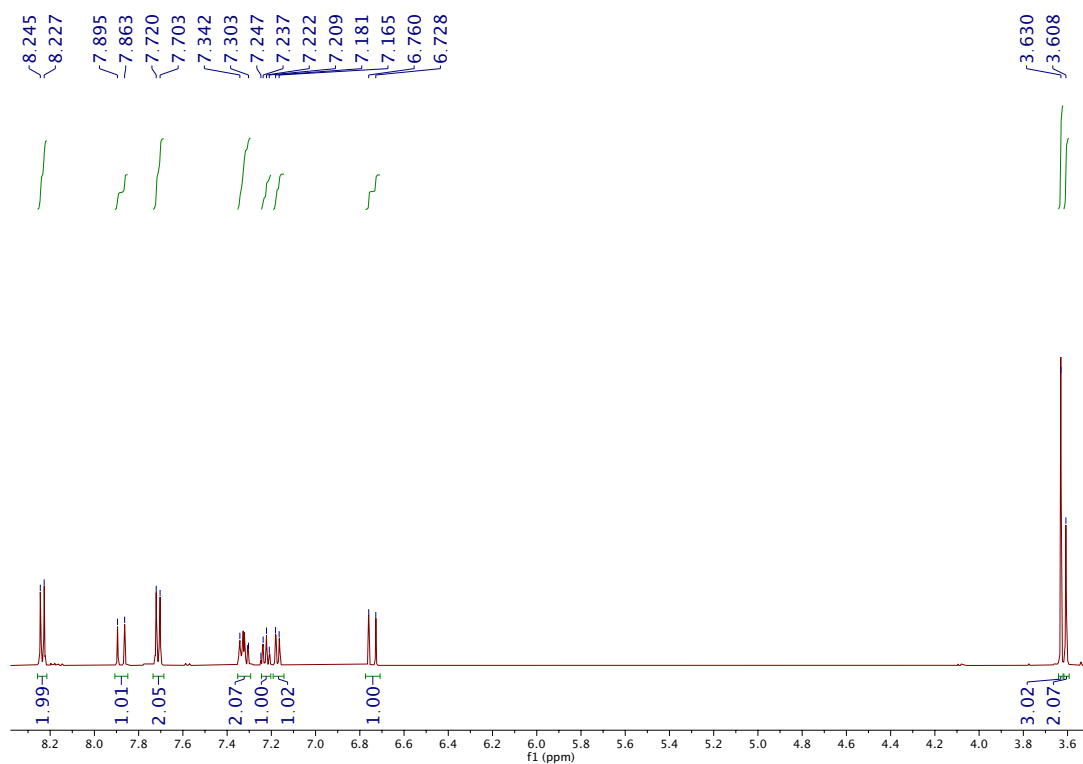


Figure 3.42 The  $^1\text{H}$  NMR spectrum of NT20

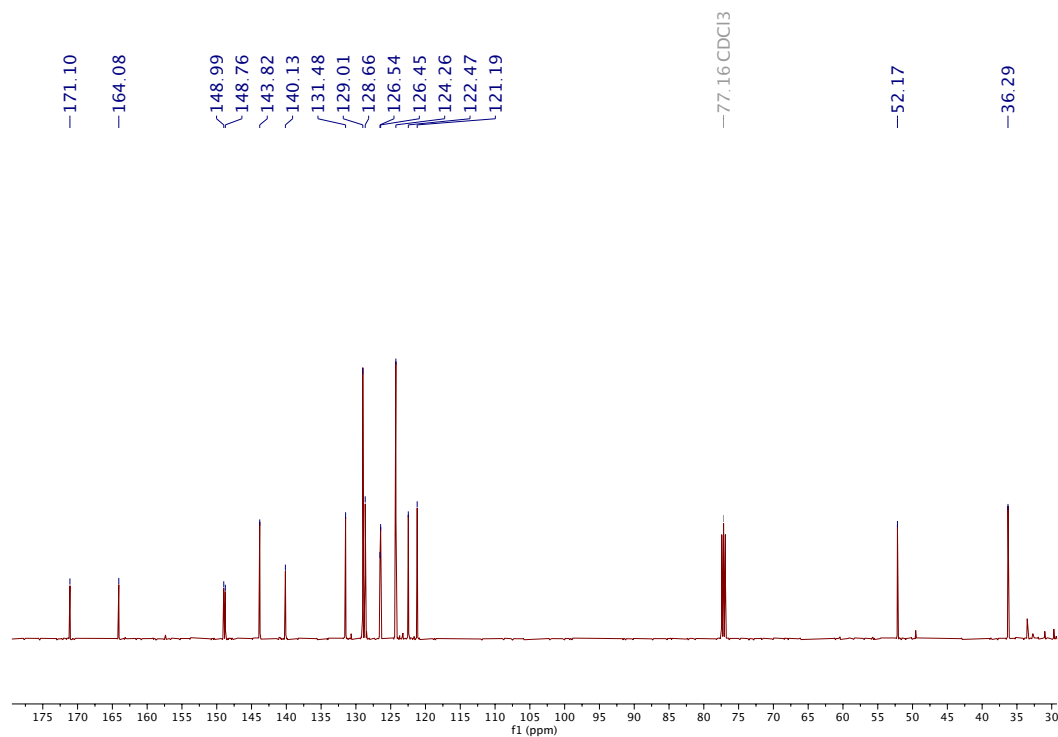


Figure 3.43 The  $^{13}\text{C}$  NMR spectrum of NT20

**Table 3.21** The  $^1\text{H}$  and  $^{13}\text{C}$  NMR spectral assignment of **NT20**

<b>NT20</b>		
Position	Chemical shift (ppm)	
	$^{13}\text{C}$	$^1\text{H}$
1	148.99	-
2	126.5	-
3	128.8	7.17 (d, $J = 8.0$ Hz, 1H)
5	131.5	7.22 (dd, $J = 7.5, 1.5$ Hz, 1H)
4	126.5	7.34-7.30 (m, 2H)
6	122.5	
7	36.3	3.61 (s, 2H)
8	171.1	-
9	52.3	3.63 (s, 3H)
1'	143.8	-
2'	140.1	7.71 (d, $J = 8.5$ Hz, 2H)
6'	140.1	
3'	124.3	8.24 (d, $J = 9.0$ Hz, 2H)
5'	124.3	
4'	148.8	-
7'	129.0	7.88 (d, $J = 16.0$ Hz, 1H)
8'	121.2	6.74 (d, $J = 16.0$ Hz, 1H)
9'	164.0	-

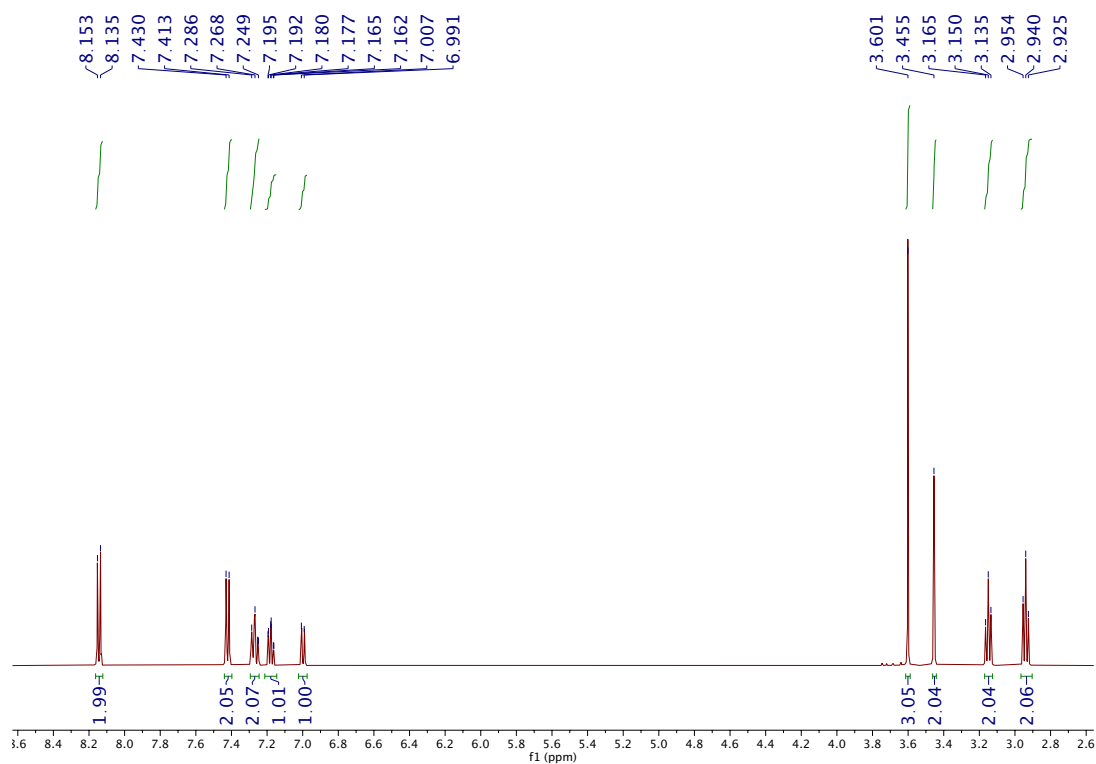


Figure 3.44 The  $^1\text{H}$  NMR spectrum of NT21

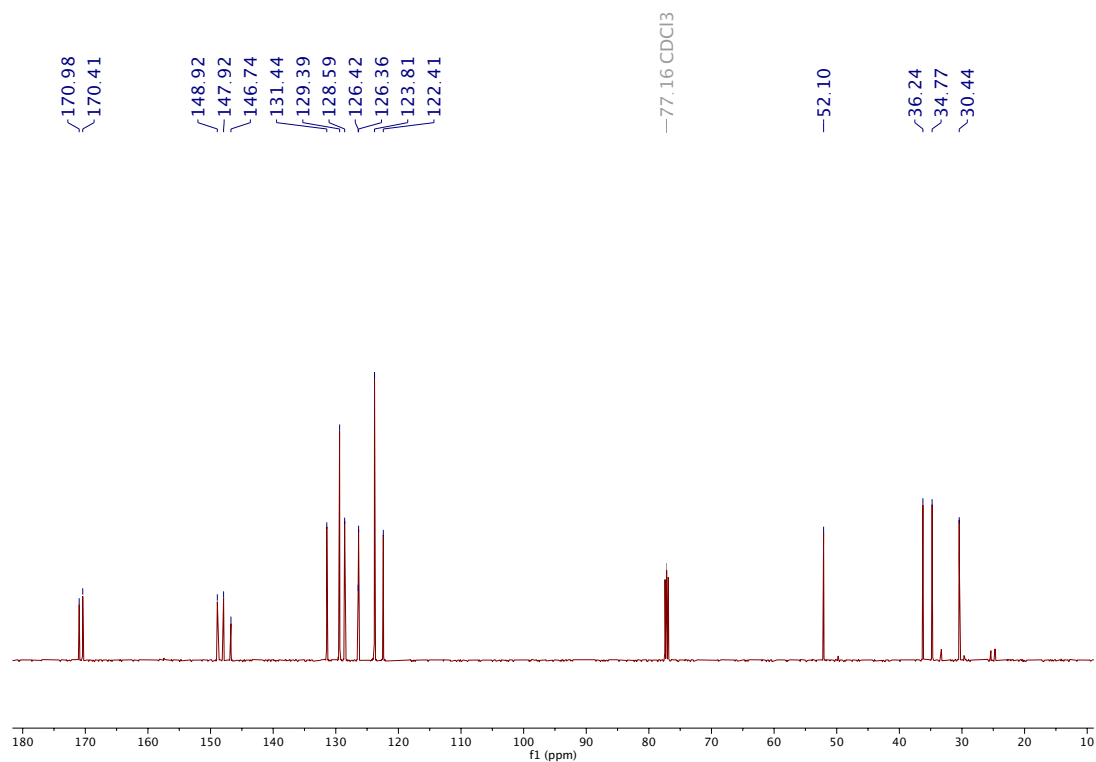


Figure 3.45 The  $^{13}\text{C}$  NMR spectrum of NT21

**Table 3.22** The  $^1\text{H}$  and  $^{13}\text{C}$  NMR spectral assignment of **NT021**

<b>NT021</b>		
Position	Chemical shift (ppm)	
	$^{13}\text{C}$	$^1\text{H}$
1	148.9	-
2	126.4	-
3	128.6	7.18 (t, $J = 7.5$ Hz, 1H)
5	131.44	7.00 (d, $J = 8$ Hz, 1H)
4	126.4	7.27 (t, $J = 9.5$ Hz, 1H)
6	122.4	7.27 (d, $J = 9.5$ Hz, 1H)
7	36.2	3.46 (s, 2H)
8	171.0	3.15 (t, $J = 7.5$ Hz, 2H)
9	52.1	3.60 (s, 3H)
1'	146.7	-
2'	123.8	7.42 (d, $J = 8.5$ Hz, 2H)
6'	123.8	
3'	129.4	8.14 (d, $J = 9.0$ Hz, 2H)
5'	129.4	
4'	147.9	-
7'	36.24	2.94 (t, $J = 7.5$ Hz, 2H)
8'	30.44	-
9'	170.4	-

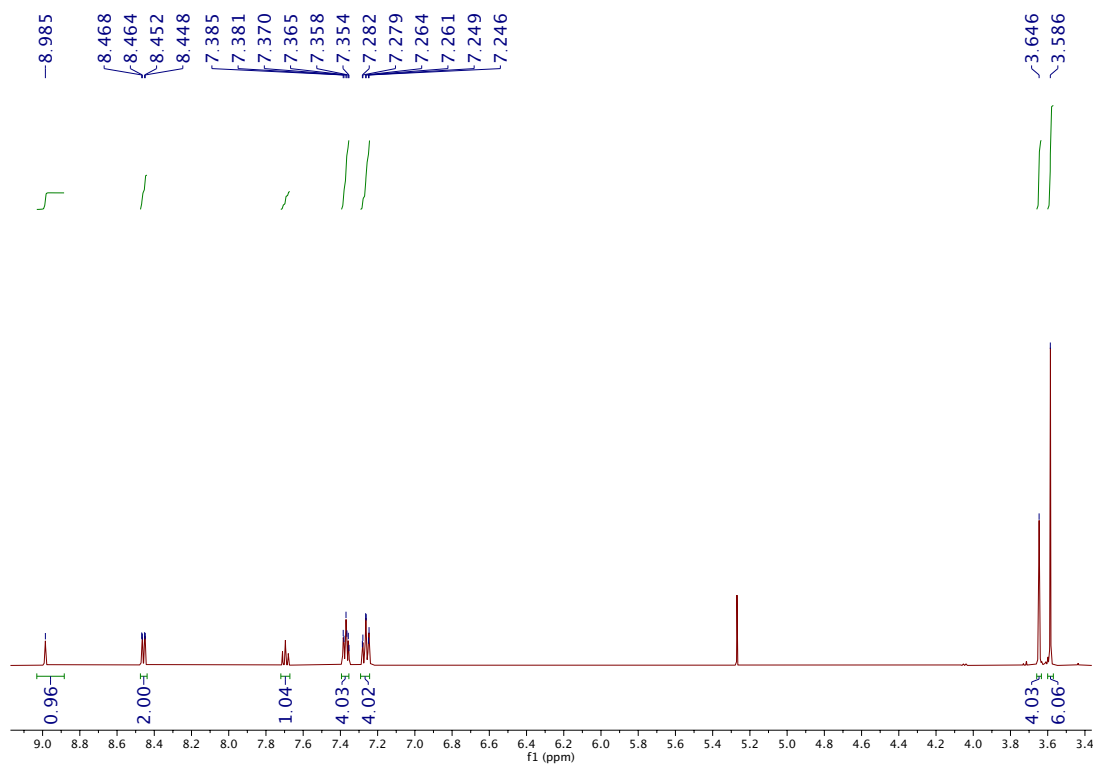


Figure 3.46 The  $^1\text{H}$  NMR spectrum of NT22

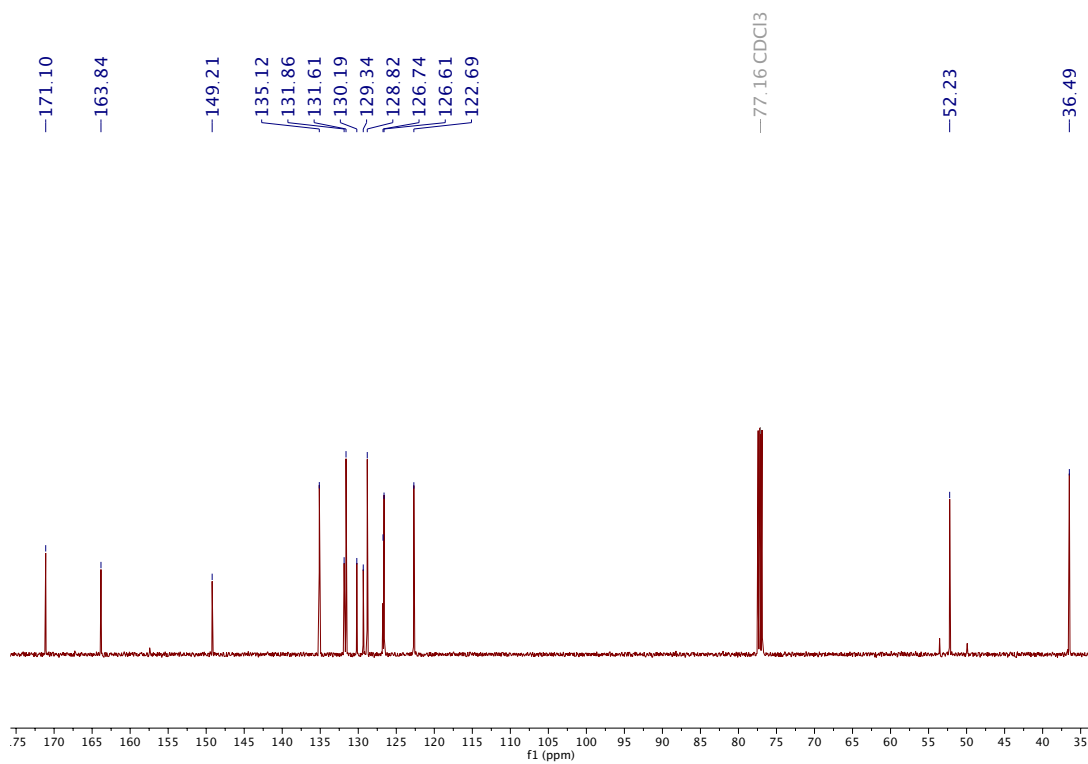


Figure 3.47 The  $^{13}\text{C}$  NMR spectrum of NT22



**Table 3.23** The  $^1\text{H}$  and  $^{13}\text{C}$  NMR spectral assignment of **NT22**

<b>NT22</b>		
Position	Chemical shift (ppm)	
	$^{13}\text{C}$	$^1\text{H}$
1	149.21	-
2	126.7	-
3	128.8	7.26 (d, $J = 9.0$ Hz, 2H)
3''	128.8	
6	122.7	7.37 (t, $J = 7.5$ Hz, 2H)
6''	122.7	
4	126.6	7.37 (t, $J = 7.5$ Hz, 2H)
4''	126.6	
5	131.6	7.26 (t, $J = 9.0$ Hz, 2H)
5''	131.6	
7	36.5	3.65 (s, 4H)
7''	36.5	
9	52.2	3.59 (s, 6H)
9''	52.2	
1'	130.2	-
2'	135.2	8.99 (s, 1H)
4'	131.9	8.46 (dd, $J = 8$ and 2 Hz, 1H)
6'	131.9	
5'	129.3	7.70 (t, $J = 7.5$ Hz, 1H)
8	163.8	-
1''	130.2	-
2''	135.2	8.99 (s, 1H)
3''	130.2	-
4''	131.9	8.46 (dd, $J = 8$ and 2 Hz, 1H)
6''	131.9	

5'	129.3	7.70 (t, $J = 7.5$ Hz, 1H)
7'	163.8	-
8'	171.1	-
1"	149.2	-
2"	126.7	-
8"	171.1	-

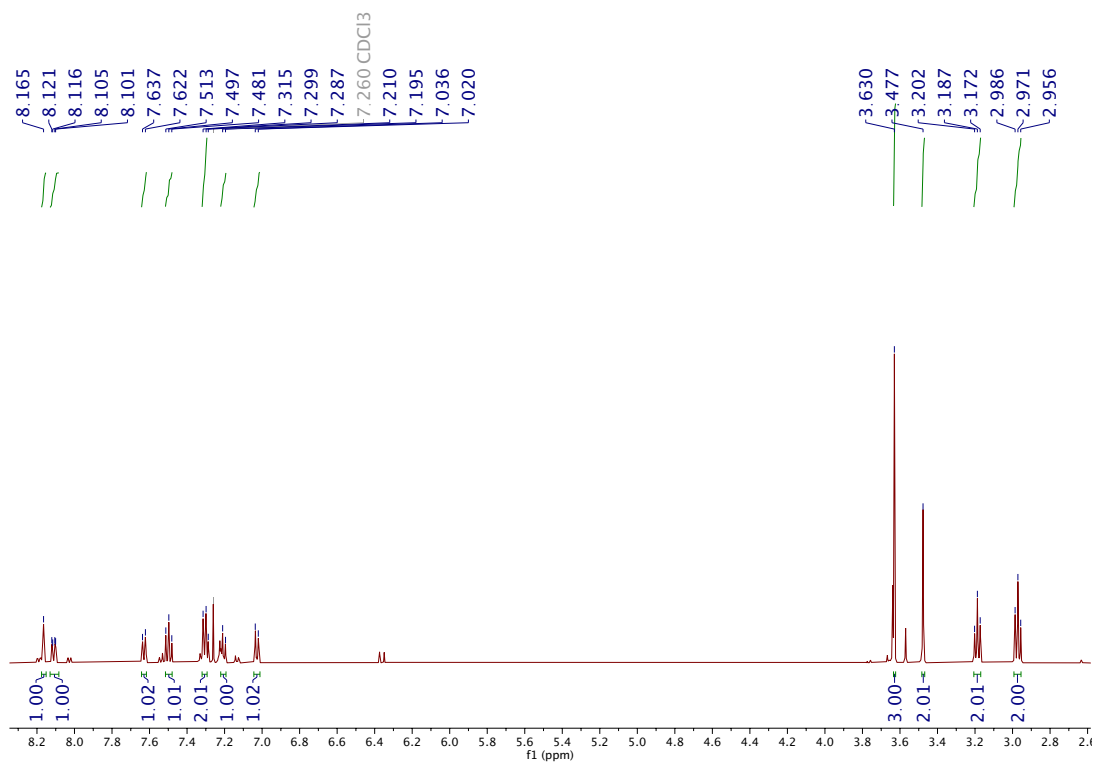


**Figure 3.48** The <sup>1</sup>H NMR spectrum of NT23

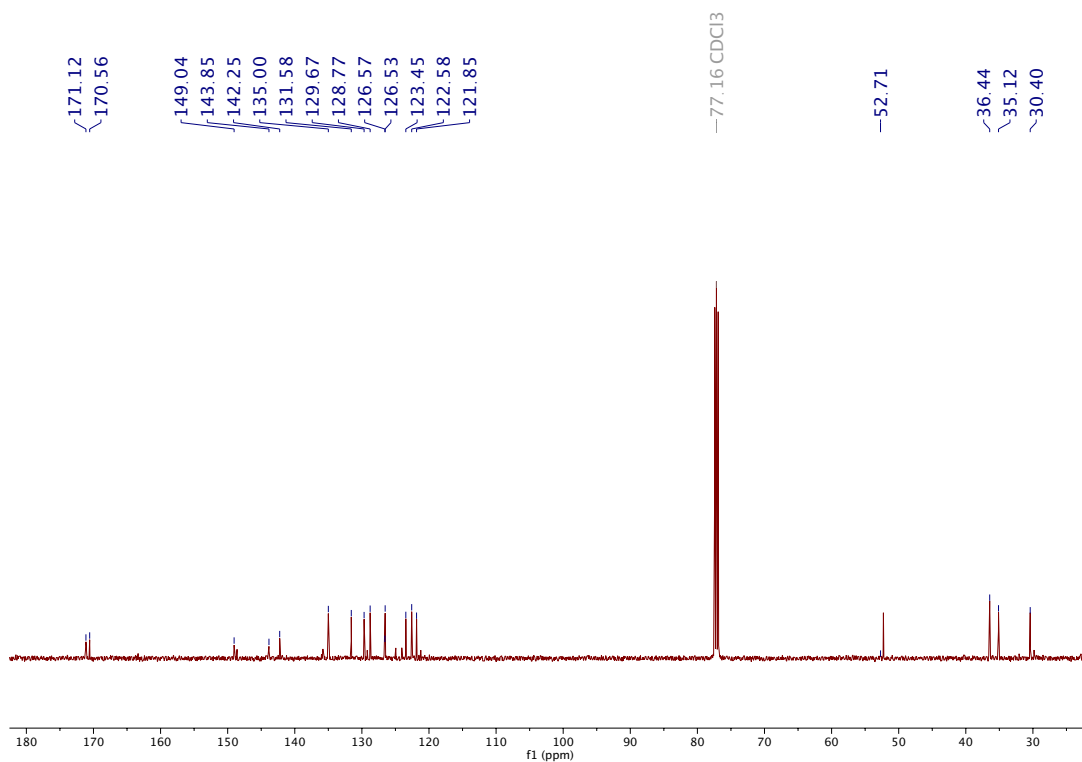


**Figure 3.49** The <sup>13</sup>C NMR spectrum of NT23

**Table 3.24** The  $^1\text{H}$  and  $^{13}\text{C}$  NMR spectral assignment of NT23

<b>NT023</b>		
Position	Chemical shift (ppm)	
	C-NMR	H-NMR
1	149	-
2	126.6	-
3	128.8	7.30 (d, $J = 8.0$ Hz, 1H)
4	126.5	7.20 (t, $J = 8.0$ Hz, 1H)
5	131.6	7.30 (t, $J = 8.0$ Hz, 1H)
6	122.6	7.03 (d, $J = 8.0$ Hz, 1H)
7	36.4	3.48 (s, 2H)
8	170.6	-
9	52.7	3.63 (s, 3H)
1'	142.2	-
2'	123.4	8.16 (s, 1H)
3'	143.8	-
4'	121.8	8.10 (d, $J = 8.0$ Hz, 1H)
5'	129.7	7.49 (t, $J = 8.0$ Hz, 1H)
6'	135	7.63 (d, $J = 7.5$ Hz, 1H)
7'	171	2.97 (t, $J = 7.5$ Hz, 2H)
8'	35.1	3.19 (t, $J = 7.5$ Hz, 2H)
9'	29.5	-

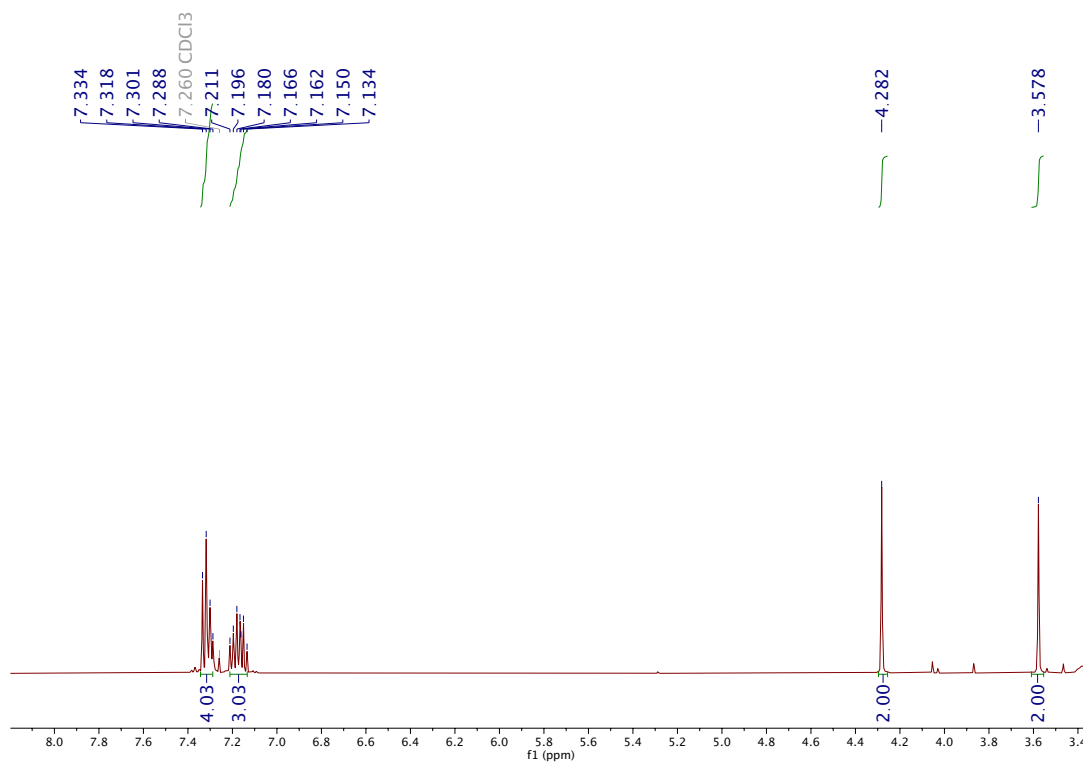


Figure 3.50 The <sup>1</sup>H NMR spectrum of NT24

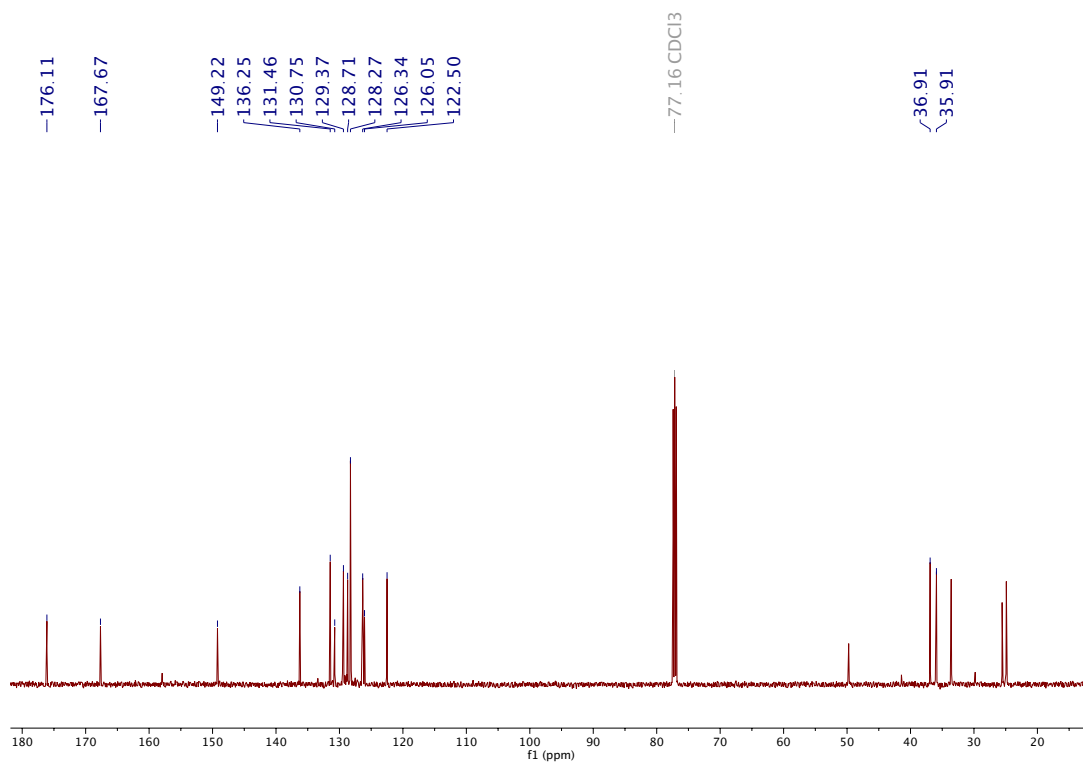


Figure 3.51 The <sup>13</sup>C NMR spectrum of NT24

**Table 3.25** The  $^1\text{H}$  and  $^{13}\text{C}$  NMR spectral assignment of **NT24**

<b>NT24</b>		
Position	Chemical shift (ppm)	
	$^{13}\text{C}$	$^1\text{H}$
1	149.2	-
2	126.1	-
3	128.7	7.34-7.29 (m, 4H)
5	131.5	
3'	128.3	
5'	128.3	
4	126.3	-
6	122.5	7.21-7.13 (m, 3H)
4'	129.4	
7	36.9	3.58 (s, 2H)
8	176.1	-
1'	130.8	-
2'	136.3	-
6'	136.3	-
7'	35.9	4.29 (s, 2H)
8'	167.7	-

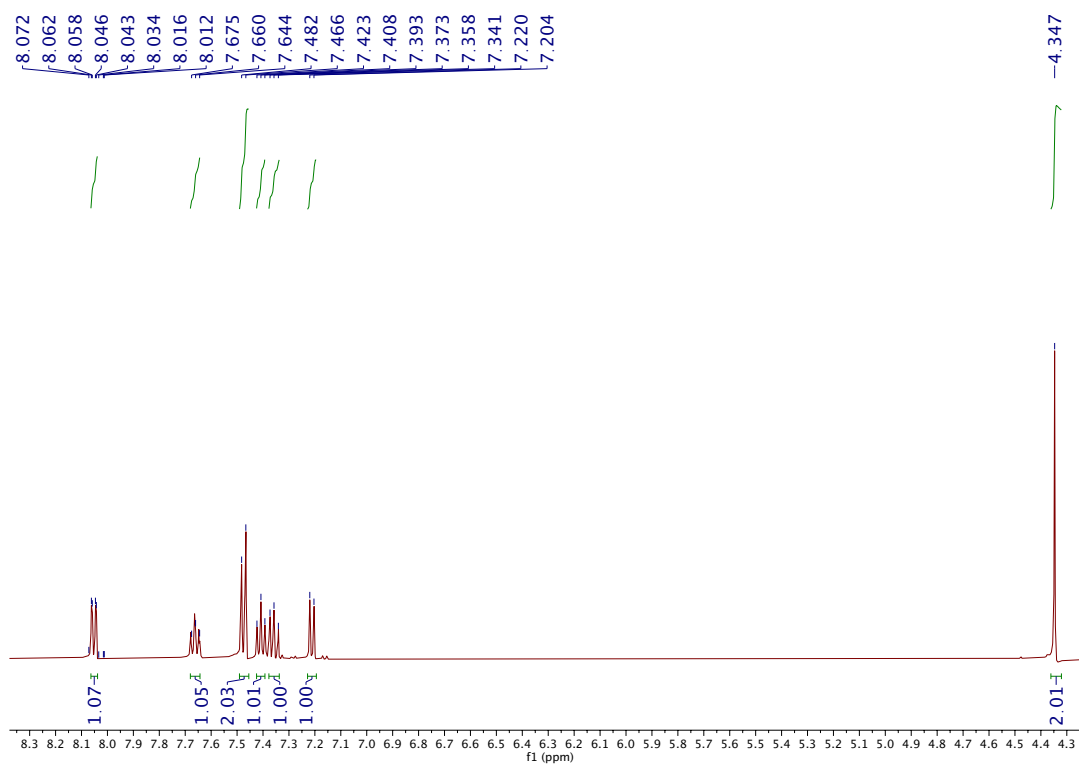


Figure 3.52 The  $^1\text{H}$  NMR spectrum of NT25

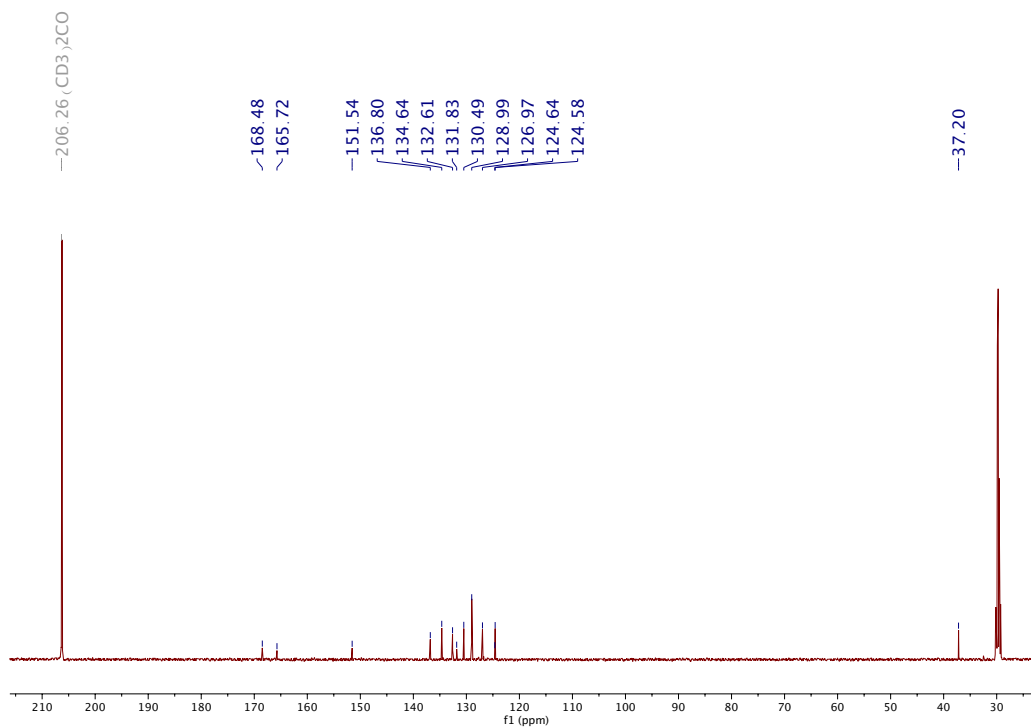


Figure 3.53 The  $^{13}\text{C}$  NMR spectrum of NT25

**Table 3.26** The  $^1\text{H}$  and  $^{13}\text{C}$  NMR spectral assignment of **NT25**

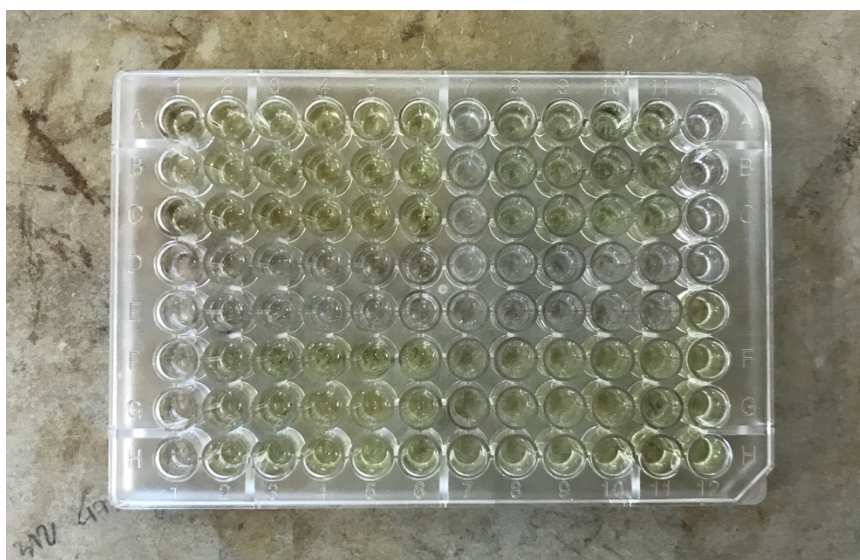
<b>NT25</b>		
Position	Chemical shift (ppm)	
	$^{13}\text{C}$	$^1\text{H}$
1	151.5	-
2	124.6	-
3	130.5	8.20 (dd, $J = 8.0$ and $7.5$ Hz, 1H)
4	126.9	7.41 (t, $J = 7.5$ Hz, 1H)
5	134.6	7.66 (td, $J = 7.5$ Hz and $2.0$ , 1H)
6	124.6	7.21 (d, $J = 8.0$ Hz, 1H)
7	165.7	-
1'	131.8	-
2'	136.8	-
3'	128.9	7.47 (d, $J = 8.0$ Hz, 1H)
4'	130.5	7.36 (d, $J = 7.5$ Hz, 1H)
5'	128.9	7.47 (d, $J = 8.0$ Hz, 1H)
6'	136.8	-
7'	168.5	-



### 3.3 Biological test of synthesized depsides

#### 3.3.1 Anti $\alpha$ -Glucosidase activity

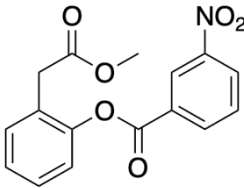
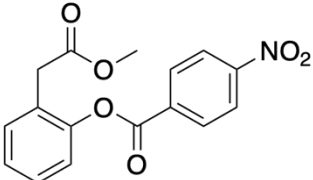
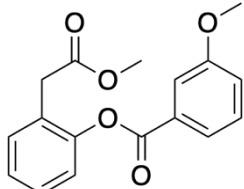
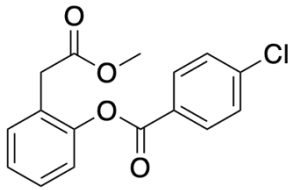
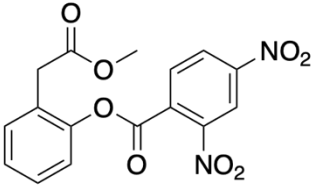
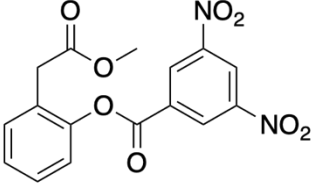
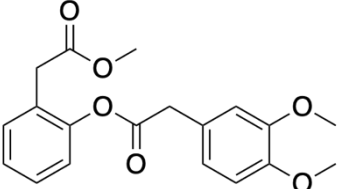
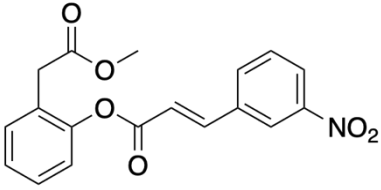
The synthetic depsides **NT1-NT25** were screened for anti  $\alpha$ -glucosidase activity. The mechanism of the inhibition is attributed to the competitive reaction between the tested compound with 4-nitrophenyl  $\alpha$ -D-glucopyranoside (substrate). During the assay, all of the synthesized compounds were added to the 96-well plates. The compounds were colorless and transformed into a yellow color after incubation with the addition of enzyme and substrate. The absorbance value obtained was further used to calculate for the % inhibition and  $IC_{50}$  value.

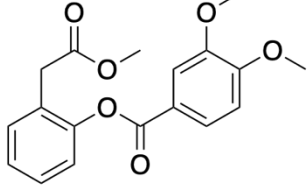
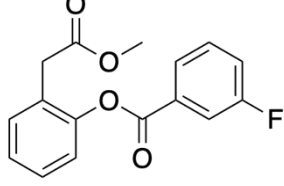
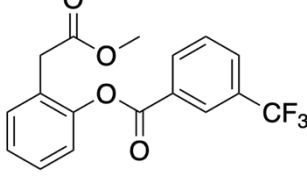
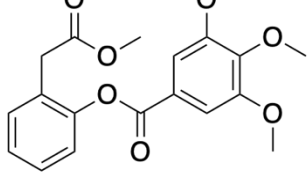
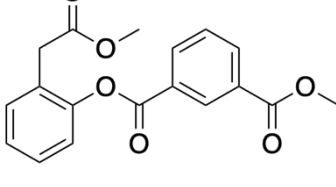
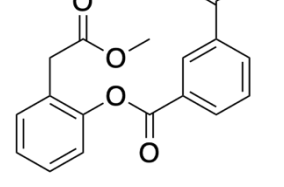
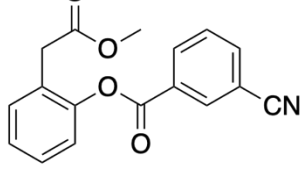
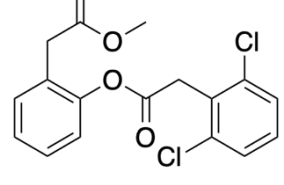


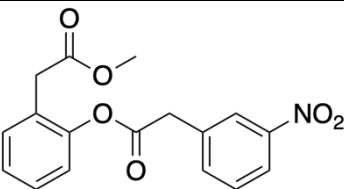
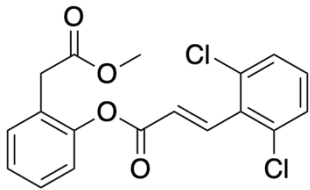
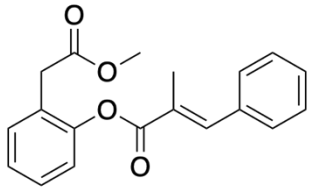
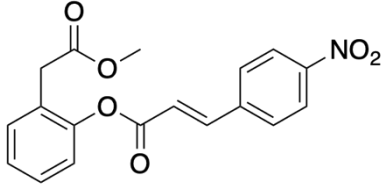
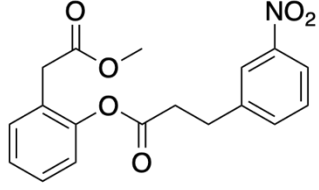
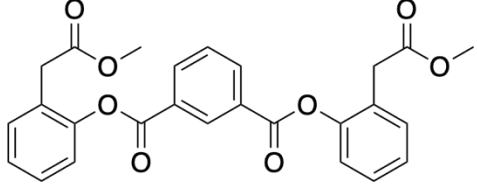
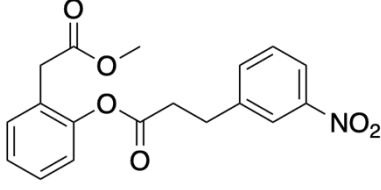
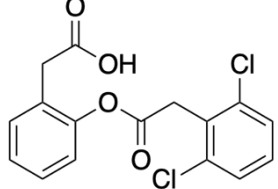
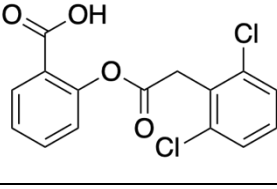
**Figure 3.54** The 96-well plate after the addition of enzyme, substrate and incubation

The percentage of the inhibition at the maximum concentration ( $200 \mu\text{M}$ ) was calculated using the equation mentioned in 2.3.8.1. It is expected to show a value of at least 50 %. In order to quantify the concentration of compounds that were required to inhibit half the rate of the enzyme-catalyzed reaction, the  $IC_{50}$  values for each compound with % inhibition higher than 50 were also calculated. The calculated data were compared to acarbose which is the reference standard ( $IC_{50} = 93.6 \mu\text{M}$ ) and the % inhibition at  $200 \mu\text{M}$  was obtained experimentally, with synthesized compounds values that are below 50% being categorized as non-active. The calculated results are shown in the table 3.27.

**Table 3.27** The anti  $\alpha$ -glucosidase activity of NT1-25 as % inhibition at 200  $\mu$ M and  $IC_{50}$  value

Compound	Structure	Inhibition at 200 $\mu$ M <sup>a</sup> (%)	$IC_{50}$ <sup>b</sup> ( $\mu$ M)
NT1		93.5	68.7 $\pm$ 7.74
NT2		85.9	160.5 $\pm$ 27.3
NT3		48.3	Non-active
NT4		52.64	Non-active
NT5		101.4	80.4 $\pm$ 7.21
NT6		49.8	Non-active
NT7		31.5	Non-active
NT8		92.7	137.8 $\pm$ 4.38

NT9		46.4	Non-active
NT10		89.3	190.7 ± 12.0
NT11		78.2	121.3 ± 25.6
NT12		48.4	Non-active
NT13		97.0	201.8 ± 6.95
NT14		49.08	Non-active
NT15		44.4	Non-active
NT16		100.1	85.1 ± 1.46

NT17		97.8	91.5 ± 5.50
NT18		84.8	84.8 ± 5.15
NT19		77.5	Non-active
NT20		59.6	239.2 ± 0.72
NT21		80.9	228.0 ± 27.7
NT22		10.1	Non-active
NT23		95.5	107.0 ± 15.0
NT24		19.8	Non-active
NT25		33.2	Non-active

<sup>a</sup> The % inhibition was reported as the average value across 2 trials

<sup>b</sup> Values are the mean  $\pm$  standard deviation

IC<sub>50</sub> values for active synthesized compounds are categorized into 4 main categories. The most promising anti  $\alpha$ -glucosidase compound is **NT1** with an IC<sub>50</sub> of 68.7  $\mu$ M, more potent than acarbose (IC<sub>50</sub> = 93.6  $\mu$ M). The structure of **NT1** consists of a NO<sub>2</sub> substituent attached to the 3'-position of ring B (Figure 3.1).

However, **NT5**, which contains two NO<sub>2</sub> groups located at R<sub>2</sub> and R<sub>4</sub>, showed an increase in IC<sub>50</sub> value of up to 80.4  $\mu$ M. In addition, by relocating the NO<sub>2</sub> substituent on the B-ring and/or an additional carbon linkage between two aromatic rings in the form of both single and double bond, the IC<sub>50</sub> values of compound **NT2**, **NT8** and **NT23** demonstrated an increasing trend, respectively, as shown in the table 3.1.

Another group of compounds which also showed potential anti- $\alpha$ -glucosidase activity are **NT16** and **NT18**. Both of these potential compounds contain two chlorine substituents which are directly attached to R<sub>2</sub> and R<sub>6</sub> of the aromatic ring, where **NT16** (IC<sub>50</sub> = 85.1  $\mu$ M) contained an extra methylene group in the ester linkage. In comparison, for **NT18**, by substituting the linkage with a unsaturated carbon along with an additional carbon located at the bridge, the IC<sub>50</sub> value reduced to 84.8  $\mu$ M. On the other hand, further modification was performed on compound **NT24** and **NT25**. The removal of the methoxy group attached to R<sub>1</sub> position in both compounds **NT24** and **NT25**, with the latter without the methylene group sprouting from the ring A, led to the colossal deterioration of their activity (from 19.8 to 33.2 % inhibition, respectively). This indicates that the carboxylic group attached directly to the A-ring increased the electron withdrawing effect which accounts for the higher % inhibition of **NT25** when compared to **NT24**. However, the % inhibition of these two compounds was less than 50% which means that they are classified as non-active compounds.

Moreover, with the presence a fluorine substituent in **NT10** and a trifluoromethyl group in **NT11**, both located at R<sub>2</sub> position, the high IC<sub>50</sub> values of up to 190.0 and 121.3  $\mu$ M were observed. Furthermore, **NT13** with an acetate group attached to R<sub>3</sub> was the least potent compound (IC<sub>50</sub> = 201.8  $\mu$ M). Apart from this, there were also compounds that are non-active, especially depsides with the methoxy group attached directly to the B-ring. This demonstrates that by increasing the number of methoxy substituent on the B-ring will not result in the improvement of the IC<sub>50</sub> value nor % inhibition at 200  $\mu$ M. In addition, other depsides containing various substituents, such as carboxylic group (**NT14**), cyano (**NT15**), and other diverse ester linkages, were synthesized and tested but the result appeared as non-active.

Therefore, modification was majorly carried out on the B-ring and the results showed more potent activity, where **NT1**, **NT5**, **NT16**, **NT17** and **NT18** showed an outstanding  $IC_{50}$  value ranging from 68.7 to 91.5  $\mu M$  which are lower than acarbose. This showed that the influence from electron-withdrawing substituents with the potency order  $NO_2$  (**NT1**, **NT5**, **NT17**) > Cl (**NT16** and **NT18**) and unsaturated carbon bridge along with the number of carbon ( $n = 1$  and  $2$ ) lead to promising anti- $\alpha$ -glucosidase inhibitors. Meanwhile substituents such as F (**NT10**) >  $CF_3$  (**NT11**) > acetate group (**NT13**) show moderate potency, **NT20** and **NT21** are the least potent compounds with an  $IC_{50}$  of up to 239  $\mu M$  and compounds with electron-donating groups such as  $OCH_3$  compounds showed non-active. Moreover, a modification at the A-ring was also carried out, the % inhibition of **NT25** was influenced by the presence of the carboxylic acid group which is a strong electron withdrawing group. The result indicated that by attaching an electron withdrawing group directly to the aromatic ring will increase the % inhibition as compared to **NT24** which has an extra methylene group ( $m = 1$ ) on the A-ring. However, the % inhibition for both **NT24** and **NT25** is lower than 50% which are classified as non-active compounds

### 3.3.2 Antioxidant activity

Antioxidant properties of synthesized compounds were also performed based on the DPPH assay. The DPPH is a free radical with a violet color which readily receives a hydrogen atom or electron that were donated from antioxidant compounds. During the assay, the observed DPPH color was violet, and the Ascorbic acid was used as the positive control. In contrast to alpha-glucosidase inhibitory assay, the result of a color change was the first indication that could predict the activeness of the compound. An example of a plate used in the assay for testing the antioxidant activity of **NT24** is shown below.

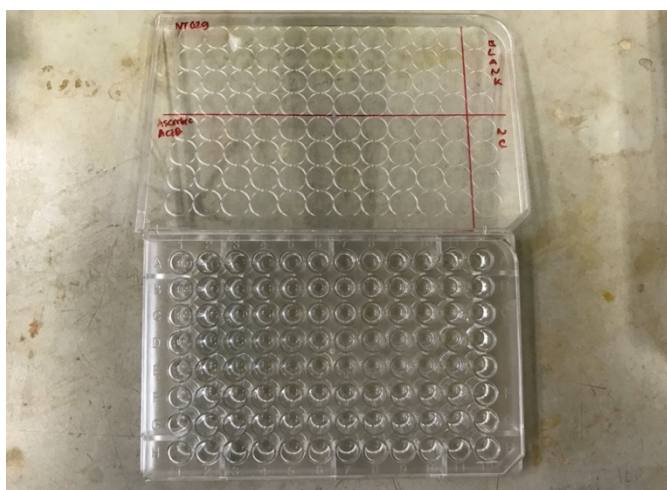


**Figure 3.56** Before the addition of DPPH

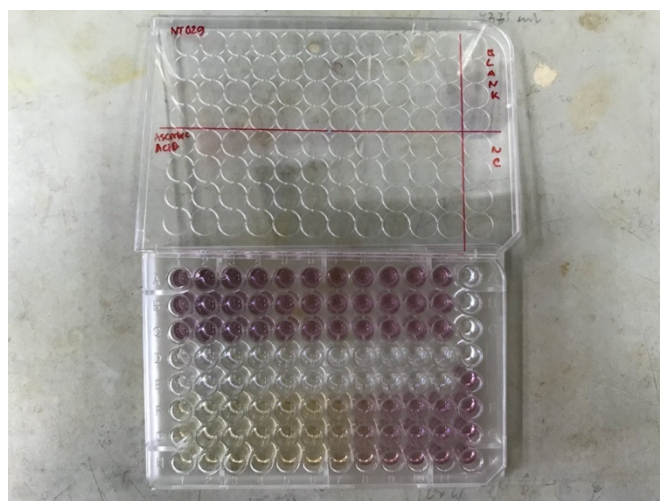


**Figure 3.57** After incubation and addition of DPPH into the samples (top 3 rows) and Ascorbic acid (bottom 3 rows)

As a result, the plate containing **NT24** was non active at 1mM which was the maximum concentration conducted in the assay. After incubation, the color remained purple, but the ascorbic acid turned yellow which is the expected color for successful antioxidants. In addition to **NT24**, the result of other tested compounds is reported in table 3.28.

**Table 3.28** The % inhibition at 1mM of **NT5**, **NT7**, **NT11-NT16**, **NT21** and **NT24**

<b>Compound</b>	<b>Inhibition at 1mM (%)</b>
<b>NT5</b>	17.4
<b>NT7</b>	23.1
<b>NT11</b>	26.4
<b>NT12</b>	6.4
<b>NT13</b>	23.4
<b>NT14</b>	18.6
<b>NT15</b>	6.9
<b>NT16</b>	14.8
<b>NT21</b>	23.3
<b>NT24</b>	11.8

The assay was conducted on a mM scale and **NT11**, containing a CF<sub>3</sub> group at R<sub>2</sub> position exhibited the highest % inhibition (26.4%) among all tested compounds. Consequently, none of the compounds displayed antioxidant properties as all % inhibition at 1mM was lower than 50%.

## Chapter 4

### Conclusion

To synthesize depsides with a core structure of Jaboticabin, an esterification was conducted. The chemicals required were methyl 2-(2-hydroxyphenyl) acetate (**NT0**) and a carboxylic acid compound, with desired substituents, as the main reactants, along with DCC and DMAP as catalysts, to help activate the carboxylic group and increase the rate of reaction, and DCM as the solvent. The esterification was carried out for 24 hours. Then the filtration technique was done to eliminate unwanted urea. Leftover starting materials were removed through extraction technique with 1 N of HCl, then 1 N of NaOH was added to remove unnecessary catalysts. Mostly, compounds with the presence of NO<sub>2</sub> substituent showed great potential as anti  $\alpha$ -glucosidase agents. 2-(2-Methoxy-2-oxoethyl)phenyl 3-nitrobenzoate (**NT1**), a compound with a core structure of jaboticabin and NO<sub>2</sub> substituent positioned at the R<sub>2</sub> of B-ring, possessed the lowest IC<sub>50</sub> value of 68.7  $\mu$ M. 2-(2-methoxy-2-oxoethyl)phenyl 2,4-dinitrobenzoate (**NT5**) contained two NO<sub>2</sub> substituents located at R<sub>2</sub> and R<sub>4</sub> of B-ring which possessed an IC<sub>50</sub> value of 80.4  $\mu$ M while compound 2-(2-methoxy-2-oxoethyl)phenyl 2-(3-nitrophenyl)acetate (**NT17**) which consist of one NO<sub>2</sub> substituent at R<sub>3</sub> position exhibited an IC<sub>50</sub> value was 91.5 $\mu$ M.

Compounds 2-(2-methoxy-2-oxoethyl)phenyl 3-(3-nitrophenyl)propanoate (**NT23**), 2-(2-methoxy-2-oxoethyl)phenyl (*E*)-3-(3-nitrophenyl)acrylate (**NT8**), 2-(2-methoxy-2-oxoethyl)phenyl 4-nitrobenzoate (**NT2**), 2-(2-methoxy-2-oxoethyl)phenyl 3-(3-nitrophenyl)propanoate (**NT21**) and 2-(2-methoxy-2-oxoethyl)phenyl (*E*)-3-(4-nitrophenyl)acrylate (**NT20**) were compounds with NO<sub>2</sub> substituent and some that are comprised of modified ester linkage with IC<sub>50</sub> values of 107.0, 137.8, 160.5, 228.0, and 239.2  $\mu$ M respectively. Moreover, not only compounds with the presence of NO<sub>2</sub> substituent that possess anti  $\alpha$ -glucosidase activity, but also compounds consisting of dichloro substituents. 2-(2-methoxy-2-oxoethyl)phenyl (*E*)-3-(2,6-dichlorophenyl)acrylate (**NT18**) and 2-(2-methoxy-2-oxoethyl)phenyl 2-(2,6-dichlorophenyl)acetate (**NT16**) are compounds that contained a dichloro positioned at R<sub>2</sub> and R<sub>6</sub>, with a difference in the type of ester linkage. The IC<sub>50</sub> values are reported as 84.8 and 85.1  $\mu$ M, respectively. The obtained value showed promising results when compared to acarbose.

A DPPH assay was carried out to test the antioxidant ability of **NT5**, **NT7**, **NT11-NT16**, **NT21** and **NT24**. However, the outcome of this test was unfortunate, the compounds did not exhibit antioxidants properties.



## REFERENCES

1. Lehman, S. The Benefits of Phenolic Acids and Where to Find Them in Your Diet. **2020**
2. Singla, R. K.; Dubey, A. K.; Garg, A.; Sharma, R. K.; Fiorino, M.; Ameen, S. M.; Haddad, M. A.; Hiary, M. A. Natural Polyphenols: Chemical Classification, Definition of Classes, Subcategories, and Structures. *AOAC inter.* **2019**, *102*, 1397-1400
3. Popa, D. E.; Dragoi, C. M.; Arsene, A. L.; Dumitrescu, I. B.; Nicolae, A. C.; Velescu, B. S.; Brucea-Dragomiroiu, G. T.A. The relationship between phenolic compounds from diet and microbiota. *Phenolic compounds - Biological activity* **2017**, 25-38
4. Cafasso, J. Caffeic Acid: Benefits, Sources, and Foods. **2020**
5. Boz, H. Ferulic acid in cereals – a review. *Czech Journal of Food Sciences* **2015**, *33*, 1-7
6. Reynertson, K. A.; Wallace, A. M.; Adachi, S.; Gil, R. R.; Yang, H.; Basile, M. J.; Armiento, J. D.; Weinstein, I. B.; Kennelly, E. J. Bioactive Depsides and Anthocyanins from Jaboticaba (*Myrciaria cauliflora*). *J. Nat. Prod.* **2006**, *69*, 1228-1230
7. Shukla, V.; Joshi, G. P.; Rawat, M. S. M. Lichens as potential natural source of bioactive compounds: a review. *Phytochem. Rev.* **2010**, *9*, 303-314
8. Thadhani, V. M.; Choudhary, M. I.; Khan, S.; Karunaratne, V. Antimicrobial and toxicological activities of some depsides and depsidones. *J. Natn. Sci. Foundation Sri Lanka* **2012**, *40*, 43-38
9. Duong, T.; Devi, A. P.; Tran, N.; Phan, H.; Huynh, N.; Sichaem, J.; Tran, H.; Alam, M.; Nguyen, T.; Nguyen, H.; Charasiri, W.; Nguyen, T. Synthesis,  $\alpha$ -glucosidase inhibition, and molecular docking studies of novel *N*-substituted hydrazide derivatives of atranorin as antidiabetic agents. *Bioorg. Med. Chem. Lett.* **2020**, *30*, xxx
10. Lv, P.; Xiao, Z.; Fang, R.; Li, H.; Zhu, H.; Liu, C. Synthesis, characterization and structure-activity relationship analysis of novel depsides as potential antibacterials. *Eur. J. Med. Chem.* **2009**, *44*, 1779-1787.
11. Lobo, V.; Phatak, P. A.; Chandra, N. Free radicals, antioxidants and functional foods: Impact on human health. *Pharmacog. Rev.* **2010**, *4*, 118-126
12. Hidalgo, M. E.; Fernandez, E. B.; Quilhot, W. P.; Lissi, E. E. Antioxidant activity of depsides and depsidones. *Phytochemistry* **1994**, *37*, 1585-1587
13. Zhang, J.; Jin, Q.; Deng, Y.; Hou, J.; Wu, W.; Guo, D. New depsides from the roots of *Salvia miltiorrhiza* and their radical- scavenging capacity and protective effects against H<sub>2</sub>O<sub>2</sub>-induced H9c2 cells. *Fitoterapia* **2017**, *121*, 46-52
14. Vu, T. H.; Lamer, A. L, Lalli, C.; Boustie, J.; Samson, M.; Devehat, F. L.; Seyec, J. L. Depsides: Lichen Metabolites Active against Hepatitis C Virus. *Plos One* **2015**, *10*, 1-14

## Biography

Miss Thamolwan Arnanthigo was born in Bangkok, Thailand on May 24, 1999. She studied primary and secondary at Regents International school pattaya before continuing her GCSE and A Level course in the United Kingdom at Queen Anne's School. Currently, she is studying a Bachelor degree at Chulalongkorn University in an international program of Science in Applied Chemistry and majoring in Material Chemistry. Her current address is 23/5 Moo 6 Naklua, Banglamung, Chonburi, Thailand, 20150.

Miss Napassakorn Chuaycharoen was born in Chanthaburi, Thailand on January 18, 1999. She finished her primary school at Anuban Chanthaburi school (English program) and continued her secondary school at Sacred Heart Convent (English program). She took a summer course in New Zealand during her 8th grade. Currently, she is studying her senior year, majoring in Material Chemistry at the Faculty of Science in Applied Chemistry (International program), Chulalongkorn University. Her current address is 17/5 Moo 5, Khlong Khut, Thamai, Chanthaburi, 22120.